Simulation of lake thermal structure, ice cover, and fish habitat in response to changing climate

By

Madeline R. Magee

A dissertation submitted in partial fulfillment of

the requirements for the degree of

Doctor of Philosophy

(Civil and Environmental Engineering)

at the

UNIVERSITY OF WISCONSIN-MADISON

2016

Date of final oral examination: 8/29/2016

The dissertation is approved by the following members of the Final Oral Committee:

Chin H. Wu, Professor, Civil and Environmental Engineering

Katherine D. McMahon, Professor, Civil and Environmental Engineering

Paul Block, Assistant Professor, Civil and Environmental Engineering

Peter B. McIntyre, Associate Professor, Limnology

Paul C. Hanson, Research Professor, Limnology

Abstract

Physical, chemical, and biological properties in lakes are all sensitive to changes in climate, but the interaction and response of these properties to changes in climate is not yet fully understood. The objective of this dissertation is to characterize the role of lake depth and lake surface area on the physical response of water temperature and ice cover to air temperature and wind speed changes and to determine the response fish habitat to climate-caused changes in the physical parameter of temperature chemical parameter of dissolved oxygen. To fulfill these objectives, a one-dimensional lake hydrodynamic, ice, and water quality model is utilized on three lakes near Madison, WI.

Water temperatures and ice cover were simulated from 1911 – 2014 for Lake Mendota, Fish Lake, and Lake Wingra, WI, three lakes of varying depth and surface area to elucidate the effects of air temperature and wind speed on lake thermal structure and ice cover. For all three lakes, epilimnetic temperatures increased, hypolimnetic temperatures decreased, stratified period lengthened, stability increased, and ice cover duration and ice thickness all decreased. For all open water variables except hypolimnion temperatures, perturbations revealed that increasing air temperatures and decreasing wind speeds both alter lake physical variables in the same direction, creating a cumulative effect on water temperatures and stratification. Interestingly, air temperature and wind speed perturbations showed that for hypolimnion temperatures, increasing air temperatures and decreasing wind speed had opposing effects. Historical changes in hypolimnion temperatures in Lake Mendota and Fish Lake show decreasing temperatures indicating that decreasing wind speed changes are driving this response rather than air temperature changes. Overall, lake depth impacts the ice cover variables more than surface area

does, but surface area influences temperature and stratification variables to a greater extent than does lake depth. In general, for the lakes studied here, the larger, deeper lake appears more susceptible to water temperature, stratification, and stability changes, while larger, shallower lakes appear more resilient to ice cover changes.

Using temperature at dissolved oxygen of 3 mg L^{-1} (TDO3) to characterize oxythermal habitat of cisco (*Coregonus artedi*) in Lake Mendota from 1976 – 2013 and multiple linear regression analysis to compare TDO3 with meteorological and water quality drivers revealed that summer (Jun – Aug) air temperatures, spring (Mar – May) phosphorus loads, and spring inflow volumes influenced TOD3 values in the lake. Model results from sensitivity analysis show that air temperature has the greatest influence on TDO3 values, followed by phosphorus loads, then inflow volumes. Under the A1B air temperature scenario, it is possible to improve oxythermal habitat, measured as lower TDO3 values, to the current levels through a 25% reduction in phosphorus load, and reduce them even further to improve habitat over historical conditions by reducing phosphorus loads by 75%. This represents a feasible mitigation strategy to offset effects of climate change and maintain cisco populations in at-risk lakes.

Finally, a novel metric, cumulative oxythermal stress dosage (COSD) was developed for yellow perch (*Perca flavescens*) in Fish Lake, WI to quantify oxythermal stress in the lake. For yellow perch COSD is a better predictor of fish declines than the TDO3 method as it accounts for both magnitude and duration of stress. COSD values are closely tied to the July – September air temperatures, and perturbation scenarios identify 3°C air temperature increase as a possible threshold for yellow perch extirpation.

Acknowledgements

I would like to thank many people and organizations who have supported me throughout my graduate studies at the University of Wisconsin-Madison. First, I must thank my advisor Dr. Chin Wu. His guidance has helped me develop as a researcher, and under his direction I have learned much about what makes a good scientist. Next, I would like to thank all my committee members, Drs. Trina McMahon, Paul, Block, Pete McIntyre, and Paul Hanson. Thanks to you all for believing in my work, offering great career and research advice, and teaching me how to become a better scientist. I would also like to thank the other professors and researchers that I have worked with, or adjacent to, during my time here: Drs. Emily Stanley, Steve Loheide, Dick Lathrop, Dale Robertson, Ken Potter, John Magnuson, David Hamilton, John Hoopes, Jordan Read, Luke Winslow, Noah Lottig, and many others. I have looked up to and respected the work you have all done and I hope one day someone regards me as highly as I do all of you.

This work was supported by a Grainger College of Engineering Graduate Research Fellowship, the National Science Foundation Long Term Ecological Research Study, the University of Wisconsin (UW) Water Resources Institute, UW Office of Sustainability SIRE Award Program, the Becker Travel Grant, and the Anna Grant Birge Memorial Award. I am also thankful for the opportunity to teach CEE 291 for three years.

I received much support from colleagues in the Water Resources Engineering and Environmental Fluid Mechanics program and those associated with LTER that was integral to my success either through feedback on research or field work. I would like to thank Adam Bechle whom I have truly looked up to these last 6 years both as a scientist and a great person. I couldn’t have finished this dissertation without your support. Yi-Fang Hsieh, thank you for helping me as I was starting on this research journey. Alex, Hoilai, Alvaro, and Nick, thanks for

being such great desk neighbors and listening to my random rambling when I'm trying to figure stuff out. Josh, Michael, Owen, Alvaro, and Bill Roznik, I have learned a lot about teaching from you all and have benefitted greatly from your support and encouragement during our time as 291 TAs together. To everyone else in the group (past and present), I am honored to have known and worked with all of you, and I thank you sincerely for your friendship, support, and constant encouragement.

Next, I would like to thank all the outstanding teachers I've had throughout my life for instilling a love of learning and the confidence that I could achieve anything I wanted. Mr. Donahoe, thank you for always pushing me in math, never letting me slack even for a moment, and for always showing, through your actions and words, that I was just as good as all the guys. Mrs. Carpenter for being the best science teacher I've ever had. Mrs. Behrens and Ms. Durkin, thank you for encouraging my love of music and art, both of which helped during rough times. Mrs. Murphey, thank you for helping to turn a shy, quiet girl into someone who no longer turns red and mumbly when speaking in public. Dr. Randall Barnes thank you for first encouraging me to go to graduate school. Dr. Otto Strack, thank you for teaching me how to be a good modeler and for being the best teacher I've ever had. Cathy Abene and Lanya Ross, thank you both for being fantastic mentors. I'm so thankful I had the opportunity to work with and learn from both of you.

Finally, I would like to thank my family and friends for their encouragement during my graduate studies. Thank you to my parents, Pat and Helen, for giving me every opportunity to learn and succeed. The advantages you have given me in life and lessons you've taught me are the reason I have become the person I am and I cannot thank you enough. Sean and Cameron, thanks for never letting me think too highly of myself and always supporting me. To my many

friend from Richland Center, Minneapolis, and Madison, thank you for all your support, encouragement, and random funny text messages when I needed them. I want to especially thank Caitlin, Heather, Kally, Ashley, and Betsy for putting up with me while I was busy, tired, and not the best friend over the last six years. Finally, I want to thank Alex and William for always loving me and giving me a reason to push through when I didn't think I could do it. William, thank you for being my reason to be the best person possible. Alex, you have always supported me, encouraged me, and picked up the slack at home when I was in the office late working. I am so thankful that I found you early in life and cannot imagine my life without you.

Table of Contents

List of Tables

List of Figures

Chapter 1 : Introduction

1.1 Background

Lakes are particularly sensitive to changes in climate, and previous research shows that physical, biological, and chemical properties of lakes all respond to climate changes (Rosenzweig et al. 2007; Adrian et al. 2009). Global increases in air temperature and precipitation lead to measurable changes in water quality (Murdoch et al. 2000), and climate changes amplify impacts of eutrophication (Jeppesen et al. 2010; Moss et al. 2011). Declines in biodiversity of freshwater ecosystems are related to climate-induced stress (Sala et al. 2000; Heino et al. 2009), and changes to the lake ecosystem affect all trophic levels (Jackson et al. 2007; Kosten et al. 2012; Jeppesen et al. 2012; Michelutti et al. 2015). Climate affects the interaction and distribution of species, shifting lake food webs (Winder and Schindler 2004a; Messner et al. 2013; Comte et al. 2013) and resulting in new competitive interactions (Van Zuiden et al. 2016). These changes have far- reaching economic impacts, and may disproportionately affect those in low-income countries that rely heavily on lakes as a food resource or for their economic value (Ogutu-Ohwayo et al. 2016).

Multi-level ecosystem changes are primarily influenced by changes in lake water temperature, stratification, and ice cover. Several studies have shown a strong coupling between lake temperatures and water chemistry, organism physiology, population abundance, community structure, and food – web dynamics (Weyhenmeyer et al. 1999; Straile 2000; Gerten and Adrian 2000; Arhonditsis et al. 2004b). Disappearance of ice cover can impact photic exposure (Leppäranta et al. 2003), nutrient cycling (Järvinen et al. 2002), oxygen conditions (Livingstone 1993; Stefan et al. 2001), and production and diversity of phytoplankton (Weyhenmeyer et al.

1999; Phillips and Fawley 2002). Changes in seasonal phytoplankton development and cyanobacteria dominance are driven by changes in water temperature (Elliot et al. 2005), and bloom-forming cyanobacteria have a competitive advantage at higher temperatures (Jöhnk et al. 2008; Paerl and Huisman 2008). Shifts in phytoplankton species composition occur in response to changing water temperatures and strong vertical stratification (Verburg et al. 2003; Winder and Schindler 2004a; Yankova et al. 2016). Similarly, stratification-induced shifts to earlier phytoplankton blooms (Winder and Schindler 2004b) have impacted zooplankton composition and abundance (Berger et al. 2014). Seasonally heterogeneous increases in air temperature cause asynchronous shifts in phenology (Straile et al. 2015). Warmer water temperatures and increased stratification duration has drastically altered fish distribution (Jiang et al. 2012; Herb et al. 2014; Van Zuiden et al. 2016) because fish populations, especially cold – and cool – water fish are especially susceptible to increases in water temperatures (Kumar et al. 2013; Feiner et al. 2016; Coulter et al. 2016). Similarly, decreases in ice cover reduces the occurrence of winter fish kills (Fang and Stefan 2000; Stefan et al. 2001), which are critical for hypoxia-tolerant but predation-sensitive fish species (Tonn and Magnuson 1982). The underlying cause of these ecological changes are changes in water temperature, stratification, and ice cover in response to climate change (Adrian et al. 2009).

Lake water temperatures and ice cover are, in part, governed by air temperature and wind speed. Previous studies showed that the warming temperatures have caused increasing epilimnetic water temperatures (Dobiesz and Lester 2009; Shimoda et al. 2011), increased the strength of stratification (Rempfer et al. 2010), prolonged the stratified period (Robertson and Ragotzkie 1990; Livingstone 2003; Wilhelm and Adrian 2008), altered thermocline depth (Schindler et al. 1990; King et al. 1997), caused later ice-on and earlier ice-off (Magnuson et al.

2000; Korhonen 2006; Jensen et al. 2007; Benson et al. 2011), thinner ice (Williams and Stefan 2006; Choiński et al. 2013; Magee et al. 2016), and less spatial ice cover (Wang et al. 2011; Bai et al. 2012). Changes in wind speed strongly affect lake mixing (Boehrer and Schultze 2008; Boehrer et al. 2008), lake heat transfer (Fu et al. 2009; Read et al. 2012), and temperature structure (Schindler et al. 1990; Desai et al. 2009). Larger wind speeds can delay ice – on by breaking up thin ice during the beginning of ice formation (Adams 1976), and large wind shear also breaks think ice during ice melting periods, especially on large lakes (Ashton 1986).

While much research has elucidated the role of climate on lake processes, some questions remain unanswered:

i. First, *what is the role of lake morphometry on expression of climate signals in lake thermal structure and ice cover?* Response of temperature and ice cover is variable based on geographic location and lake morphometry (Adrian et al. 2009; Shimoda et al. 2011). Particularly, the behavior of hypolimnetic water temperatures is complex, exhibiting both warming (Livingstone 2003) and cooling behavior (Bueche and Vetter 2014). Furthermore, the persistence of climate signals vary substantially among lakes with different sizes and mixing regimes (Arhonditsis et al. 2004a).

ii. Second, it is unclear *what role the interaction of changing climate and cultural eutrophication have on fish populations?* and *can climate – induced reductions in fish habitat be offset through eutrophication management?* Cultural eutrophication can reduce fish habitat (Evans et al. 1996; Jacobson et al. 2010; Honsey et al. 2016), and climate changes, specifically air temperature increases, can further exacerbate the decline of fish populations due to cultural eutrophication (De Stasio et al. 1996; Jacobson et al. 2010; Herb et al. 2014). Foley et al. (2012) found that both eutrophication and climate change

(specifically air temperature and wind speed) drive changes in volumetric hypolimnetic dissolved oxygen, an important component in cold-water fish habitat. However, little research looks at both factors together (Jacobson et al. 2010; Herb et al. 2014), and fewer still investigate the role of eutrophication management as a means of habitat improvement (Honsey et al. 2016).

iii. Third, *how do fish populations respond to changes in climate and what habitat metrics are appropriate for assessing these changes*? Interactions between climate change and lake biota are complex since other factors such as resource availability, density, and predation strongly control the abundance and distribution of biota (Adrian et al. 2009). A lakes' internal physical structure, morphometry, hydrological setting, and biota can alter the primary mechanisms by which climate affects indicator variables (Adrian et al. 2009). As a result, variables that show response to climate change in one lake may exhibit a very different response in another (Weyhenmeyer et al. 2011), leading to uncertainty when using different indicator variables

1.2 Research objectives

The aim of this dissertation is investigate the response of changing climate in Madison – area lakes with a specific focus on the role of lake morphometry and the response of fish habitat to changes in climate. Guided by currently unanswered questions on lake response to changing climate, specific objectives of the dissertation are as follows:

1. Investigate how lake depth and surface area influence the response of water temperature and stratification to changes in air temperature and wind speed.
2. Determine how the response of lake ice cover duration and ice thickness to changes in air temperature is impacted by the depth and surface area of the lake.

3. Determine how meteorological and water quality parameters influence year-to-year and long-term changes in cisco habitat in one lake and determine if reductions in habitat under a future climate could be mitigated by reducing phosphorus loading into the lake.
4. Develop a novel metric to quantify oxythermal stress for a cool-water fish species and determine how stress changes with air temperature perturbations.

1.3 Introduction to the dissertation

Chapter 2 uses a modelling approach to examine the response of water temperature, stratification, and surface heat fluxes to historical increases in air temperature and decreases in wind speeds and to perturbations of air temperatures and wind speeds on three morphometrically different Madison-areas lakes. In Chapter 3, ice dates, ice cover duration, and ice thickness are simulated on the same three lakes to characterize the response of ice cover variables to past and projected changes in air temperatures. Chapter 4 determines the main meteorological and water quality drivers of cisco oxythermal habitat in Lake Mendota, examines the ability of a multiple linear regression model to estimate oxythermal habitat in comparison to a mechanistic one – dimensional hydrodynamic and water quality model, and investigates what phosphorus loadings would be necessary to offset habitat loss that occurs under the future A1B air temperature scenario. A novel metric for quantifying oxythermal habitat in yellow perch, a cool-water fish species, is proposed in Chapter 5 and compared to a current metric, TDO3, which has been applied to cold-water fish in the northern Midwest and Canada. Finally, conclusions and recommendations for future work are offered in Chapter 6.

1.4 References

Adams, W. 1976. Diversity of lake-cover and its implications. Musk-Ox **18**: 86–98.

Adrian, R., C. M. O'Reilly, H. Zagarese, and others. 2009. Lakes as sentinels of climate change. Limnol. Oceanogr. **54**: 2283–2297.

Arhonditsis, G. B., M. T. Brett, C. L. DeGasperi, and D. E. Schindler. 2004a. Effects of Climatic Variability on the Thermal Properties of Lake Washington. Limnol. Oceanogr. **49**: 256–270.

Arhonditsis, G. B., M. Winder, M. T. Brett, and D. E. Schindler. 2004b. Patterns and mechanisms of phytoplankton variability in Lake Washington (USA). Water Res. **38**: 4013–4027. doi:10.1016/j.watres.2004.06.030

Ashton, G. D. 1986. River and lake ice engineering, Water Resources Publications.

Bai, X., J. Wang, C. Sellinger, A. Clites, and R. Assel. 2012. Interannual variability of Great Lakes ice cover and its relationship to NAO and ENSO. J. Geophys. Res. Oceans **117**: C03002. doi:10.1029/2010JC006932

Benson, B. J., J. J. Magnuson, O. P. Jensen, and others. 2011. Extreme events, trends, and variability in Northern Hemisphere lake-ice phenology (1855–2005). Clim. Change **112**: 299–323. doi:10.1007/s10584-011-0212-8

Berger, S. A., S. Diehl, H. Stibor, P. Sebastian, and A. Scherz. 2014. Separating effects of climatic drivers and biotic feedbacks on seasonal plankton dynamics: no sign of trophic mismatch. Freshw. Biol. **59**: 2204–2220. doi:10.1111/fwb.12424

Boehrer, B., R. Fukuyama, and K. Chikita. 2008. Stratification of very deep, thermally stratified lakes. Geophys. Res. Lett. **35**. doi:10.1029/2008GL034519

Boehrer, B., and M. Schultze. 2008. Stratification of lakes. Rev. Geophys. **46**. doi:10.1029/2006RG000210

Bueche, T., and M. Vetter. 2014. Future alterations of thermal characteristics in a medium-sized lake simulated by coupling a regional climate model with a lake model. Clim. Dyn. **44**: 371–384. doi:10.1007/s00382-014-2259-5

Choiński, A., M. Ptak, and Strzelczak. 2013. Areal variation in ice cover thickness on lake morskie oko (Tatra mountains). Carpathian J. Earth Environ. Sci. **8**: 97–102.

Comte, L., L. Buisson, M. Daufresne, and G. Grenouillet. 2013. Climate-induced changes in the distribution of freshwater fish: observed and predicted trends. Freshw. Biol. **58**: 625–639. doi:10.1111/fwb.12081

Coulter, D. P., M. S. Sepúlveda, C. D. Troy, and T. O. Höök. 2016. Species-specific effects of subdaily temperature fluctuations on consumption, growth and stress responses in two physiologically similar fish species. Ecol. Freshw. Fish **25**: 465–475. doi:10.1111/eff.12227

De Stasio, B. T., D. K. Hill, J. M. Kleinhans, N. P. Nibbelink, and J. J. Magnuson. 1996. Potential effects of global climate change on small north-temperate lakes: Physics, fish, and plankton. Limnol. Oceanogr. **41**: 1136–1149. doi:10.4319/lo.1996.41.5.1136

Desai, A. R., J. A. Austin, V. Bennington, and G. A. McKinley. 2009. Stronger winds over a large lake in response to weakening air-to-lake temperature gradient. Nat. Geosci. **2**: 855–858. doi:10.1038/ngeo693

Dobiesz, N. E., and N. P. Lester. 2009. Changes in mid-summer water temperature and clarity across the Great Lakes between 1968 and 2002. J. Gt. Lakes Res. **35**: 371–384. doi:10.1016/j.jglr.2009.05.002

Elliot, A. J., S. J. Thackeray, C. Huntingford, and R. G. Jones. 2005. Combining a regional climate model with a phytoplankton community model to predict future changes in phytoplankton in lakes. Freshw. Biol. **50**: 1404–1411. doi:10.1111/j.1365-2427.2005.01409.x

Evans, D. O., K. H. Nicholls, Y. C. Allen, and M. J. McMurtry. 1996. Historical land use, phosphorus loading, and loss of fish habitat in Lake Simcoe, Canada. Can. J. Fish. Aquat. Sci. **53**: 194–218. doi:10.1139/f96-012

Fang, X., and H. G. Stefan. 2000. Projected Climate Change Effects on Winterkill in Shallow Lakes in the Northern United States. Environ. Manage. **25**: 291–304.

Feiner, Z. S., D. P. Coulter, S. C. Guffey, and T. O. Höök. 2016. Does overwinter temperature affect maternal body composition and egg traits in yellow perch Perca flavescens? J. Fish Biol. **88**: 1524–1543. doi:10.1111/jfb.12929

Foley, B., I. D. Jones, S. C. Maberly, and B. Rippey. 2012. Long-term changes in oxygen depletion in a small temperate lake: effects of climate change and eutrophication. Freshw. Biol. **57**: 278–289. doi:10.1111/j.1365-2427.2011.02662.x

Fu, G., S. P. Charles, and J. Yu. 2009. A critical overview of pan evaporation trends over the last 50 years. Clim. Change **97**: 193–214. doi:10.1007/s10584-009-9579-1

Gerten, D., and R. Adrian. 2000. Climate-driven changes in spring plankton dynamics and the sensitivity of shallow polymictic lakes to the North Atlantic Oscillation. Limnol. Oceanogr. **45**: 1058–1066. doi:10.4319/lo.2000.45.5.1058

Heino, J., R. Virkkala, and H. Toivonen. 2009. Climate change and freshwater biodiversity: detected patterns, future trends and adaptations in northern regions. Biol. Rev. **84**: 39–54. doi:10.1111/j.1469-185X.2008.00060.x

Herb, W. R., L. B. Johnson, P. C. Jacobson, and H. G. Stefan. 2014. Projecting cold-water fish habitat in lakes of the glacial lakes region under changing land use and climate regimes. Can. J. Fish. Aquat. Sci. **71**: 1334–1348. doi:10.1139/cjfas-2013-0535

Honsey, A. E., S. B. Donabauer, and T. O. Höök. 2016. An Analysis of Lake Morphometric and Land-Use Characteristics that Promote Persistence of Cisco in Indiana. Trans. Am. Fish. Soc. **145**: 363–373. doi:10.1080/00028487.2015.1125949

Jackson, L. J., T. L. Lauridsen, M. SøNdergaard, and E. Jeppesen. 2007. A comparison of shallow Danish and Canadian lakes and implications of climate change. Freshw. Biol. **52**: 1782–1792. doi:10.1111/j.1365-2427.2007.01809.x

Jacobson, P. C., H. G. Stefan, and D. L. Pereira. 2010. Coldwater fish oxythermal habitat in Minnesota lakes: influence of total phosphorus, July air temperature, and relative depth. Can. J. Fish. Aquat. Sci. **67**: 2002–2013. doi:10.1139/F10-115

Järvinen, M., M. Rask, J. Ruuhijärvi, and L. Arvola. 2002. Temporal coherence in water temperature and chemistry under the ice of boreal lakes (Finland). Water Res. **36**: 3949–3956. doi:10.1016/S0043-1354(02)00128-8

Jensen, O. P., B. J. Benson, J. J. Magnuson, V. M. Card, M. N. Futter, P. A. Soranno, and K. M. Stewart. 2007. Spatial analysis of ice phenology trends across the Laurentian Great Lakes region during a recent warming period. Limnol. Oceanogr. **52**: 2013–2026. doi:10.4319/lo.2007.52.5.2013

Jeppesen, E., T. Mehner, I. J. Winfield, and others. 2012. Impacts of climate warming on the long-term dynamics of key fish species in 24 European lakes. Hydrobiologia **694**: 1–39. doi:10.1007/s10750-012-1182-1

Jeppesen, E., B. Moss, H. Bennion, and others. 2010. Interaction of Climate Change and Eutrophication, p. 119–151. *In* rtin Kernan, R.W. Battarbee, and B. Moss [eds.], Climate Change Impacts on Freshwater Ecosystems. Wiley-Blackwell.

Jiang, L., X. Fang, H. G. Stefan, P. C. Jacobson, and D. L. Pereira. 2012. Oxythermal habitat parameters and identifying cisco refuge lakes in Minnesota under future climate scenarios using variable benchmark periods. Ecol. Model. **232**: 14–27. doi:10.1016/j.ecolmodel.2012.02.014

Jöhnk, K. D., J. Huisman, J. Sharples, B. Sommeijer, P. M. Visser, and J. M. Stroom. 2008. Summer heatwaves promote blooms of harmful cyanobacteria. Glob. Change Biol. **14**: 495–512. doi:10.1111/j.1365-2486.2007.01510.x

King, J. R., B. J. Shuter, and A. P. Zimmerman. 1997. The response of the thermal stratification of South Bay (Lake Huron) to climatic variability. Can. J. Fish. Aquat. Sci. **54**: 1873–1882. doi:10.1139/f97-093

Korhonen, J. 2006. Long-term trends in lake ice cover in Finland. *Proceedings of the 18th IAHR international symposium on ice*. 71–78.

Kosten, S., V. L. M. Huszar, E. Bécares, and others. 2012. Warmer climates boost cyanobacterial dominance in shallow lakes. Glob. Change Biol. **18**: 118–126. doi:10.1111/j.1365-2486.2011.02488.x

Kumar, R., S. J. Martell, T. J. Pitcher, and D. A. Varkey. 2013. Temperature-Driven Decline of a Cisco Population in Mille Lacs Lake, Minnesota. North Am. J. Fish. Manag. **33**: 669–681. doi:10.1080/02755947.2013.785992

Leppäranta, M., A. Reinart, A. Erm, H. Arst, M. Hussainov, and L. Sipelgas. 2003. Investigation of Ice and Water Properties and Under-ice Light Fields in Fresh and Brackish Water Bodies. Hydrol. Res. **34**: 245–266.

Livingstone, D. M. 1993. Lake Oxygenation: Application of a One-box Model with Ice Cover. Int. Rev. Gesamten Hydrobiol. Hydrogr. **78**: 465–480. doi:10.1002/iroh.19930780402

Livingstone, D. M. 2003. Impact of Secular Climate Change on the Thermal Structure of a Large Temperate Central European Lake. Clim. Change **57**: 205–225. doi:10.1023/A:1022119503144

Magee, M. R., C. H. Wu, D. M. Robertson, R. C. Lathrop, and D. P. Hamilton. 2016. Trends and abrupt changes in 104 years of ice cover and water temperature in a dimictic lake in response to air temperature, wind speed, and water clarity drivers. Hydrol Earth Syst Sci **20**: 1681–1702. doi:10.5194/hess-20-1681-2016

Magnuson, J. J., D. M. Robertson, B. J. Benson, and others. 2000. Historical Trends in Lake and River Ice Cover in the Northern Hemisphere. Science **289**: 1743–1746. doi:10.1126/science.289.5485.1743

Messner, J. S., M. M. Maclennan, and R. D. Vinebrooke. 2013. Higher temperatures enhance the effects of invasive sportfish on mountain zooplankton communities. Freshw. Biol. **58**: 354–364. doi:10.1111/fwb.12062

Michelutti, N., A. P. Wolfe, C. A. Cooke, W. O. Hobbs, M. Vuille, and J. P. Smol. 2015. Climate Change Forces New Ecological States in Tropical Andean Lakes. PLOS ONE **10**: e0115338. doi:10.1371/journal.pone.0115338

Moss, B., S. Kosten, M. Meerhof, and others. 2011. Allied attack: climate change and eutrophication. Inland Waters **1**: 101–105.

Murdoch, P. S., J. S. Baron, T. L. Miller, and others. 2000. Potential effects of climate change on surface-water quality in North America. J. Am. Water Resour. Assoc. **36**: 347–366.

Ogutu-Ohwayo, R., V. Natugonza, L. Musinguzi, M. Olokotum, and S. Naigaga. 2016. Implications of climate variability and change for African lake ecosystems, fisheries productivity, and livelihoods. J. Gt. Lakes Res. **42**: 498–510. doi:10.1016/j.jglr.2016.03.004

Paerl, H. W., and J. Huisman. 2008. Blooms Like It Hot. Science **320**: 57–58. doi:10.1126/science.1155398

Phillips, K. A., and M. W. Fawley. 2002. Winter phytoplankton community structure in three shallow temperate lakes during ice cover. Hydrobiologia **470**: 97–113. doi:10.1023/A:1015667803372

Read, J. S., D. P. Hamilton, A. R. Desai, and others. 2012. Lake-size dependency of wind shear and convection as controls on gas exchange. Geophys. Res. Lett. **39**: L09405. doi:10.1029/2012GL051886

Rempfer, J., D. M. Livingstone, C. Blodau, R. Forster, P. Niederhauser, and R. Kipfer. 2010. The effect of the exceptionally mild European winter of 2006-2007 on temperature and oxygen profiles in lakes in Switzerland: A foretaste of the future? Limnol. Oceanogr. **55**: 2170–2180. doi:10.4319/lo.2010.55.5.2170

Robertson, D. M., and R. A. Ragotzkie. 1990. Changes in the thermal structure of moderate to large sized lakes in response to changes in air temperature. Aquat. Sci. **52**: 360–380. doi:10.1007/BF00879763

Rosenzweig, C., D. J. Karoly, A. Imeson, and others. 2007. Assessment of observed changes and responses in natural and managed systems, p. 79–131. *In* M.L. Parry, O.F. Canziani, J.P. Palutikof, P.J. Van der Linden, and C.E. Hanson [eds.], Climate Change 2007: impacts, adaptation and vulnerability: contribution of Working Group II to the fourth assessment report of the Intergovernmental Panel on Climate Change. Cambridge University Press.

Sala, O. E., F. S. Chapin, Iii, and others. 2000. Global Biodiversity Scenarios for the Year 2100. Science **287**: 1770–1774. doi:10.1126/science.287.5459.1770

Schindler, D. W., K. G. Beaty, E. J. Fee, and others. 1990. Effects of climatic warming on lakes of the central boreal forest. Science **250**: 967–970. doi:10.1126/science.250.4983.967

Shimoda, Y., M. E. Azim, G. Perhar, M. Ramin, M. A. Kenney, S. Sadraddini, A. Gudimov, and G. B. Arhonditsis. 2011. Our current understanding of lake ecosystem response to climate change: What have we really learned from the north temperate deep lakes? J. Gt. Lakes Res. **37**: 173–193. doi:10.1016/j.jglr.2010.10.004

Stefan, H. G., X. Fang, and J. G. Eaton. 2001. Simulated Fish Habitat Changes in North American Lakes in Response to Projected Climate Warming. Trans. Am. Fish. Soc. **130**: 459–477. doi:10.1577/1548-8659(2001)130<0459:SFHCIN>2.0.CO;2

Stefan, H. G., M. Hondzo, X. Fang, J. G. Eaton, and J. H. McCormick. 1996. Simulated long term temperature and dissolved oxygen characteristics of lakes in the north-central United States and associated fish habitat limits. Limnol. Oceanogr. **41**: 1124–1135. doi:10.4319/lo.1996.41.5.1124

Straile, D. 2000. Meteorological forcing of plankton dynamics in a large and deep continental European lake. Oecologia **122**: 44–50. doi:10.1007/PL00008834

Straile, D., O. Kerimoglu, and F. Peeters. 2015. Trophic mismatch requires seasonal heterogeneity of warming. Ecology **96**: 2794–2805. doi:10.1890/14-0839.1

Tonn, W. M., and J. J. Magnuson. 1982. Patterns in the Species Composition and Richness of Fish Assemblages in Northern Wisconsin Lakes. Ecology **63**: 1149–1166. doi:10.2307/1937251

Van Zuiden, T. M., M. M. Chen, S. Stefanoff, L. Lopez, and S. Sharma. 2016. Projected impacts of climate change on three freshwater fishes and potential novel competitive interactions. Divers. Distrib. **22**: 603–614. doi:10.1111/ddi.12422

Verburg, P., R. E. Hecky, and H. Kling. 2003. Ecological Consequences of a Century of Warming in Lake Tanganyika. Science **301**: 505–507. doi:10.1126/science.1084846

Wang, J., X. Bai, H. Hu, A. Clites, M. Colton, and B. Lofgren. 2011. Temporal and Spatial Variability of Great Lakes Ice Cover, 1973–2010. J. Clim. **25**: 1318–1329. doi:10.1175/2011JCLI4066.1

Weyhenmeyer, G. A., T. Blenckner, and K. Pettersson. 1999. Changes of the plankton spring outburst related to the North Atlantic Oscillation. Limnol. Oceanogr. **44**: 1788–1792. doi:10.4319/lo.1999.44.7.1788

Weyhenmeyer, G. A., D. M. Livingstone, M. Meili, O. Jensen, B. Benson, and J. J. Magnuson. 2011. Large geographical differences in the sensitivity of ice-covered lakes and rivers in the Northern Hemisphere to temperature changes: GLOBAL CHANGE ON LAKE AND RIVER ICE-COVER. Glob. Change Biol. **17**: 268–275. doi:10.1111/j.1365-2486.2010.02249.x

Wilhelm, S., and R. Adrian. 2008. Impact of summer warming on the thermal characteristics of a polymictic lake and consequences for oxygen, nutrients and phytoplankton. Freshw. Biol. **53**: 226–237. doi:10.1111/j.1365-2427.2007.01887.x

Williams, S. G., and H. G. Stefan. 2006. Modeling of Lake Ice Characteristics in North America Using Climate, Geography, and Lake Bathymetry. J. Cold Reg. Eng. **20**: 140–167. doi:10.1061/(ASCE)0887-381X(2006)20:4(140)

Winder, M., and D. E. Schindler. 2004a. Climate Change Uncouples Trophic Interactions in an Aquatic Ecosystem. Ecology **85**: 2100–2106.

Winder, M., and D. E. Schindler. 2004b. Climatic effects on the phenology of lake processes. Glob. Change Biol. **10**: 1844–1856. doi:10.1111/j.1365-2486.2004.00849.x

Yankova, Y., J. Villiger, J. Pernthaler, F. Schanz, and T. Posch. 2016. Prolongation, deepening and warming of the metalimnion change habitat conditions of the harmful filamentous cyanobacterium Planktothrix rubescens in a prealpine lake. Hydrobiologia **776**: 125–138. doi:10.1007/s10750-016-2745-3

Chapter 2 : Response of water temperatures and stratification to changing climate in three lakes with different morphometry

The following is currently in review at *Hydrology and Earth Systems Sciences*

Magee MR and CH Wu. Response of water temperatures and stratification to changing climate in three lakes with different morphometry, Hydrol. Earth Syst. Sci. Discuss., doi:10.5194/hess-2016-262, in review, 2016

2.1 Abstract

Water temperatures in three morphometrically different lakes are simulated using a one-dimensional hydrodynamic lake model over 104-years (1911-2014) to elucidate the effects of increasing air temperature and decreasing wind speed on lake thermal variables (water temperature, stratification dates, strength of stratification, and surface heat fluxes). During the study period, epilimnetic temperatures increased, hypolimnetic temperatures decreased, and the length of the stratified season increased due to earlier stratification onset and later fall overturn. Additionally, there was an abrupt change in epilimnion temperature after 1930 in both Lake Mendota and Lake Wingra, and three changes, after 1934, 1995, and 2008 for Fish Lake. There was a significant change in the rate of change in stratification duration after 1940 in Lake Mendota and a significant rate change after 1981 for Fish Lake. Schmidt stability showed a statistically significant increasing trend for both deep lakes, with the larger trend and greater variability in the larger surface area lake. Sensible heat flux in all three lakes increased over the simulation period, while longwave heat flux decreased. The shallow study lake had a greater change in latent heat flux and net heat flux, illustrating the role of lake depth to surface heat fluxes. Sensible heat flux in all three lakes had similar timing of abrupt changes, but the magnitude of the change increased with increasing depth. Abrupt changes in latent heat flux appear to be independent of lake morphometry, indicating that the timing of change may be

primarily driven by climate. Air temperature and wind speed perturbations showed that increasing air temperature and decreasing wind speed yields earlier stratification onset and later fall overturn. Increasing air temperature warmed hypolimnetic waters, while decreasing wind speed cooled the hypolimnion, indicating that changing hypolimnetic temperatures may be influenced by wind speed changes. Overall, lake depth impacts the presence of stratification and magnitude of Schmidt stability, while lake surface area influences differences in hypolimnion temperature, hypolimnetic heating, variability of Schmidt stability, and stratification onset and fall overturn dates.

2.2 Introduction

Air temperature and wind speeds have changed drastically over the past century. Globally averaged land and ocean surface temperature anomalies increased from 1850-2012 (IPCC 2013), and in the Northern Hemisphere, 1983-2012 was likely the warmest 30-year period of the last 1400 years (IPCC 2013). Studies suggest that more intense and longer lasting heat waves will appear in the future (Meehl and Tebaldi 2004). In Wisconsin, the air temperature increased by 0.61°C from 1950 to 2006 (Kucharik et al. 2010). Meanwhile, both increases and decreases in wind speeds have been observed globally. Wintertime wind energy increased in Northern Europe (Pryor et al. 2005), while modest declines in mean wind speeds were observed in the United States (Breslow and Sailor 2002). Similarly, on the regional scale, Klink (2002) reported a decreasing trend in annual wind speed at five of seven stations in and around Minnesota from 1959 to 1995 and Magee et al. (2016) showed a decrease in wind speeds occurring in Madison, Wisconsin after 1994. Overall, evidence suggest that significant air temperature and wind speed changes over the last century will likely continue to change in the future.

Lake water temperature is closely related to air temperature and wind speed. Warming air temperatures increase epilimnetic water temperatures (Dobiesz and Lester 2009; Shimoda et al. 2011; Bueche and Vetter 2014), increase the strength of stratification (Rempfer et al. 2010; Kerimoglu and Rinke 2013), prolong stratification (Livingstone 2003; Bueche and Vetter 2014), and alter thermocline depth (Schindler et al. 1990). For instance, Lakes Superior, Michigan, and Huron exhibited increasing water temperature and increased stratification duration between 1979 – 2006 (Austin and Colman 2007). In contrast, hypolimnetic temperatures have undergone both warming (Livingstone 2003) and cooling trends (Bueche and Vetter 2014). Changes in wind speed strongly affect lake mixing (Boehrer and Schultze 2008), lake heat transfer (Boehrer and Schultze 2008; Read et al. 2012), and temperature structure (Schindler et al. 1990; Desai et al. 2009; Kerimoglu and Rinke 2013). Stefan et al. (1996) found that decreasing wind speeds resulted in increased stratification and increased epilimnetic temperatures in inland lakes, and Kerimoglue and Rinke (2013) found that wind speed to be a critical variable, with a 30% increase in wind speed offsetting a 5.5 ℃ increase in air temperature. In recent years, we have improved understanding of changing air temperature and wind speed on alterations of water temperature and stratification (Kerimoglu and Rinke 2013; Magee et al. 2016), but there is still uncertainty in the response of water temperatures to solitary and combined changes in air temperature and wind speed.

The lake ecosystem is significantly impacted by changes in lake water temperature (MacKay et al. 2009). For example, increasing water temperatures led to changing plankton community composition and abundance (Rice et al. 2015), altered fish populations (Lynch et al. 2015), and enhanced the dominance of cyanobacteria (Jöhnk et al. 2008). Changes in these populations affect the biodiversity of freshwater ecosystems (Mantyka-Pringle et al. 2014).

Furthermore, increased thermal stratification of lakes can intensify lake anoxia (Palmer et al. 2014), enhance the growth of bloom-forming cyanobacteria (Paerl and Paul 2012), and induce changes to internal nutrient loading and lake productivity (Verburg and Hecky 2009). Variations in water temperature impact the distribution, behavior, community composition, reproduction, and evolutionary adaptations of organisms (Thomas et al. 2004). Further assessment of the response of lake water temperature to changes in air temperature and wind speed will improve our understanding of ecosystem response, which can better prepare management, adaptation, and mitigation efforts for a range of lake sizes.

Lake morphometry can complicate the response of lake water temperatures to air temperature and wind speed changes by altering physical processes of wind mixing, water circulation, and heat storage (Adrian et al. 2009). Basin morphometric characteristics such as mean depth, surface area, and volume can strongly affect lake stratification (Butcher et al. 2015; Kraemer et al. 2015). Large surface areas increase the effects of vertical wind mixing, an important mechanism for transferring heat to the lake bottom (Rueda and Schladow 2009) and thermocline shifts may be dampened in large lakes where the depth of the thermocline is constrained by the lake's fetch (Boehrer and Schultze 2008; MacIntyre and Melack 2010). Winslow *et al*., (2015) showed that differences in wind-driven mixing may explain the inconsistent response of hypolimnetic temperatures between small and large lakes. While previous research efforts have investigated the response of individual lakes (Livingstone 2003; Kerimoglu and Rinke 2013; Voutilainen et al. 2014) and the bulk response of lakes in a geographic region to changing climate (Magnuson et al. 1990; Kirillin 2010), few studies have focused on elucidating the effects of lake depth and surface area on response of water temperatures to long-term changes in air temperature and wind speed.

The purpose of this paper is to investigate the role of lake depth and surface area on the response of water temperatures and stratification to changes in air temperature and wind speed. A one-dimensional hydrodynamic lake-ice model, allowing for additional investigation into quantities that are not available in limnological records, was employed to run continuous long-term simulations of water temperature during open water and ice covered seasons of three lakes with different morphometry. The lakes vary in surface area and depth and were close enough to each other (<30 km distance) to experience similar daily average air temperature and wind speed over the simulation period 1911-2014. Long-term changes in water temperature (epilimnetic and hypolimnetic temperatures), stratification variables (stratification onset, overturn, and duration), heat fluxes, and stability from observations and model outputs reveal how lake depth and surface area influence and alter thermal structure among the three study lakes.

2.3 Methods

2.3.1 Study sites

Three morphometrically different lakes, Lake Mendota, Fish Lake, and Lake Wingra, located near Madison, Wisconsin, United States of America (USA), were selected for this study. These lakes are chosen for (i) their morphometry differences, (ii) their close proximity to one another, and (iii) the availability of long-term limnological records for model calibration.

Lake Mendota (43°6' N; 89°24'W; Figure 2-1; Table 2-1), is a dimictic, eutrophic, drainage lake in an urbanizing agricultural watershed (Carpenter and Lathrop, 2008). The lake stratifies during the summer, and typical stratification periods lasts from May to September. During the summer months (1 June - 31 August), the mean surface water temperature is 22.4 °C, and hypolimnetic temperatures range in value from 11°C to 15 °C. Normal secchi depth during

the summer is 3.0 meters (Lathrop et al., 1996). Fish Lake (43°17'N; 89°39'W; Figure 2- 1; Table 2-1) is a dimictic, eutrophic, shallow seepage lake located in northwestern Dane County. From 1966 to 2001, the water level of the lake rose by 2.75 meters (Krohelski et al. 2002). The lake experiences summer stratification lasting from the beginning of May to mid-September. Mean surface water temperature 23.9°C and hypolimnetic temperatures are normally near 8°C during summer months; however, some years do not experience complete mixing in the spring and reach temperatures of only 4−5°C in the bottom waters by the end of the summer. The average Secchi depth during the summer months is 2.4 m. Lake Wingra (43°3' N; 89°26' W; Figure 2- 1; Table 2-1) is a very shallow, eutrophic, drainage lake. Due to its shallow depth, Lake Wingra does not experience thermal stratification in the summer. During the summer, the mean water temperature is 23.9°C and mean secchi depth is 0.7 meters.

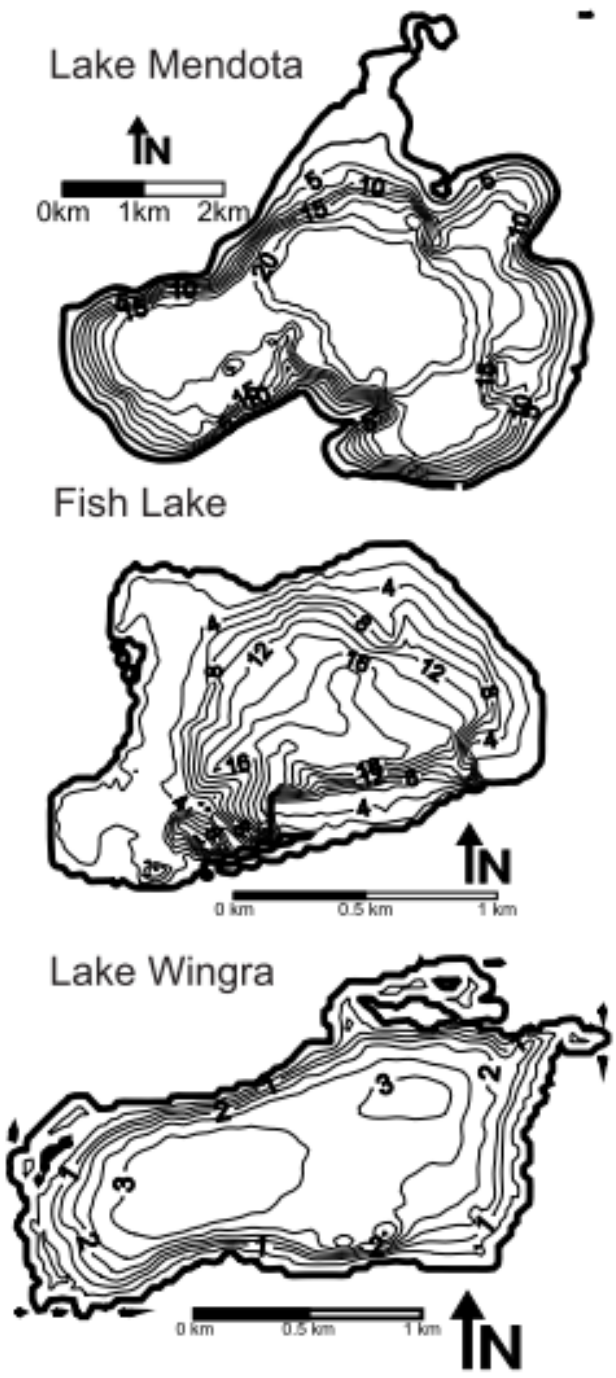

Figure 2-1: Bathymetric maps of Lake Mendota, Fish Lake, and Lake Wingra

Table 2-1: Morphometry and hydrology of the three study lakes

	Lake Mendota	Fish Lake	Lake Wingra
Mean Depth (m)	12.8	6.6	2.7
Max Depth (m)	25.3	18.9	4.7
Surface Area (ha)	3937.7	87.4	139.6
Shoreline Length (km)	33.8	4.3	5.9
Groundwater	Groundwater Discharge	Groundwater Flowthrough	Groundwater Flowthrough
Surface Water	Drainage	Seepage	Drainage
Groundwater Input (%)	30	6	35

2.3.2 Data

Meteorological data used in the model consisted of daily solar radiation, air temperature, vapor pressure, wind speed, cloud cover, rainfall, and snowfall from 1911 to 2014. Air temperature, wind speed, vapor pressure, and cloud cover were computed as an average of the whole day, while solar radiation, rainfall, and snowfall were the daily totals. Meteorological data was gathered from Robertson (1989), who compiled a continuous daily meteorological dataset for Madison Wisconsin from 1884 to 1988 by adjusting for changes in site location. Appended to this dataset is data from the National Climate Data Center weather station at the Dane County Regional Airport. All data other than solar radiation can be obtained from http://www.ncdc.noaa.gov/, for Madison (MSN), and solar radiation can be obtained from http://www.sws.uiuc.edu/warm/weather/. Adjustments to wind speed were made based on changes in observational techniques occurring in 1996 (McKee et al. 2000) by comparing data from the Dane County Airport with that collected from the Atmospheric and Oceanic Science Building instrumentation tower at the University of Wisconsin-Madison (http://ginsea.aos.wisc.edu/labs/mendota/index.htm). Detail of this adjustment can be found in Magee et al. (2016).

Seasonal Secchi depths were used to determine light extinction coefficients. Lathrop et al. (1996) compiled Secchi depth data for Lake Mendota between 1900 and 1993 (1701 daily Secchi depth readings from 70 calendar years), and summarized the data for six seasonal periods: winter (ice-on to ice-out), spring turnover (ice-out to 10 May), early stratification (11 May to 29 June), summer (30 June to 2 September), destratification (3 September to 12 October), and fall turnover (13 October to ice-on). After 1993, Secchi depths are obtained from the North Temperate Lake Long Term Ecological Research (NTL-LTER) program (https://portal.lternet.edu/nis/home.jsp#). For Fish Lake and Lake Wingra, Secchi depths were compiled for 1995 to the present from the NTL-LTER program. For years with no Secchi data, the long-term mean seasonal Secchi depths were used. Light extinction coefficients were estimated from Secchi depth using Equation 2.1, adapted from Williams *et al.*, (1980):

$$k = 1.1/z_s^{0.73} \tag{2.1}$$

where k is the light extinction coefficient and z_s is the Secchi depth (m).

Inflow and outflow measurements were collected from gauging stations (http://waterdata.usgs.gov/wi/nwis/sw/), and complied to calculate daily totals. In cases where inflow and outflow measurements were not available, they were estimated as the residual unknown term of the water budget balancing precipitation, evaporation, and lake level. The residual term was distributed evenly across the number of days between water level measurements. For Lake Mendota, water level was recorded since 1916 (http://waterdata.usgs.gov/wi/nwis/dv). Water level at Fish Lake was recorded almost daily from 1966-2003 (http://waterdata.usgs.gov/wi/nwis/dv/?site_no=05406050&agency_cd=USGS&referred_module=sw). For Lake Wingra, water level was recorded sporadically during the period of interest. When lake level information was unavailable, the long-term mean

lake level was assumed for water budget calculations. Only Lake Mendota has inflowing surface water streams. Inflow temperatures were estimated following the method in (Magee et al. 2016). Groundwater temperature measurements near each lake were used to estimate the temperature of groundwater fluxes.

Observation data used for model calibration came from a variety of sources. For Lake Mendota, long term water temperature records for Lake Mendota were collected from Robertson (1989) and the NTL-LTER (2012a). Ice thickness data were gathered from E. Birge, University of Wisconsin (unpublished); D. Lathrop, Wisconsin Department of Natural Resources (unpublished); Stewart (1965); and the NTL-LTER program (2012b). Frequency of temperature data varied from one or two profiles per year to several profiles for a given week. Additionally, the vertical resolution of the water profiles varied greatly. For Fish Lake and Lake Wingra, water temperature data were collected from NTL-LTER only from 1996-2014 (2012a).

2.3.3 Model description

The DYRESM-WQ (DYnamic REservoir Simulation Model-Water Quality) model (Hamilton and Schladow 1997) employs discrete horizontal Lagrangian layers to simulate vertical water temperature, salinity, and density with input including inflows, outflows, and mixing (Imberger et al. 1978). A one-dimensional layer structure is adopted based on the vertical density stratification over horizontal density variations and destabilizing forces such as wind stress and surface cooling abbreviated to ensure a one dimensional structure (Antenucci and Imerito 2003). Mixing and surface layer dynamics depend on a turbulent kinetic energy budget and potential energy required for mixing (Sherman et al. 1978; Hamilton and Schladow 1997). Hypolimnetic mixing is parameterized through a vertical eddy diffusion coefficient, which accounts for turbulence created by the damping of basin-scale internal waves on the bottom

boundary and lake interior (Yeates and Imberger 2003). More information on the simulation of water temperature and mixing can be found in Imberger and Patterson (1981) and Yeates and Imberger (2003).

The ice model added into the DYRESM-WQ model and called DYRESM-WQ-I model is based on the MLI model of Rogers et al., (1995), with the additions of two-way coupling of the hydrodynamic and ice models and time-dependent sediment heat flux for all horizontal layers. Details of the ice model can be found in Magee et al., (2016). The model assumes that the time scale for heat conduction through the ice is short relative to the time scale of meteorological forcing (Patterson and Hamblin 1988; Rogers et al. 1995), an assumption which is valid with a Stefan number less than 0.1 (Hill and Kucera 1983).

Model inputs include lake hypsography, initial vertical profiles for water temperature and salinity, Secchi depth, meteorological variables, and inflow/outflow. The model calculates the surface heat fluxes using meteorological variables: total daily shortwave radiation, daily cloud cover, air vapor pressure, daily average wind speed, air temperature, and precipitation. During the entire simulation period, all parameters and coefficients are kept constant. The time step in the model for calculating water temperature, water budget, and ice thickness is 1 hr. Snow ice compaction, snowfall and rainfall components are updated at a daily time step, corresponding to the frequency of meteorological data input. Cloud cover, air pressure, wind speed, and temperature are assumed constant throughout the day, and precipitation is assumed uniformly distributed. Shortwave radiation distribution throughout the day was computed based on the lake latitude and the Julian day. Hydrodynamic and ice model parameters are identical for all three study lakes and can be found in Table 1 of Magee et al. (2016). After calibrating the model, we

run the simulation period for all three lakes over 104 years, starting on 7 April 1911 and ending on 31 October 2014 without termination.

2.3.4 Model calibration and evaluation

Using known inflows, outflow, and water elevation, the water balance was closed in the method described in Section 2.3.2 to match measured water levels if known and long term average water levels when elevation information was unknown. We assumed that evaporative water flux and heat flux were properly parameterized by the DYRESM-WQ-I model, although we did not validate model evaporation rates. Parameters used in the model were derived from literature values (Table 1 in Magee et al., 2016) with the exception of light extinction estimate from observed Secchi depth (see Sect. 2.3.2) and adjustment of the minimum layer thickness. To calibrate water temperature, minimum layer thickness was varied from 0.05 to 0.5 m in intervals of 0.025 m for the period 1995-2000 for all three lakes, similar to the method in Tanentzap et al. (2007) and Weinburger and Vetter (2012). One minimum layer thickness was chosen for all three lakes, and the final thickness was chosen to be 0.125 m as it minimized the overall deviation between simulated and observed temperature values for the three lakes.

Three statistical measures were used to evaluate model output against observational data (Table 2-2): absolute mean error (AME), root mean square error (RMSE), and Nash-Suttcliffe efficiencies (NS) were used to compare simulated and observed temperature values for volumetrically-averaged epilimnion temperature, volumetrically-averaged hypolimnion temperature, and all individual water temperature measurements for unique depth and sampling time combinations. Simulated and observed values are compared directly, with the exception of aggregation of water temperature measurements to daily intervals where sub-daily intervals are available. Water temperatures were evaluated for the full range of available data on each lake.

2.3.5 Analysis

In this study, the surface mixed layer depth was determined with LakeAnalyzer (Read et al. 2011). We quantified the resistance to mechanical mixing as the average summer (15 July to 15 August) Schmidt number for each lake based on Idso's version of Schmidt Stability (Idso 1973). Linear regression was used to determine the trend of long-term changes in lake variables. Breakpoints in variables over the study period were determined using a piecewise linear regression (Ying et al. 2015; Magee et al. 2016). A sequential t-test (Rodionov 2004; Rodionov and Overland 2005) was used to detect abrupt changes in the mean value of lake variables. The variables were tested on data with trends removed using a threshold significance level of p = 0.05, a Huber weight parameter of h = 2, and a cut-off length L = 10 years. Finally, the coherence of lake variables (Magnuson et al. 1990) between lake pairs was determined with a Pearson correlation coefficient (Baron and Caine 2000).

2.4 Results

2.4.1 Changes in air temperature and wind speed

Both yearly average air temperatures and seasonal air temperatures from 1911−2014 (Figure 2-2 a). Yearly air temperature increased at a rate of 0.145°C decade^{-1} (p<0.01); winter air temperature increased at a rate of 0.225°C decade-1 (p<0.01); spring air temperature increased at a rate of 0.165°C decade^{-1} (p<0.01); summer air temperature increased at a rate of 0.081°C decade^{-1} (p<0.05); and fall air temperature increased at a rate of 0.110°C decade^{-}1 (p<0.05). All five sets of data were further analyzed for significant changes in slope and for abrupt changes in mean. Yearly average air temperature showed a significant change in slope from 0.081°C decade^{-1} to 0.334°C decade^{-1} occurring in 1981, but seasonal changes in air temperature showed no significant changes in slope over the study period. Summer air temperatures did show

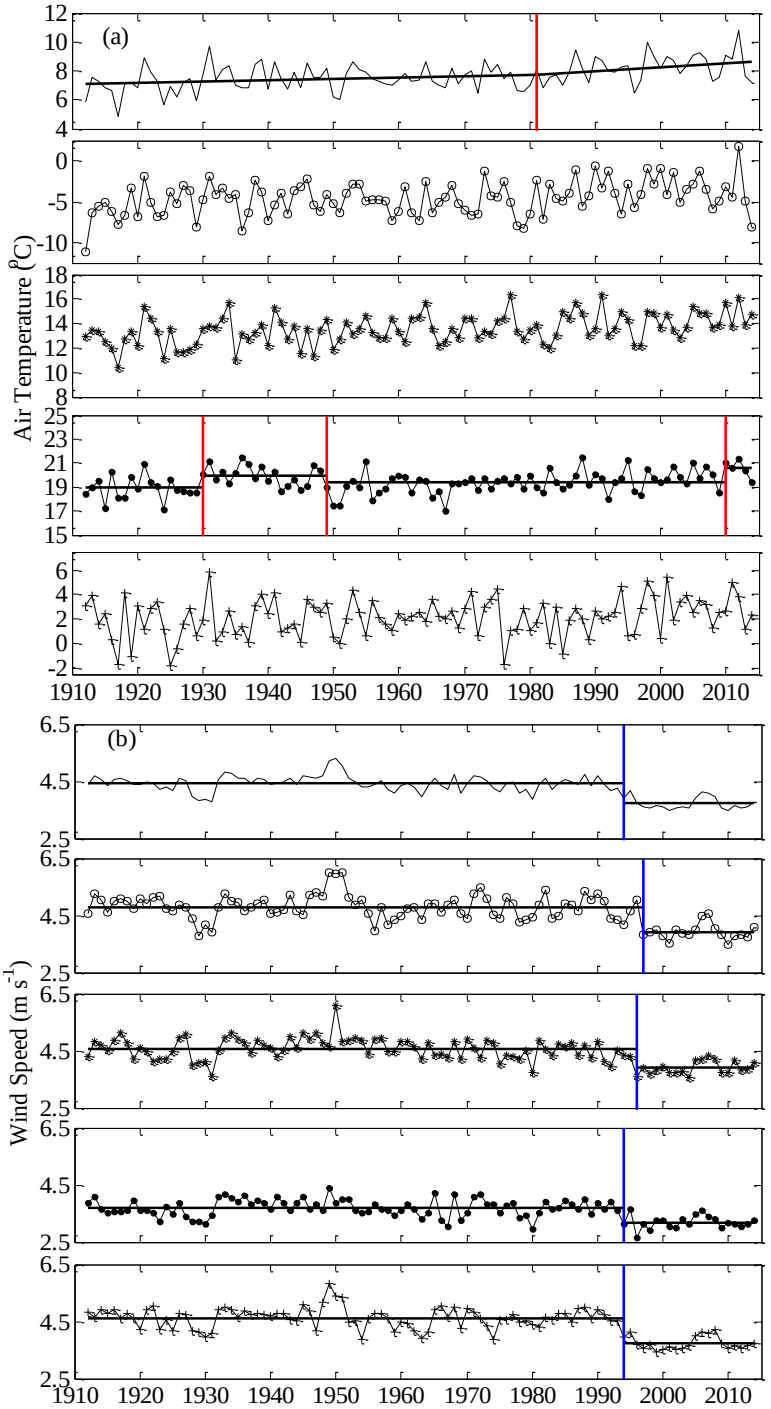

significant abrupt changes in the mean value in 1930 from 18.88°C to 19.96 °C (p <0.01); in 1949 from 19.96°C to 19.37 °C (p<0.05); and in 2010 from 19.37 °C to 20.54°C (p<0.05).

Wind speeds for both yearly and seasonal average exhibited significant decreased in trend over the period 1911−2014 (Figure 2-2 b). Yearly wind speed decreased at a rate of 0.073 m s^{-1} $decade^{-1}$ (p<0.01); winter decreased at a rate of 0.083 m s^{-1} $decade^{-1}$ (p<0.01); spring decreased at a rate of 0.071 m s^{-1} $decade^{-1}$ (p<0.01); summer decreased at a rate of 0.048 m s^{-1} $decade^{-1}$ (p<0.01); and fall

Figure 2-2: Yearly (solid line) winter (open circle), spring (asterisk), summer (solid circles), and fall (cross) average (a) air temperature and (b) wind speeds for Madison, WI, USA> Red line in yearly air temperature figure represents a breakpoint in the trend of average air temperature increase from 0.081° C decade-1 to 0.334 °C decade-1 occurring in 1981. Red lines in summer air temperature figure represents abrupt changes in average summer air temperature occurring in 1930, 1949, and 2010. Blue lines in wind speed figures represent abrupt changes in average wind speed occurring in each season and in the overall yearly wind speeds. Yearly wind speed change in 1994; winter in 1997; spring in 1996; summer in 1994; and fall in 1994.

decreased at a rate of 0.088 m s^{-1} $decade^{-1}$ (p<0.01). Additionally, all five sets of wind speed data showed statistically significant abrupt changes in the mean value occurring in the mid-nineties. For yearly average wind speed, a shift from 4.43 m s^{-1} to 3.74 m s^{-1} (p<0.01) occurred after 1994; for winter wind speeds, a shift from 4.72 m s^{-1} to 3.92 m s^{-1} (p<0.01) occurred after 1997; for spring wind speeds, a shift from 4.59 m s^{-1} to 3.90 m s^{-1} (p<0.01) occurred after 1996; for summer, a shift from 3.70 m s^{-1} to 3.66 m s^{-1} (p<0.01) occurred after 1994; and for fall, a shift from 4.64 m s^{-1} to 3.75 m s^{-1} (p<0.01) occurred after 1994.

2.4.2 Model evaluation

Model output including epilimnetic (Table 2-2), hypolimnetic (Table 2-2), and temperature at 1 m intervals (Table 2-2; Figure 2-3) for the three study lakes compared well with observations. The model was validated with all available data for all three lakes during the period 1911−2014. AME and RMSE for all variables were low and less than standard deviations for the variables. NS efficiencies were high (>0.85) and most above 0.90, indicating high model accuracy.

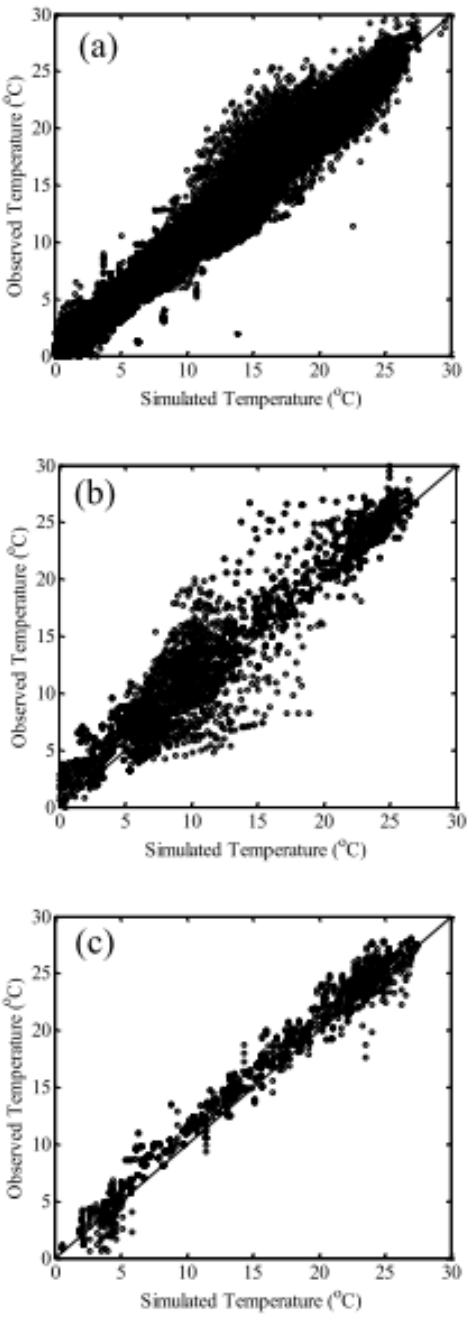

Figure 2-3: Comparison of observed and simulated water temperatures for (a) Lake Mendota, (b) Fish Lake, and (c) Lake Wingra. Each point represents one observation vs. simulation pair with unique date and lake depth

Table 2-2: Absolute mean error (AME), root-mean square error (RMSE), and Nash-Sutcliff efficiency (NS) for water temperatures on Lake Mendota, Fish Lake, and Lake Wingra. n = number of measurements, N/A represents errors that cannot be determined because Lake Wingra is polymictic and does not have a defined epilimnion or hypolimnion.

	Lake Mendota				Fish Lake				Lake Wingra			
Variable	n	AME	RMSE	NS	n	AME	RMSE	NS	n	AME	RMSE	NS
Epilimnetic temperature (°C)	3,239	0.69	0.3	0.99	263	1.23	1.45	0.95	N/A	N/A	N/A	N/A
Hypolimnetic temperature (°C)	3,239	1.04	0.53	0.96	263	1.63	1.94	0.92	N/A	N/A	N/A	N/A
temperature at 1m interval (°C) overall range of values for depths	85,566	0.5-1.56	0.25-0.75	0.95-0.99	5,522	0.85-1.93	1.98-2.42	0.85-0.91	1,897	0.63-0.85	0.41-0.96	0.99

2.4.3 Water temperatures

Epilimnion for Lake Mendota (Figure 2-4a) and Fish Lake (Figure 2-4b) were defined as 0-10 m depth and 0-5 m depth, respectively, based on the surface mixed layer depth from observation and model data using LakeAnalyzer analysis (Read et al. 2011). For Lake Wingra (Figure 2-4c), the whole water column was "epilimnetic" because the lake did not stratify during the summer months. Lake Mendota temperatures ranged from 19.65°C to 26.1°C (mean (M) = 22.8°C, standard deviation (SD) = 1.07°C, range (R) =6.4°C); Fish Lake temperatures ranged from 25.8°C to 19.0°C (M = 22.5°C, SD = 1.3, R = 6.7); Lake Wingra temperatures ranged from 27.5°C to 20.6°C (M = 23.8, SD = 1.27, R = 6.9). Lake Mendota and Lake Wingra had similar increasing trends of 0.069°C decade^{-1} and 0.079°C decade^{-1}, respectively, while Fish Lake had a larger trend increase of 0.138°C decade^{-1} (Table 2-3). All three lakes have statistically significant (p<0.01) abrupt changes in mean values over the study period. For Lake Mendota, there is an abrupt change after 1930 from 22.09 °C to 22.99 °C. For Fish Lake there are three shifts: first after 1934 from 21.68°C to 22.50°C, then after 1995 from 22.50°C to 24.26°C, and finally in

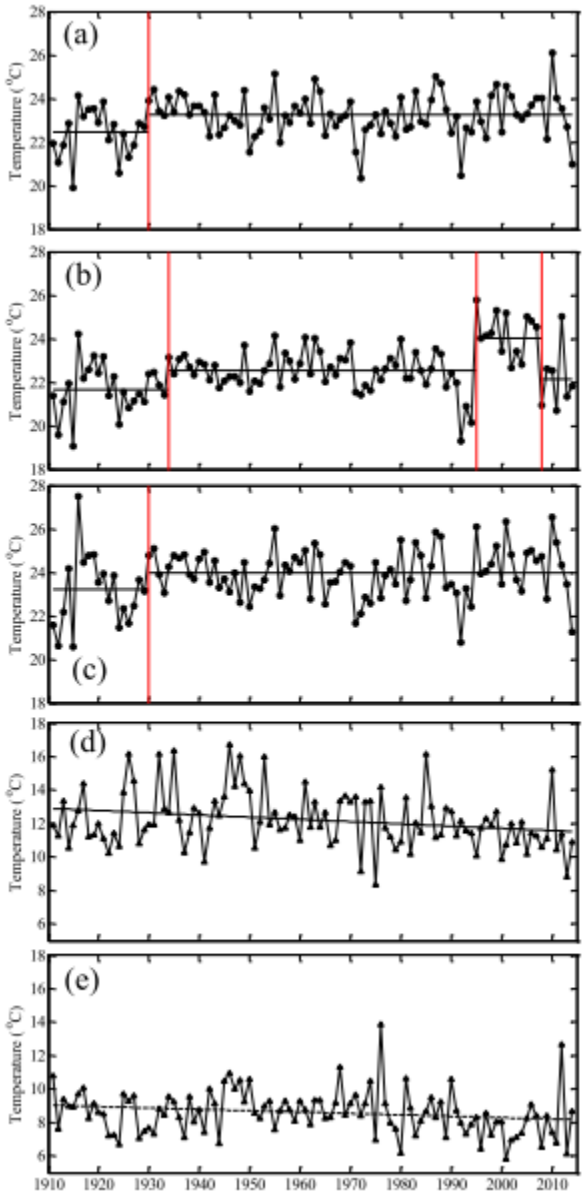

Figure 2-4: Mean summertime (July15-August15) epilimnetic temperatures for (a) Lake Mendota, (b) Fish Lake, and (c) Lake Wingra, and mean summertime (July 15-August 15) hypolimnetic temperatures for (d) Lake Mendota and (e) Fish Lake. In (a), (b), and (c), solid red lines represent statistically significant ($p < 0.5$) locations of abrupt changes in epilimnion temperatures and solid lines represent mean temperatures for each period. In (d) and (e) solid lines represent the long-term trend over the period 1911-2014. Hypolimnetic temperatures show no significant abrupt changes. Neither epilimnetic nor hypolimnetic temperatures for any lakes have significant changes in long-term trends.

2008 from 24.26°C to 22.14°C. For Lake Wingra, there is an abrupt change after 1930 from 23.13°C to 24.02°C. None of the three lakes show any significant breakpoint in the trend of epilimnetic temperatures.

Hypolimnetic water temperatures for Lake Mendota (Figure 2-4d) and Fish Lake (Figure 2-4e) were defined as 18−25 m and 13−20 m, respectively, based upon the long term bottom of metalimnion depth calculated with LakeAnalyzer (Read et al. 2011). Hypolimnetic water temperatures for Lake Mendota ranged from 8.3°C to 16.7 °C (M = 12.2°C, SD = 1.7 °C, R = 8.4 °C); Fish Lake temperatures ranged from 5.8°C to 13.8°C (M = 8.6°C, SD = 1.3°C; R = 8.0°C). Opposite to those of the epilimnion, Lake Mendota and Fish Lake both experienced statistically significant decreases in summer-time hypolimnetic water temperatures of 0.131°C decade^{-1} and 0.083°C decade^{-1}, respectively Table 2-3). The hypolimnetic heating from 15 July to 15 August was also calculated (Table

Table 2-3: Trends in lake physical variables for the three studied lakes from 1911-2014. Trends are represented as units decade-1

	Lake Mendota	Fish Lake	Lake Wingra
Summer Epilimnetic Temperature (°C)	+ 0. 069$^{\Delta}$	+ 0.138*	+ 0.079*
Summer Hypolimnetic Temperature (°C)	- 0.131*	- 0.083*	N/A
Stratification Onset (days)	1.15 days earlier*	0.81 days earlier*	N/A
Fall Overturn (days)	1.18 days later*	1.05 days later*	N/A
Stratification Duration (days)	+ 2.68*	+ 1.86*	N/A
Hypolimnetic heating (°C)	- 0.011*	-0.0011*	N/A
Summer Schmidt stability number (J m^{-2})	+11.7*	+1.44*	no trend

*indicates significant to p<0.05, $^{\Delta}$ indicates significant to p<0.1

2-3), showing a range from 0.04 °C to 2.3°C (M = 0.84°C, SD = 0.37°C, R = 2.2°C) for Lake Mendota and a range from 0.17°C to 0.72°C (M = 0.48, SD = 0.11, R = 0.50) for Fish Lake. Neither lake has a significant abrupt change in temperature nor a significant breakpoint in linear trend during the study period.

2.4.4 Stratification and stability

In this paper, summer stratification was characterized by 3 variables: stratification onset, fall overturn, and duration of stratification. The dates of onset of stratification and fall turnover were defined as the day when the surface-to-bottom temperature difference was greater than (for stratification) or less than (for overturn) 2°C (Robertson and Ragotzkie 1990). Since Lake Wingra did not experience seasonal stratification, only Lake Mendota and Fish Lake are considered here.

For stratification onset, Lake Mendota (Figure 2-5 a) ranged from 15 April to 28 June (M = 20 May; SD = 15 days; R = 74 days) and Fish Lake (Figure 2-5b) ranged from 19 March to 14 May (M = 24 April, SD = 8.2 days, R = 56 days). For fall overturn, Lake Mendota (Figure 5a)

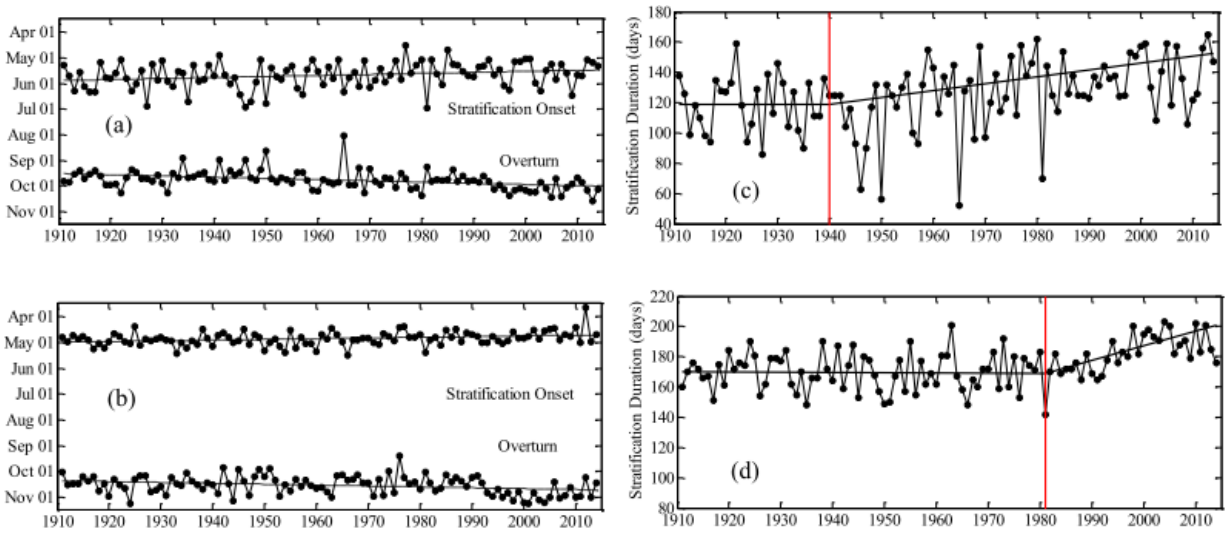

Figure 2-5: Stratification onset and overturn dates for (a) Lake Mendota and (b) Fish Lake. Stratification duration for (c) Lake Mendota and (d) Fish Lake. In (a) and (b) solid lines represent the long-term trend in stratification onset and overturn dates. In (c) and (d), solid red lines represent the timing of a statistically significant ($p<0.01$) change in trend and solid black lines represent the trend during the periods.

ranged from 31 July to 17-October (M = 21 September; SD = 11.4 days; R = 78 days) and Fish Lake (Figure 2-5) ranged from 9 September to 6 November (M = 15 October, SD = 11.0 days, R = 56 days). Stratification duration for Lake Mendota (Figure 2-5c) ranged from 52 days to 165 days (M = 124.7, SD = 22.8, R = 113) and for Fish Lake (Figure 2-5d) ranged from 142 days to 203 days (M = 173.9, SD = 13.7, R = 61). Both lakes experienced earlier stratification onset, later fall overturn, and longer stratification duration, with Lake Mendota having larger trends in all 3 variables (Table 2-3). For both lakes, there was a statistically significant ($p<0.01$) change in the long term mean of 13.3 days earlier occurring after 1994 for Lake Mendota and of 15.1 days earlier occurring after 1993 for Fish Lake. Stratification duration in Lake Mendota exhibited a significant change in trend from 0.067 days earlier decade^{-1} to 4.5 days earlier decade^{-1} after 1940. Similarly, stratification duration in Fish Lake exhibited a significant change in trend from 0.19 days later decade^{-1} to 9.6 days earlier decade^{-1} after 1981.

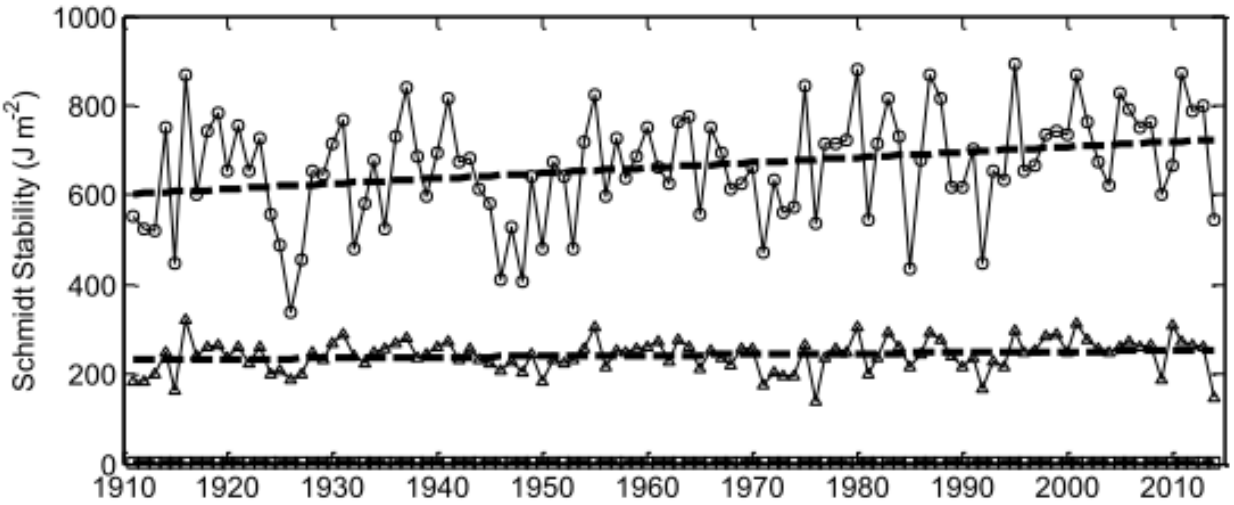

Figure 2-6: Yearly average summer-time (15 July - 15 August) Schmidt stability values for Lake Mendota (circle), Fish Lake (triangle), and Lake Wingra (square).

For lake stability, Lake Wingra had an average Schmidt stability value near 0 (Figure 2-6), indicating that the lake was easily mixed and polymictic during the period. In contrast, both Lake Mendota and Fish Lake had significantly higher stability values (Figure 2-6) and both lakes were stratified and more resistant to mixing. While the shallow lake Wingra showed no trend (Figure 2-6), Lake Mendota and Fish Lake exhibited statistically significant changes in trend. Furthermore, Lake Mendota had larger mean values than Fish Lake (Figure 2-6). A larger trend was also observed in Lake Mendota (Table 2-3), possibly due to both a larger change in stratification variables and changing hypolimnion temperature, increasing stability. There was no significant abrupt shift or change in trend for any of the three lakes during the study period.

2.4.5 Surface heat fluxes

The modelled surface heat fluxes (Figure 2-7) including (a) net shortwave radiative flux; (b) net longwave radiative flux; (c) sensible heat flux; (d) latent heat flux; and (e) total heat flux for the study lakes over the 104-year period are examined here. There is no statistically

significant trend in shortwave flux, latent flux, or total heat flux, but longwave flux exhibits trend toward larger magnitude flux (decreasing absolute value; -5.85 J m^{-2} for Lake Mendota, -5.80 J m^{-2} for Fish Lake, and -4.59 J m^{-2} for Lake Wingra, $p<0.05$ for all three lakes) and sensible heat fluxes displays an increasing trend (less negative values; 4.10 J m^{-2} for Lake Mendota, 3.65 J m^{-2} for Fish Lake, and 5.65 J m^{-2} for Lake Wingra, $p<0.05$ for all three lakes). For shortwave radiation, an abrupt change from 1.14 J m^{-2} to -4.92 J m^{-2} occurred in Lake Mendota after 1992($p<0.01$); a change from -1.97 J m^{-2} to 3.34 J m^{-2} after 1945 ($p<0.01$) and from 3.34 J m^{-2} to -4.84 J m^{-2} after 1992 ($p<0.01$) for Fish Lake; and from -4.34 J m^{-2} to 4.07 J m^{-2} after 1937 ($p<0.01$) and from 4.07 J m^{-2} to -5.98 J m^{-2} after 1992 ($p<0.01$) for Lake Wingra. For longwave radiation, multiple abrupt changes occurred in all three lakes. For Lake Mendota: -2.09 J m^{-2} to 2.54 J m^{-2} after 1923 ($p<0.01$), 2.54 J m^{-2} to -0.68 J m^{-2} after 1937 ($p<0.01$), -0.68 J m^{-2} to 2.60 J m^{-2} after 1981 ($p<0.01$), and 2.60 J m^{-2} to -0.86 J m^{-2} after 1998 ($p<0.01$). For Fish Lake: -2.23 J m^{-2} to 2.53 J m^{-2} after 1923 ($p<0.01$), and 2.53 J m^{-2} to 0.10 J m^{-2} after 1937 ($p<0.01$). For Lake Wingra: -1.98 J m^{-2} to 3.09 J m^{-2} after 1924 ($p<0.01$), 3.09 J m^{-2} to -0.81 J m^{-2} after 1937 ($p<0.01$), and -0.81 J m^{-2} to 1.42 J m^{-2} after 1981 ($p<0.01$). Sensible heat flux had an abrupt change after 1926 for Lake Mendota (-1.67 J m^{-2} to 0.26 J m^{-2}, $p<0.01$) and after 1921 for both Fish Lake (-2.23 J m^{-2} to 0.26 J m^{-2}, $p<0.01$) and Lake Wingra (-3.68 J m^{-2} to 0.36 J m^{-2}, $p<0.01$). While the timing of the abrupt change was similar in all three lakes, the magnitude of the change appears to increase with lake depth. Latent heat flux shows statistically significant ($p<0.01$) changes in mean after 1926 (Lake Mendota 5.78 J m^{-2} to -2.32 J m^{-2}; Fish Lake 5.43 J m^{-2} to -2.14 J m^{-2}; Lake Wingra 6.42 J m^{-2} to -2.70 J m^{-2}) and 1996 (Lake Mendota -2.32 J m^{-2} to 5.22 J m^{-2}; Fish Lake -2.14 J m^{-2} to 4.77 J m^{-2}; Lake Wingra -2.70 J m^{-2} to 6.20 J m^{-2}) for all three lakes. Abrupt changes in latent heat flux appear to be independent of lake morphometry,

suggesting that the timing of change may be primarily driven by climate. Net heat flux shows no significant abrupt change for Lake Mendota, two changes for Fish Lake (-0.33 J m^{-2} to 4.00 J m^{-2} after 1964, $p<0.01$, and 4.00 J m^{-2} to -0.55 J m^{-2} after 1975, $p<0.01$), and one change for Lake Wingra (-1.15 J m^{-2} to 0.28 J m^{-2} after 1930, $p<0.01$). Differences in magnitude and timing of abrupt changes in shortwave, longwave, and net heat fluxes emphasize that while morphometry may play a role, it is unclear how or what the specific role may be.

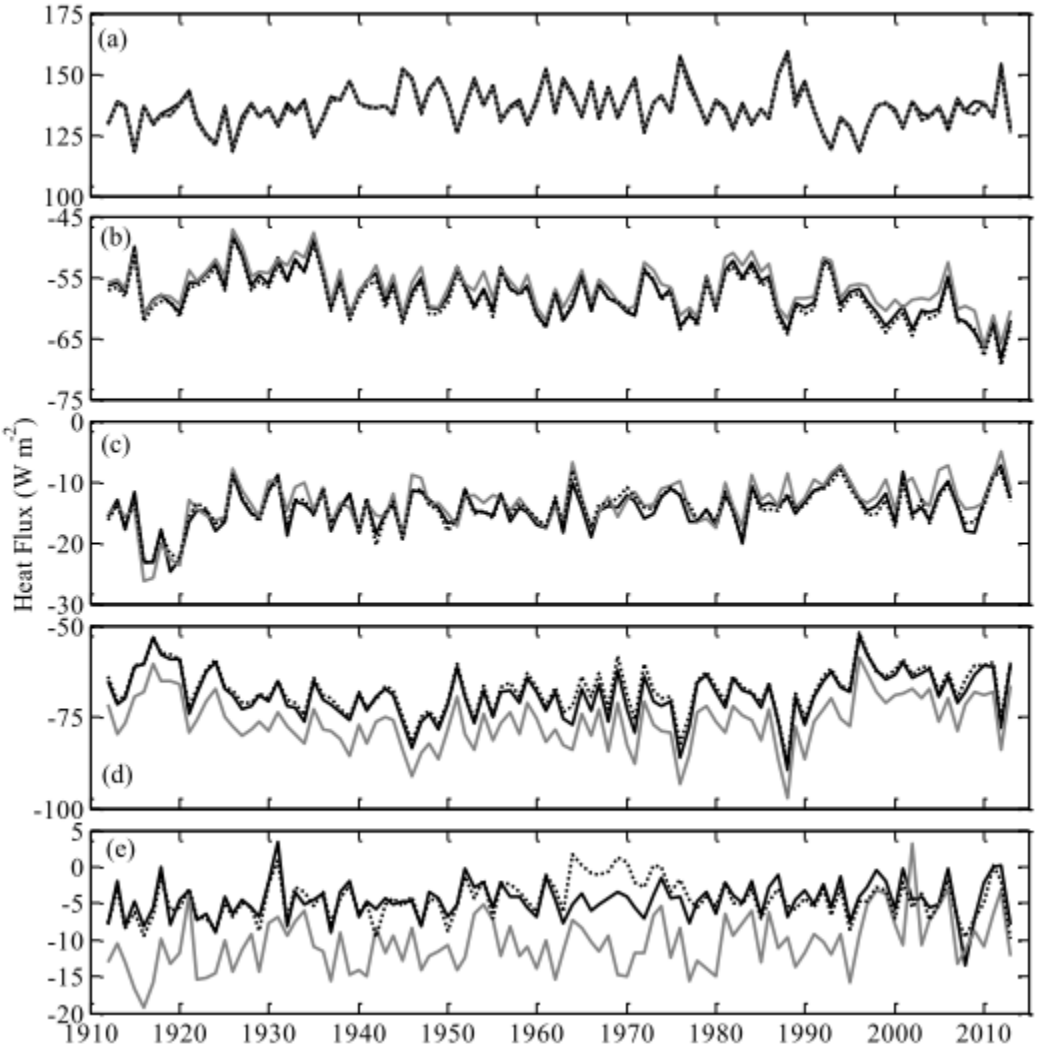

Figure 2-7: Yearly average (a) solar radiation flux, (b) longwave radiative flux, (c) sensible heat flux, (d) latent heat flux, and (e) total heat flux at the lake surface for Lake Mendota (solid black line), Fish Lake (black dashed line) and Lake Wingra (solid grey line). Trends and abrupt changes in heat fluxes are not shown on the plots for clarity.

2.5 Discussion

2.5.1 Model performance and comparison

The DYRESM-WQ-I model reliably simulated long – term water temperatures (Table 2-2, Figure 2-3). Input averaging, particularly daily averaging of air temperature and wind speed, and differences between observed and simulated thermocline depth contribute to deviation between observed and simulated temperatures. In general, thermocline depths were within 1 m between observed and simulated, but some years differ by as much as 2.5 m. Model performance is similar to that of other studies. Perroud et al. (2009) performed a comparison of one-dimensional lake models on Lake Geneva, and RMSE for water temperatures were as high as 2°C for the Hostetler model (Hostetler and Bartlein 1990), 1.7°C for DYRESM (Tanentzap et al. 2007), 2°C for SIMSTRAT, and 4°C for Freshwater Lake (FLake) model (Golosov et al. 2007; Kirillin et al. 2012). For all four models, errors were lower in the upper layers and larger in the bottom of the water column (Perroud et al. 2009), similar to errors found in here (Table 2-2). Fang and Stefan (1996) gave standard errors of water temperature of 1.37°C for the open water season and 1.07°C for the total simulation period for Thrush Lake, MN, which are in the range of those found here for all three lakes. Results of Nash-Sutcliff efficiency coefficients for study lakes were within the ranges found in Yao et al. (2014) for the Simple Lake Model (SIM; Jöhnk et al., 2008), Hostetler (Hostetler and Bartlein 1990), Minlake (Fang and Stefan 1996), and General Lake Model (GLM; Hipsey et al., 2014) models for Harp Lake, Ontario, Canada water temperatures.

Limitations in the model and simulations presented here arise from the assumption of one-dimensionality in both model and field data and from uncertainties in observations and model parameters. Quantifying this type of uncertainty is difficult (Tebaldi et al. 2005; Gal et al.

2014). Simulation results rely on the assumption of one-dimensionality because small, stratified lakes generally lack large horizontal temperature gradients (Imberger and Patterson 1981). However, short-term deviations in water temperature and thermocline depth may exist due to internal wave activity, especially in larger lakes (Tanentzap et al. 2007) and spatial variations in wind stress can produce horizontal variations in temperature profiles (Imberger and Parker 1985). Neither of these are captured in the one-dimensional model approach nor by the collection of observation data at a single in-lake location. Light extinction estimated from Secchi depths can have a large degree of measurement uncertainty (Smith and Hoover 2000), leading to uncertainty in water temperature simulations as light extinction significantly impacts thermal stratification (Hocking and Straškraba 1999). Locations and techniques of meteorological measurements changed at various times throughout the 104-year study period, adding uncertainty to model drivers, although adjustments have been made to minimize this uncertainty. While inflow and outflow measurements were assessed by the USGS for quality assurance and control, uncertainty for both quantity and temperature is unknown, especially in consideration of having to fill in missing data to fully simulate the time period. Effects of inflow uncertainties are likely not large as inflow and outflow are small in comparison to lake volume. Model parameters used to characterize the lake hydrodynamics were taken from literature values. These values are expected to have some small variability between lakes, but previous studies have shown that many of the hydrodynamic parameters are insensitive to changes of ±10% (Tanentzap et al. 2007). In this study, the model was validated against an independent dataset for each lake to determine if the model fits measured data and functions adequately, with errors within the range of those from other studies. As all parameters and observational methods were kept consistent among the three lakes, the validity of the model in predicting temperature differences due to lake

depth and surface area is adequate. We reason that the model accuracy is sufficient to meet the objectives of identifying morphometry-caused differences in lake response for both past and future climate changes.

2.5.2 Coherence among lakes

Adjacent lakes generally respond coherently to climate (Magnuson et al. 1990; Thompson et al. 2005), and lakes with comparable physical features exhibit higher coherence than lakes with different physical properties (Novikmec et al. 2013). Large correlation coefficients, indicative of high temporal coherence between lakes, are largely due to synchronous patterns in lake variables driven by climate (Magnuson et al. 1990; Palmer et al. 2014). In this study, the three lakes were grouped into three distinct pairs to compare the coherence of water temperature and stratification variables. Pair 1, Lake Mendota (deep, large surface area) and Fish Lake (deep, small surface area), illustrates the effects of surface area differences. Pair 2, Lake Wingra (shallow, small surface area) and Fish Lake, addresses the effects of lake depth. Pair 3, Lake Mendota and Lake Wingra, illustrate differences in both morphometry characteristics. Pearson correlation coefficients (Table 2-4) in lake variables were calculated for pairs of the study lakes. This method allows us to easily identify coherence differences that may be driven by lake surface area or lake depth while simultaneously accounting for differences in climate that may impact the results of similar analysis covering lakes over a broad region.

Epilimnetic temperature exhibited high coherence for the three lake pairs (Table 2-4), suggesting that inter-annual variability in epilimnion temperatures was primarily driven by climate drivers such as air temperature and wind speed. Specifically, the Mendota/Wingra pair is highly correlated and Mendota and Wingra differ significantly in both depth and surface area. Furthermore, comparing the Mendota/Fish pair (similar depth) and the Fish/Wingra pair (similar

surface area) suggests that both surface area and depth impact coherence between lake pairs; and surface area differences may drive asynchronous patterns to a greater extent than does depth differences for epilimnetic water temperature. The lower correlation for the Mendota/Fish and Fish/Wingra pairs of lakes may be due to the large change in lake depth from 1966−2001 (Krohelski et al. 2002), compared to the Mendota and Wingra, which have relatively little year – to – year variation in water levels..

Hypolimnion temperature, unlike epilimnion temperature, showed only moderate coherence between Lake Mendota and Fish Lake (Table 2-4), suggesting that inter-annual variability in hypolimnion water temperatures was influenced by factors non – climatological factors, such as lake morphometry. For example, differences in thermocline depth (~10 m in Lake Mendota and ~6 m in Fish Lake) may filter climate signals into the hypolimnion. This result is consistent with other studies that show lake morphometry parameters affect timing of climatic signals, especially for temperature stored in the lake system (Thompson et al. 2005). Strength of stratification and fetch differences may also drive differences in the stratification onset, further affecting hypolimnetic temperatures. Arvola (2009) showed that hypolimnion temperatures were primarily determined by the conditions during the previous spring turnover. In

Table 2-4: Correlation coefficients for temperature and stratification variables grouped by lake pairs

	Lake Pair		
Lake Variable	**Mendota/Fish**	**Wingra/Fish**	**Mendota/Wingra**
Epilimnion Temperature	0.605	0.742	0.804
Hypolimnion Temperature	0.482	N/A	N/A
Stratification Onset	0.260	N/A	N/A
Fall Overturn	0.388	N/A	N/A
Schmidt Stability Number	0.761	0.405	0.346

our study, the relatively low hypolimnetic coherence (Table 2-4) suggests that lake morphometry plays a role in hypolimnion temperatures.

Coherence for stratification onset and fall overturn dates were low for the Mendota/Fish lake pair (Table 2-4), suggesting that surface area influences differences in stratification onset and overturn. Schmidt stability showed high coherence for the Mendota/Fish lake pair, but low coherence between the Wingra/Fish and Mendota/Wingra lake pairs, suggesting that lakes of differing depth have asynchronous behavior, but that climate is the main factor in stability when comparing lakes of similar depth.

2.5.3 Sensitivity to changes in air temperature and wind speed

We perturbed air temperatures from -10°C to +10°C in 1°C increments and wind speeds from 70% to 130% of the historical value in 5% increments, respectively, to determine sensitivity of lake water temperature and stratification to both drivers. For each scenario, meteorological inputs remained the same as in the original simulation, but snowfall (rainfall) was converted if the air temperature scenarios increased (decreased) above 0°C. Similarly, the water balance is maintained so that the long-term water levels in both lakes matches the historical record. Results of lake response to all perturbation scenarios will be discussed in the following.

2.5.3.1 Stratification onset

Increasing (decreasing) air temperature resulted in earlier (later) stratification onset in both lakes (Figure 2-8 a and b). Lake Mendota exhibited a linear trend of 2.0 days earlier (later) stratification for each degree (°C) increase (decrease) in air temperature, but Fish Lake has a nonlinear change in stratification onset with a 1°C increase causing 1.5 days earlier stratification and 1°C decrease causing 2.7 days later stratification. Standard deviations in Lake Mendota onset

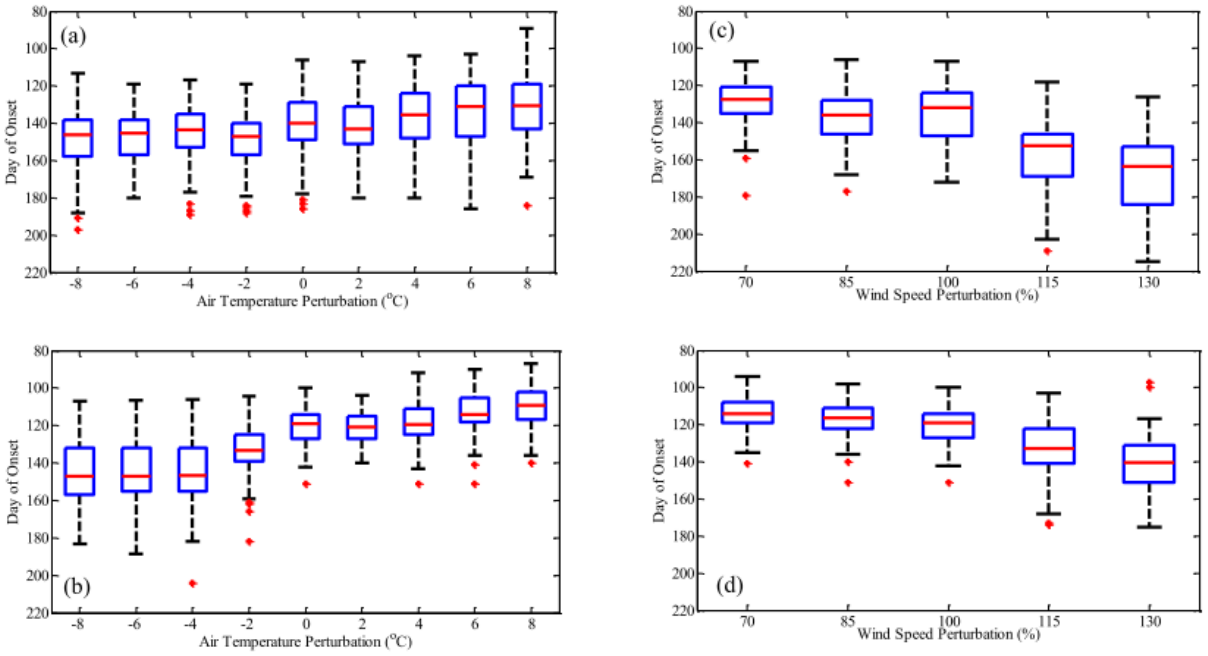

Figure 2-8: Day of stratification onset under select air temperature perturbation scenarios for (a) Lake Mendota and (b) Fish Lake and day of stratification onset under select wind speed perturbation scenarios for (c) Lake Mendota and (d) Fish Lake. Boxes represent the 25th and 75th quartiles and the central lines are median values. The whiskers extend to the minimum and maximum data point in cases where there are no outliers, which are plotted individually.

remained fairly consistent, ranging from 15.5 to 18 days. In contrast, the standard deviation for Fish Lake onset decreased from 17.5 days to 12 days as air temperature increased. This may be due to an early limit in stratification onset for Fish Lake, reducing the variability of onset dates with increasing air temperatures. These results suggest that lake surface area can complicate the response of stratification onset to changes in air temperatures.

For both Lake Mendota and Fish Lake (Figure 2-8 c and d), decreased (increased) wind speed results in earlier (later) stratification onset, however the change is nonlinear. For Lake Mendota each 1m s^{-1} decrease in wind speed results in 3.4 days earlier stratification onset and each 1m s^{-1} increase in wind speed results in 10.5 days later stratification onset; meanwhile, Fish Lake shows 3.6 days earlier stratification onset for each 1m s^{-1} decrease in wind speed and 8.1 days later stratification onset for each 1m s^{-1} increase in wind speed. Standard deviations in both

lakes see large decreases (increases) with decreasing (increasing) wind speed. For Lake Mendota, standard deviation changes from 20 days at 130 % of historical wind speed to 12 days at 70% of historical wind speed, and for Fish Lake standard deviation changes from 15.6 days at 130 % of historical wind speed to 8.7 days at 70 % of historical wind speed. As wind speed decreases (increases), the likelihood of the wind-induced kinetic energy being sufficient to mix the lake also decreases (increases). Additionally, the number of higher wind events is decreased (increased) under this scenario, leading to less (more) kinetic energy available to mix the lake later (earlier) in the season. The change in stratification onset date for both lakes is nonlinear, but Lake Mendota experiences a greater difference between decreasing and increasing wind speeds due to the large surface area of the lake increasing the nonlinear response of thermal structure to wind speed changes. Additionally, standard deviations are much larger for Lake Mendota because the large fetch of the lake causes greater variability in wind stress than for the smaller Fish Lake.

2.5.3.2 Stratification overturn

Air temperature increases (decreases) result in a linear change in stratification overturn of 0.68 days later (earlier) for 1°C increase (decrease) in air temperature for Lake Mendota (Figure 2-9 a). The change in Fish Lake (Figure 2-9 b) is nonlinear: stratification overturn is 1.81 days later for a 1°C increase in air temperature, but 0.77 days earlier for air temperature decreases of 1°C. Standard deviation for Lake Mendota decreased from 14 days to 11 days over the ±10°C perturbation range, and Fish Lake had a consistent standard deviation of 13 days (±0.75 days). Results imply that air temperature changes have a limited impact on the variability of the stratification overturn dates, and a larger impact on the average date of stratification overturn.

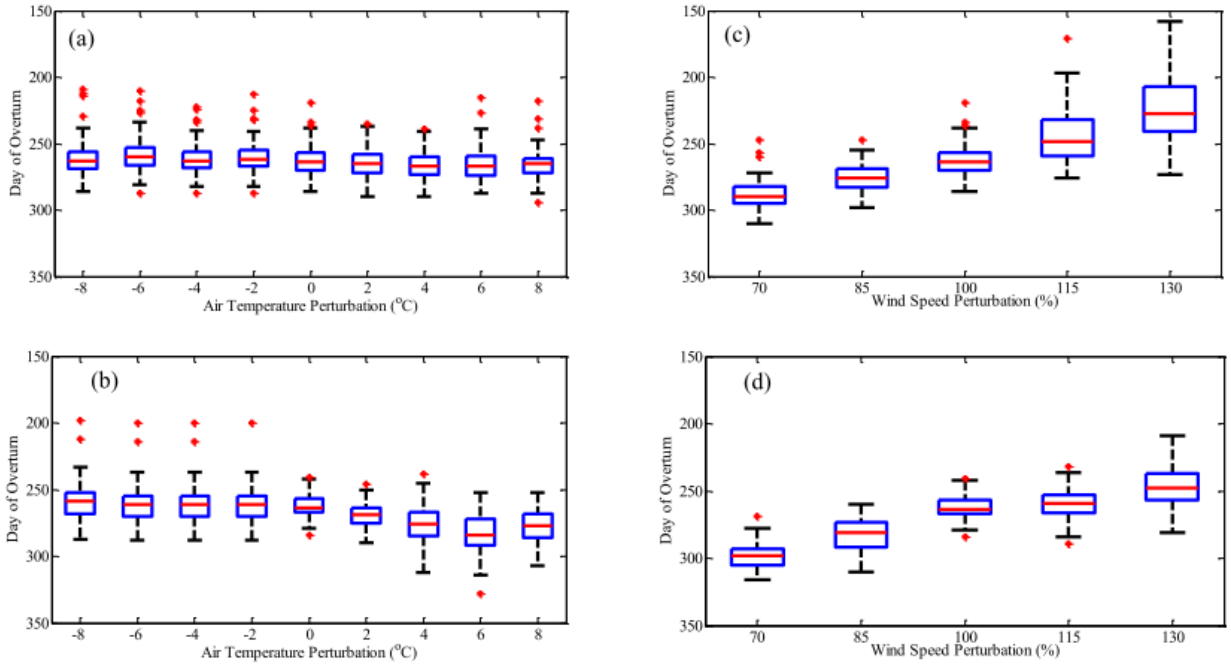

Figure 2-9: Day of stratification overturn under select air temperature perturbation scenarios for (a) Lake Mendota and (b) Fish Lake and day of stratification onset under select wind speed perturbation scenarios for (c) Lake Mendota and (d) Fish Lake. Boxes represent the 25th and 75th quartiles and the central lines are median values. The whiskers extend to the minimum and maximum data point in cases where there are no outliers, which are plotted individually.

For wind speed perturbations, both lakes show a nonlinear change for later (earlier) stratification overturn with decreases (increases) in wind speed. For Lake Mendota (Figure 2-9 c), decreases in wind speed cause a change of 13.9 days later with each 1 m s^{-1} decrease in wind speed and a change of 17.1 days earlier with each 1 m s^{-1} increase in wind speed. For Fish Lake (Figure 2-9 d), decreases in wind speed cause a change of 16.4 days later with each 1 m s^{-1} decrease in wind speed and a change of 8.5 days earlier with each 1 m s^{-1} increase in wind speed. This result suggests that stratification overturn dates are more sensitive to wind speed decrease in lakes with large surface areas. As with stratification onset, decreasing (increasing) wind speeds decrease (increase) variability in overturn dates (27.6 to 10.6 days for Lake Mendota and 15.1 to 9.2 for Fish Lake).

2.5.3.3 Hypolimnetic water temperature

For Lake Mendota (Figure 2-10 a), a 1°C increase (decrease) in air temperature resulted in a linear change of 0.18°C increase (decrease) in hypolimnetic temperature. For Fish Lake (Figure 2-10 b), a 1°C increase in air temperature yielded a hypolimnion temperature increase of 0.25°C, and a 1°C decrease in air temperature resulted in a hypolimnion temperature decrease of 0.18°C. Standard deviations for Lake Mendota and Fish Lake remain consistent with increasing (decreasing) temperature and range from approximately 2.3°C to 2.7°C for Lake Mendota and from 1.7°C to 2.2°C for Fish Lake. Air temperature changes alter mean hypolimnetic temperatures, but do not affect hypolimnetic temperature variability.

For wind speed, hypolimnion temperature changes are non – linear for both lakes. In Lake Mendota (Figure 2-10 c) decreasing wind speed decreases hypolimnion temperature at a rate of 1.1°C for each m s^{-1} decrease in wind speed and increasing wind speed increases hypolimnion temperature at a rate of 1.8°C for each m s^{-1} increase in wind speed. For Fish Lake (Figure 2-10 d), decreasing wind speed yields a 1.2°C decrease in hypolimnion temperature for each m s^{-1} decrease in wind speed and increasing wind speed yields a 0.8°C increase in hypolimnion temperature for each m s^{-1} increase in wind speed. Standard deviation in Lake Mendota decreased (increased) with decreasing (increasing) wind speeds, changing from 2.6°C at 130 % of historical wind speed to 1.8 °C at 70 % of historical wind speeds, but standard deviation in Fish Lake were constant over the perturbation scenarios, ranging from 1.3°C to 1.6°C. This indicates that wind speed changes have a much larger impact on the variability of hypolimnetic temperatures for the larger surface area lake than for smaller surface area lake. Overall, the increasing temperature perturbations show increasing hypolimnetic water temperature, while decreasing wind speed perturbations show decreasing hypolimnetic water

temperatures. Simulation results (Figure 2-10 d and e) indicate that hypolimnetic temperatures decreased in both study lakes during the historical period. Combining the effects of air temperature and wind speed suggest that wind speed decreases are a larger driver to hypolimnetic water temperature changes than increasing air temperatures for both lakes. For example, in Lake Mendota, a 5% decrease in wind speed will offset the impacts to hypolimnetic temperature of a 1°C increase in air temperature, while in Fish Lake, a 12-13% decrease in wind speed is necessary to offset the effects of a 1°C increase in air temperature. In other words, lakes with larger surface areas that also experience decreasing wind speeds may be more resilient to changing hypolimnion temperatures as a result of warmer air temperatures.

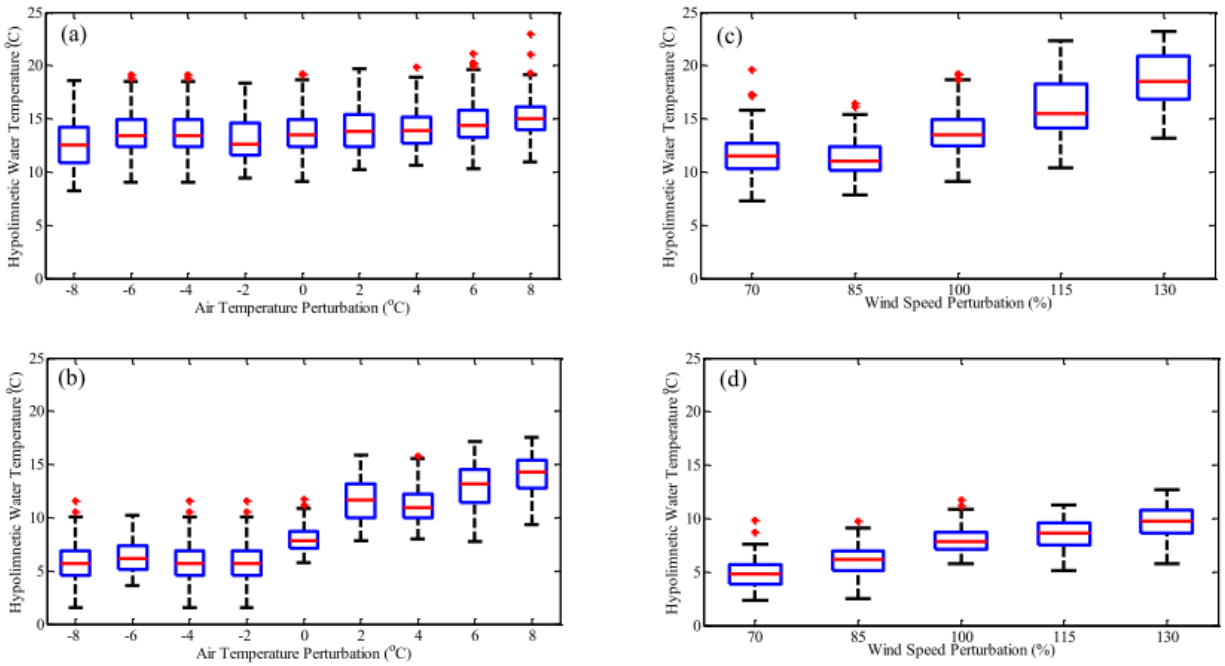

Figure 2-10: Hypolimnetic water temperatures under select air temperature perturbation scenarios for (a) Lake Mendota and (b) Fish Lake and day of stratification onset under select wind speed perturbation scenarios for (c) Lake Mendota and (d) Fish Lake. Boxes represent the 25th and 75th quartiles and the central lines are median values. The whiskers extend to the minimum and maximum data point in cases where there are no outliers, which are plotted individually.

2.5.4 Role of morphometry on water temperature and stratification

2.5.4.1 Lake depth

Lakes with different depths (e.g., Lake Wingra and Fish Lake) responded differently to climate change. In this study, Lake Wingra, the shallowest of the three, did not stratify, while the deeper lakes, Lake Mendota and Fish Lake, did. Results show increased Schmidt Stability over the long term for Fish Lake and Lake Mendota (Table 2-3), but no trend in Lake Wingra. Indeed, Kraemer et al. (2015) showed that mean lake depths explain the largest amount of variation in stratification trends and lakes with greater mean depths have larger changes in their stability, consistent with our results for Lake Mendota and Fish Lake (Table 2-3). Due to lower heat capacity, shallow lakes respond more directly to short-term variations in the weather (Arvola et al. 2009), and heat can be transferred easily throughout the water column by wind mixing (Nõges et al. 2011). Deep lakes have a higher heat capacity so greater wind speeds are required to completely mix the lake during the summer months, resulting in more temperature stability and higher Schmidt stability values for deeper Lake Mendota and Fish Lake. For radiative fluxes at the surface of the lake, shallow Lake Wingra had a similar magnitude of shortwave, longwave, and sensible heat fluxes as Lake Mendota and Fish Lake, but relatively larger magnitude of latent and net heat fluxes. This result indicates that lake depth may play a large role in the magnitude of latent heat fluxes and amount of evaporation amount due to the overall warmer temperatures throughout the water column compared to lakes that stratify. Additionally, the magnitude of abrupt changes in sensible heat flux appear to be influenced by water depth, with increasing depth decreasing the magnitude of shift in mean sensible heat flux after the abrupt change.

2.5.4.2 Surface area

Lake size can influence the response of epilimnetic temperatures to increases in air temperature and decreases in wind speed. Air temperature is a main driver of epilimnetic water temperatures (Boehrer and Schultze 2008; Palmer et al. 2014), and increasing air temperatures increase epilimnion temperatures (Robertson and Ragotzkie 1990; Livingstone 2003). However, wind mixing, a more dominant mechanism of heat transfer (Nõges et al. 2011), can act to dampen the effects of air temperature increase and cool the epilimnion through increased surface mixed-layer deepening. As a result, decreasing wind speeds cause an additional increase in epilimnion temperatures (Table 2-3; Figure 2-4). Nevertheless, larger fetch also increases mixing and vertical transfer of heat to bottom waters, reducing epilimnion temperatures (Boehrer and Schultze 2008) and increasing the rate of lake cooling (Nõges et al. 2011). For this reason, Lake Mendota, with a larger surface area, experiences a smaller increase in epilimnetic temperature than Fish Lake (Table 2-3). Trend and variability of Schmidt stability may also be affected by lake size. Compared with Fish Lake, Lake Mendota experiences greater variability in Schmidt stability and a larger trend in long – term changes when compared to Fish Lake (Figure 2-6).

Sensitivity results indicate that lake surface area influences the nonlinear response and variability of stratification onset, stratification overturn, and hypolimnetic temperatures to wind speed perturbations. The magnitude of the nonlinear changes and changes in variability are larger for Lake Mendota than Fish Lake. The larger surface area for Lake Mendota results in greater wind stress on the water surface, increasing the variability and non – linearity of response. Larger wind speeds produce more variability in wind stress on lakes with large fetch, so the resulting change in turbulence is also highly variable. Results of this study indicate that lakes with larger surface areas will have a more nonlinear response to changes in wind speed than

lakes with smaller surface areas for stratification onset (Figure 2-8), fall overturn (Figure 2-9), and hypolimnetic water temperature (Figure 2-10).

2.5 Conclusion

Study results show that in three different lakes, the combination of increasing air temperature and decreasing wind speeds prompt a warmer epilimnion, colder hypolimnion, earlier stratification onset, later stratification overturn, longer stratification duration, less hypolimnetic heating, and greater stability. Longer stratification and greater stability may have lasting impacts on fish populations (Gunn 2002; Sharma et al. 2011; Jiang et al. 2012) and warmer epilimnion temperatures affect the phytoplankton community (Francis et al. 2014; Rice et al. 2015). Historical analysis indicates that smaller surface area promotes less wind mixing while larger and deeper lakes respond more readily to changes in climate. Stability differences between the larger Lake Mendota and smaller Fish Lake suggest that larger surface areas promote more variability in lake stability. Climate perturbations support these historical results and provide additional insight on the individual and combined effects of air temperature and wind speed changes. Increasing air temperature and decreasing wind speeds have a doubling effect toward longer stratification duration. Wind speed plays a larger role in stratification onset and overturn and hypolimnetic temperatures, indicating that air temperature increases are not the only climate variable that managers should consider when developing mitigation and adaptation techniques. Previous research has shown differences in the directionality of hypolimnion temperature changes, but perturbation scenarios here indicate that increasing hypolimnion temperatures may be primarily determined by local increases or decreases in wind speed.

2.6 Acknowledgements

The authors specifically acknowledge Yi-Fang Hsieh for further developing an ice module into the DYRESM-WQ model that was provided by David Hamilton. We would like to thank Dale Robertson at Wisconsin USGS and Richard (Dick) Lathrop at Center of Limology for providing valuable long-term observation data for the three study lakes. In addition, we thank John Magnuson at Center of Limnology for his insightful suggestions and valuable comments regarding climate change on ice. Research funding was provided in part by the U.S. National Science Foundation Long-Term Ecological Research Program, University of Wisconsin (UW) Water Resources Institute USGS 104(B) Research Project, and UW Office of Sustainability SIRE Award Program. In addition, funding support for the first author by the College of Engineering Grainer Wisconsin Distinguished Graduate Fellowship is acknowledged.

2.7 References

Adrian, R., C. M. O'Reilly, H. Zagarese, and others. 2009. Lakes as sentinels of climate change. Limnol. Oceanogr. **54**: 2283–2297.

Antenucci, J., and A. Imerito. 2003. The CWR dynamic reservoir simulation model DYRESM. Centre for Water Research: The University of Western Australia.

Arvola, L., G. George, D. M. Livingstone, and others. 2009. The Impact of the Changing Climate on the Thermal Characteristics of Lakes, p. 85–101. *In* G. George [ed.], The Impact of Climate Change on European Lakes. Springer Netherlands.

Austin, J. A., and S. M. Colman. 2007. Lake Superior summer water temperatures are increasing more rapidly than regional air temperatures: A positive ice-albedo feedback. Geophys. Res. Lett. **34**: L06604. doi:10.1029/2006GL029021

Baron, J., and N. Caine. 2000. Temporal coherence of two alpine lake basins of the Colorado Front Range, U.S.A. Freshw. Biol. **43**: 463–476. doi:10.1046/j.1365-2427.2000.00517.x

Boehrer, B., and M. Schultze. 2008. Stratification of lakes. Rev. Geophys. **46**. doi:10.1029/2006RG000210

Breslow, P. B., and D. J. Sailor. 2002. Vulnerability of wind power resources to climate change in the continental United States. Renew. Energy **27**: 585–598. doi:10.1016/S0960-1481(01)00110-0

Bueche, T., and M. Vetter. 2014. Future alterations of thermal characteristics in a medium-sized lake simulated by coupling a regional climate model with a lake model. Clim. Dyn. **44**: 371–384. doi:10.1007/s00382-014-2259-5

Butcher, J. B., D. Nover, T. E. Johnson, and C. M. Clark. 2015. Sensitivity of lake thermal and mixing dynamics to climate change. Clim. Change **129**: 295–305. doi:10.1007/s10584-015-1326-1

Desai, A. R., J. A. Austin, V. Bennington, and G. A. McKinley. 2009. Stronger winds over a large lake in response to weakening air-to-lake temperature gradient. Nat. Geosci. **2**: 855–858. doi:10.1038/ngeo693

Dobiesz, N. E., and N. P. Lester. 2009. Changes in mid-summer water temperature and clarity across the Great Lakes between 1968 and 2002. J. Gt. Lakes Res. **35**: 371–384. doi:10.1016/j.jglr.2009.05.002

Fang, X., and H. G. Stefan. 1996. Long-term lake water temperature and ice cover simulations/measurements. Cold Reg. Sci. Technol. **24**: 289–304. doi:10.1016/0165-232X(95)00019-8

Francis, T. B., E. M. Wolkovich, M. D. Scheuerell, S. L. Katz, E. E. Holmes, and S. E. Hampton. 2014. Shifting Regimes and Changing Interactions in the Lake Washington, U.S.A., Plankton Community from 1962–1994. PLoS ONE **9**: e110363. doi:10.1371/journal.pone.0110363

Gal, G., V. Makler-Pick, and N. Shachar. 2014. Dealing with uncertainty in ecosystem model scenarios: Application of the single-model ensemble approach. Environ. Model. Softw. **61**: 360–370. doi:10.1016/j.envsoft.2014.05.015

Golosov, S., O. A. Maher, E. Schipunova, A. Terzhevik, G. Zdorovennova, and G. Kirillin. 2007. Physical background of the development of oxygen depletion in ice-covered lakes. Oecologia **151**: 331–340. doi:10.1007/s00442-006-0543-8

Gunn, J. M. 2002. Impact of the 1998 El Niño event on a Lake Charr, Salvelinus Namaycush, Population Recovering from Acidification. Environ. Biol. Fishes **64**: 343–351. doi:10.1023/A:1016058606770

Hamilton, D. P., and S. G. Schladow. 1997. Prediction of water quality in lakes and reservoirs. Part I — Model description. Ecol. Model. **96**: 91–110. doi:10.1016/S0304-3800(96)00062-2

Hill, J. M., and A. Kucera. 1983. Freezing a saturated liquid inside a sphere. Int. J. Heat Mass Transf. **26**: 1631–1637. doi:10.1016/S0017-9310(83)80083-0

Hipsey, M. R., L. C. Bruce, and D. P. Hamilton. 2014. GLM - General Lake Model: Model overview and user information. AED Report #26. AED Report #26 The University of Western Perth.

Hocking, G. C., and M. Straškraba. 1999. The Effect of Light Extinction on Thermal Stratification in Reservoirs and Lakes. Int. Rev. Hydrobiol. **84**: 535–556. doi:10.1002/iroh.199900046

Hostetler, S. W., and P. J. Bartlein. 1990. Simulation of lake evaporation with application to modeling lake level variations of Harney-Malheur Lake, Oregon. Water Resour. Res. **26**: 2603–2612. doi:10.1029/WR026i010p02603

Idso, S. B. 1973. On the concept of lake stability. Limnol. Oceanogr. **18**: 681–683.

Imberger, J., I. Loh, B. Hebbert, and J. Patterson. 1978. Dynamics of Reservoir of Medium Size. J. Hydraul. Div. **104**: 725–743.

Imberger, J., and G. Parker. 1985. Mixed layer dynamics in a lake exposed to a spatially variable wind field. Limnol. Oceanogr. **30**: 473–488.

Imberger, J., and J. C. Patterson. 1981. Dynamic reservoir simulation model - DYRESM: 5, p. 310–361. *In* H.B. Fischer [ed.], Transport Models for Inland and Coastal Waters. Academic Press.

IPCC. 2013. Summary for Policymakers, p. 3–29. *In* T. Stocker, D. Qin, G.-K. Plattner, et al. [eds.], Climate Change 2013: The Physical Science Basis. Contribution of Working Group I to the Fifth Assessment Report of the Intergovernmental Panel on Climate Change. Cambridge University Press.

Jiang, L., X. Fang, H. G. Stefan, P. C. Jacobson, and D. L. Pereira. 2012. Oxythermal habitat parameters and identifying cisco refuge lakes in Minnesota under future climate scenarios using variable benchmark periods. Ecol. Model. **232**: 14–27. doi:10.1016/j.ecolmodel.2012.02.014

Jöhnk, K. D., J. Huisman, J. Sharples, B. Sommeijer, P. M. Visser, and J. M. Stroom. 2008. Summer heatwaves promote blooms of harmful cyanobacteria. Glob. Change Biol. **14**: 495–512. doi:10.1111/j.1365-2486.2007.01510.x

Kerimoglu, O., and K. Rinke. 2013. Stratification dynamics in a shallow reservoir under different hydro-meteorological scenarios and operational strategies. Water Resour. Res. **49**: 7518–7527. doi:10.1002/2013WR013520

Kirillin, G. 2010. Modeling the impact of global warming on water temperature and seasonal mixing regimes in small temperate lakes. Boreal Environ. Res. **15**: 279–293.

Kirillin, G., M. Leppäranta, A. Terzhevik, and others. 2012. Physics of seasonally ice-covered lakes: a review. Aquat. Sci. **74**: 659–682. doi:10.1007/s00027-012-0279-y

Klink, K. 2002. Trends and Interannual Variability of Wind Speed Distributions in Minnesota. J. Clim. **15**: 3311–3317. doi:10.1175/1520-0442(2002)015<3311:TAIVOW>2.0.CO;2

Kraemer, B. M., O. Anneville, S. Chandra, and others. 2015. Morphometry and average temperature affect lake stratification responses to climate change: LAKE STRATIFICATION RESPONSES TO CLIMATE. Geophys. Res. Lett. **42**: 4981–4988. doi:10.1002/2015GL064097

Krohelski, J. T., Y.-F. Lin, W. J. Rose, and R. J. Hunt. 2002. Simulation of Fish, Mud, and Crystal Lakes and the shallow ground-water system, Dane County, Wisconsin. USGS Numbered Series 2002–4014. 2002–4014 U.S. Geological Survey.

Kucharik, C. J., S. P. Serbin, S. Vavrus, E. J. Hopkins, and M. M. Motew. 2010. Patterns of Climate Change Across Wisconsin From 1950 to 2006. Phys. Geogr. **31**: 1–28. doi:10.2747/0272-3646.31.1.1

Lathrop, R. C., S. R. Carpenter, and L. G. Rudstam. 1996. Water clarity in Lake Mendota since 1900: responses to differing levels of nutrients and herbivory. Can. J. Fish. Aquat. Sci. **53**: 2250–2261. doi:10.1139/f96-187

Livingstone, D. M. 2003. Impact of Secular Climate Change on the Thermal Structure of a Large Temperate Central European Lake. Clim. Change **57**: 205–225. doi:10.1023/A:1022119503144

Lynch, A. J., W. W. Taylor, T. D. Beard Jr., and B. M. Lofgren. 2015. Climate change projections for lake whitefish (Coregonus clupeaformis) recruitment in the 1836 Treaty Waters of the Upper Great Lakes. J. Gt. Lakes Res. **41**: 415–422. doi:10.1016/j.jglr.2015.03.015

MacIntyre, S., and J. M. Melack. 2010. Mixing dynamics in lakes across climatic zones, p. 86–95. *In* G.E. Likens [ed.], Lake Ecosystem Ecology: A Global Perspective. Academic Press.

MacKay, M. D., P. J. Neale, C. D. Arp, and others. 2009. Modeling lakes and reservoirs in the climate system. Limnol. Oceanogr. **54**: 2315–2329. doi:10.4319/lo.2009.54.6_part_2.2315

Magee, M. R., C. H. Wu, D. M. Robertson, R. C. Lathrop, and D. P. Hamilton. 2016. Trends and abrupt changes in 104 years of ice cover and water temperature in a dimictic lake in response to air temperature, wind speed, and water clarity drivers. Hydrol Earth Syst Sci **20**: 1681–1702. doi:10.5194/hess-20-1681-2016

Magnuson, J. J., B. J. Benson, and T. K. Kratz. 1990. Temporal coherence in the limnology of a suite of lakes in Wisconsin, U.S.A. Freshw. Biol. **23**: 145–159. doi:10.1111/j.1365-2427.1990.tb00259.x

Mantyka-Pringle, C. S., T. G. Martin, D. B. Moffatt, S. Linke, and J. R. Rhodes. 2014. Understanding and predicting the combined effects of climate change and land-use

change on freshwater macroinvertebrates and fish. J. Appl. Ecol. **51**: 572–581. doi:10.1111/1365-2664.12236

McKee, T. B., N. J. Doesken, C. A. Davey, and Pielke, Sr. 2000. Climate data continuity with ASOS. Report for period April 1996 through June 2000. Climno Report 00-3. Climno Report 00-3 Colorado Climate Center, Department of Atmospheric Science, Colorado State University.

Meehl, G. A., and C. Tebaldi. 2004. More Intense, More Frequent, and Longer Lasting Heat Waves in the 21st Century. Science **305**: 994–997. doi:10.1126/science.1098704

Nõges, P., T. Nõges, M. Ghiani, B. Paracchini, J. Pinto Grande, and F. Sena. 2011. Morphometry and trophic state modify the thermal response of lakes to meteorological forcing. Hydrobiologia **667**: 241–254. doi:10.1007/s10750-011-0691-7

Novikmec, M., M. Svitok, D. Kočický, F. Šporka, and P. Bitušík. 2013. Surface Water Temperature and Ice Cover of Tatra Mountains Lakes Depend on Altitude, Topographic Shading, and Bathymetry. Arct. Antarct. Alp. Res. **45**: 77–87. doi:10.1657/1938-4246-45.1.77

NTL LTER. 2012a. North Temperature Lakes LTER: Physical Limnology of Primary Study Lakes 1981-current.

NTL LTER. 2012b. North Temperate Lakes LTER: Snow and Ice Depth 1982 - current.

Paerl, H. W., and V. J. Paul. 2012. Climate change: Links to global expansion of harmful cyanobacteria. Water Res. **46**: 1349–1363. doi:10.1016/j.watres.2011.08.002

Palmer, M. E., N. D. Yan, and K. M. Somers. 2014. Climate change drives coherent trends in physics and oxygen content in North American lakes. Clim. Change **124**: 285–299. doi:10.1007/s10584-014-1085-4

Patterson, J. C., and P. F. Hamblin. 1988. Thermal simulation of a lake with winter ice cover. Limnol. Oceanogr. **33**: 323–338. doi:10.4319/lo.1988.33.3.0323

Perroud, M., S. Goyette, A. Martynov, M. Beniston, and O. Anneville. 2009. Simulation of multiannual thermal profiles in deep Lake Geneva: A comparison of one-dimensional lake models. Limnol. Oceanogr.-Methods **54**: 1574–1594.

Pryor, S. C., R. J. Barthelmie, and E. Kjellström. 2005. Potential climate change impact on wind energy resources in northern Europe: analyses using a regional climate model. Clim. Dyn. **25**: 815–835. doi:10.1007/s00382-005-0072-x

Read, J. S., D. P. Hamilton, A. R. Desai, and others. 2012. Lake-size dependency of wind shear and convection as controls on gas exchange. Geophys. Res. Lett. **39**: L09405. doi:10.1029/2012GL051886

Read, J. S., D. P. Hamilton, I. D. Jones, K. Muraoka, L. A. Winslow, R. Kroiss, C. H. Wu, and E. Gaiser. 2011. Derivation of lake mixing and stratification indices from high-resolution lake buoy data. Environ. Model. Softw. **26**: 1325–1336. doi:10.1016/j.envsoft.2011.05.006

Rempfer, J., D. M. Livingstone, C. Blodau, R. Forster, P. Niederhauser, and R. Kipfer. 2010. The effect of the exceptionally mild European winter of 2006-2007 on temperature and oxygen profiles in lakes in Switzerland: A foretaste of the future? Limnol. Oceanogr. **55**: 2170–2180. doi:10.4319/lo.2010.55.5.2170

Rice, E., H. G. Dam, and G. Stewart. 2015. Impact of Climate Change on Estuarine Zooplankton: Surface Water Warming in Long Island Sound Is Associated with Changes in Copepod Size and Community Structure. Estuaries Coasts **38**: 13–23. doi:10.1007/s12237-014-9770-0

Robertson, D. M. 1989. The use of lake water temperature and ice cover as climatic indicators. PhD Thesis. University of Wisconsin-Madison.

Robertson, D. M., and R. A. Ragotzkie. 1990. Changes in the thermal structure of moderate to large sized lakes in response to changes in air temperature. Aquat. Sci. **52**: 360–380. doi:10.1007/BF00879763

Rodionov, S. N. 2004. A sequential algorithm for testing climate regime shifts. Geophys. Res. Lett. **31**. doi:10.1029/2004GL019448

Rodionov, S., and J. E. Overland. 2005. Application of a sequential regime shift detection method to the Bering Sea ecosystem. ICES J. Mar. Sci. J. Cons. **62**: 328–332. doi:10.1016/j.icesjms.2005.01.013

Rogers, C. K., G. A. Lawrence, and P. F. Hamblin. 1995. Observations and numerical simulation of a shallow ice-covered midlatitude lake. Limnol. Oceanogr. **40**: 374–385. doi:10.4319/lo.1995.40.2.0374

Rueda, F., and G. Schladow. 2009. Mixing and stratification in lakes of varying horizontal length scales: Scaling arguments and energy partitioning. Limnol. Oceanogr. **54**: 2003–2017. doi:10.4319/lo.2009.54.6.2003

Schindler, D. W., K. G. Beaty, E. J. Fee, and others. 1990. Effects of climatic warming on lakes of the central boreal forest. Science **250**: 967–970. doi:10.1126/science.250.4983.967

Sharma, S., M. J. Vander Zanden, J. J. Magnuson, and J. Lyons. 2011. Comparing Climate Change and Species Invasions as Drivers of Coldwater Fish Population Extirpations H. Browman [ed.]. PLoS ONE **6**: e22906. doi:10.1371/journal.pone.0022906

Sherman, F. S., J. Imberger, and G. M. Corcos. 1978. Turbulence and Mixing in Stably Stratified Waters. Annu. Rev. Fluid Mech. **10**: 267–288. doi:10.1146/annurev.fl.10.010178.001411

Shimoda, Y., M. E. Azim, G. Perhar, M. Ramin, M. A. Kenney, S. Sadraddini, A. Gudimov, and G. B. Arhonditsis. 2011. Our current understanding of lake ecosystem response to climate change: What have we really learned from the north temperate deep lakes? J. Gt. Lakes Res. **37**: 173–193. doi:10.1016/j.jglr.2010.10.004

Smith, D. G., and M. Hoover. 2000. Standardization of Secchi disk measurements, including use of a viewer box. *Proceedings of the 2000 National Water Quality Monitoring Conference*.

Stefan, H. G., M. Hondzo, X. Fang, J. G. Eaton, and J. H. McCormick. 1996. Simulated long term temperature and dissolved oxygen characteristics of lakes in the north-central United States and associated fish habitat limits. Limnol. Oceanogr. **41**: 1124–1135. doi:10.4319/lo.1996.41.5.1124

Tanentzap, A. J., D. P. Hamilton, and N. D. Yan. 2007. Calibrating the Dynamic Reservoir Simulation Model (DYRESM) and filling required data gaps for one-dimensional thermal profile predictions in a boreal lake. Limnol. Oceanogr. Methods **5**: 484–494. doi:10.4319/lom.2007.5.484

Tebaldi, C., R. L. Smith, D. Nychka, and L. O. Mearns. 2005. Quantifying Uncertainty in Projections of Regional Climate Change: A Bayesian Approach to the Analysis of Multimodel Ensembles. J. Clim. **18**: 1524–1540. doi:10.1175/JCLI3363.1

Thomas, C. D., A. Cameron, R. E. Green, and others. 2004. Extinction risk from climate change. Nature **427**: 145–148. doi:10.1038/nature02121

Thompson, R., C. Kamenik, and R. Schmidt. 2005. Ultra-sensitive Alpine lakes and climate change. J. Limnol. **64**: 139–152.

Verburg, P., and R. E. Hecky. 2009. The physics of the warming of Lake Tanganyika by climate change. Limnol. Oceanogr. **54**: 2418–2430.

Voutilainen, A., T. Huttula, J. Juntunen, M. Rahkola-Sorsa, K. Rasmus, and M. Viljanen. 2014. Diverging site-specific trends in the water temperature of a large boreal lake in winter and summer due to mixed effects of local features and climate change. Boreal Environ. Res. **19**: 104–114.

Weinberger, S., and M. Vetter. 2012. Using the hydrodynamic model DYRESM based on results of a regional climate model to estimate water temperature changes at Lake Ammersee. Ecol. Model. **244**: 38–48. doi:10.1016/j.ecolmodel.2012.06.016

Williams, D. T., G. R. Drummond, D. E. Ford, and D. L. Robey. 1980. Determination of light extinction coefficients in lakes and reservoirs. *Proceedings of the Symposium on Surface Water Impoundments*. Proceedings of the Symposium on Surface Water Impoundments. 1329–1335.

Winslow, L. A., J. S. Read, G. J. A. Hansen, and P. C. Hanson. 2015. Small lakes show muted climate change signal in deepwater temperatures. Geophys. Res. Lett. **42**: 2014GL062325. doi:10.1002/2014GL062325

Yao, H., N. R. Samal, K. D. Joehnk, X. Fang, L. C. Bruce, D. C. Pierson, J. A. Rusak, and A. James. 2014. Comparing ice and temperature simulations by four dynamic lake models in Harp Lake: past performance and future predictions. Hydrol. Process. **28**: 4587–4601. doi:10.1002/hyp.10180

Yeates, P. S., and J. Imberger. 2003. Pseudo two-dimensional simulations of internal and boundary fluxes in stratified lakes and reservoirs. Int. J. River Basin Manag. **1**: 297–319. doi:10.1080/15715124.2003.9635214

Ying, L., Z. Shen, and S. Piao. 2015. The recent hiatus in global warming of the land surface: Scale-dependent breakpoint occurrences in space and time: SCALE-DEPENDENT HIATUS IN SPACE AND TIME. Geophys. Res. Lett. **42**: 6471–6478. doi:10.1002/2015GL064884

Chapter 3 : Effects of changing climate on ice cover in three morphometrically different lakes

The following has been accepted at *Hydrological Processes*

Magee MR and CH Wu. Effects of changing climate on ice cover in three morphometrically different lakes, *Hydrological Processes*, in press

3.1 Abstract

A one-dimensional hydrodynamic lake model (DYRESM-WQ-I) is employed to simulate ice cover and water temperatures over the period 1911-2014. The effects of climate changes (air temperature and wind speed) on ice cover (ice-on, ice-off, ice cover duration, and maximum ice thickness) are modeled and compared for three lakes with different morphometry: Fish Lake, Lake Wingra, and Lake Mendota, located in Madison, Wisconsin, United States of America. Ice cover period has decreased due to later ice-on dates and earlier ice-off dates, and the annual maximum ice cover thickness has decreased for the three lakes during the last century. Based upon simulated perturbations of daily mean air temperatures across the range of -10 ℃ to +10 ℃ of historical values, Fish Lake has the most occurrences of no ice cover and Lake Wingra still remains ice covered under extreme conditions (+10°C). Overall shallower lakes with larger surface areas appear more resilient to ice cover changes caused by climate changes.

3.2 Introduction

Lake ice cover responds to changes in climate (Magnuson et al. 2000, 2006; Adrian et al. 2009). Alterations of ice cover due to changing climate can stimulate significant changes to lake thermodynamics and ecosystems (MacKay et al. 2009; Kirillin et al. 2012). For example, disappearance of ice cover can considerably affect photic exposure (Leppäranta et al. 2003),

nutrient cycling (Järvinen et al. 2002), and oxygen conditions (Livingstone 1993), which in turn can change the production and diversity of phytoplankton (Weyhenmeyer et al. 1999; Phillips and Fawley 2002). Decreases in ice cover duration may lessen the prevalence of low oxygen conditions and reduce the occurrence of winter fish kills (Fang and Stefan 2000; Stefan et al. 2001). While those effects can be positive for large fish species, it may hurt other species as winterkill is critical for the maintenance of hypoxia-tolerant but predation-sensitive fish species (Tonn and Magnuson 1982). As a result, understanding how lakes respond to climate drivers is of great interest to the scientific and lake management communities (Magnuson et al. 1997; Fang and Stefan 2009). Furthermore, assessing the variations and long-term trend of ice cover in response to climate change can allow for better management of lake ecosystems.

Climate over the past century has been changing significantly, unconditionally affecting the ice regime of lakes (Kirillin et al. 2012). For example, Magnuson et al. (2000) showed that there was later ice-on and earlier ice-off over a century (1846-1995) for Northern Hemisphere lakes and rivers. Trends of later ice-on and earlier ice-off were found in small inland lakes in the Laurentian Great Lakes region from 1975-2004 (Jensen et al. 2007). Similarly, (Korhonen 2006) showed a statistically significant change towards earlier ice-off and later ice-on in Finland. Meanwhile, global average air temperature has increased by 0.74°C over the last 100 years (IPCC 2007) and various studies have reported both increasing (Pryor et al. 2005; Austin and Colman 2007) and decreasing (Klink 2002; Pryor et al. 2009) wind speeds. Air temperature drives lake ice cover duration and thickness (Robertson et al. 1992; Williams and Stefan 2006; Butcher et al. 2015); and ice-on is strongly dependent on the synoptic conditions present over a lake and quickly follow the date of air temperature falling below the freezing point (Kirillin et al. 2012). Greater wind speeds increase lake heat transfer (Read et al. 2012) but delay ice-on by

breaking up thin ice during the beginning of ice formation (Adams 1976). Large wind shear also breaks thin ice during ice melting periods, especially on large lakes (Ashton 1986). Understanding the response of lake ice cover to changes in air temperature and wind speed will provide insight into the response to the future climate. While the climate plays a significant role in lake ice cover, detailed research has been limited until recently.

Lake morphometry (i.e., lake depth and surface area) plays a significant role in affecting physical processes like wind mixing, water circulation, and heat storage (Jeffries and Morris 2007; Adrian et al. 2009), which can in turn influence ice cover (Brown and Duguay 2010; Bernhardt et al. 2011). Ice growth and decay is determined in part by heat stored in the lake, which is a function of lake depth, surface area, and volume (Williams 1965). Deeper lakes usually take longer to freeze as a greater volume per surface area must be cooled (Williams and Stefan 2006; Leppäranta 2010; Kirillin et al. 2012). Lakes with larger fetch may experience differences in ice cover early in the season and break up of skim ice (Adams 1976) since surface area plays a role in terms of wind stress. While previous research has investigated the response of individual lakes (Austin and Colman 2007; Perroud and Goyette 2010; Voutilainen et al. 2014) and the bulk response of lakes in a geographic region to changing climate (Magnuson et al. 1990, 2000, Weyhenmeyer et al. 2004, 2011; Kirillin 2010), very few studies elucidate the role of lakes of varying morphometry on the sensitivity of ice cover in response to a long-term (over a century) changing climate.

The purpose of this paper is to investigate the role of lake morphometry in long-term (1911-2014) changes, variability, and sensitivity of lake ice cover in response to increasing air temperatures and decreasing wind speed. A one-dimensional hydrodynamic lake-ice model is used to run continuous long-term simulations of ice cover and water temperature of three

Madison, Wisconsin area lakes that vary in surface area and depth, and are close to each other (<30 km distance) to experience similar daily meteorological forcing over the period 1911-2014. The application of the model allows for quantifying dates of ice cover and maximum ice thickness which are difficult to obtain through long-term limnological records.

3.3 Methods

3.3.1 Study sites

Table 3-1: Morphometric and hydrologic characteristics of the three study lakes

	Fish Lake	Lake Wingra	Lake Mendota
Mean Depth (m)	6.6	2.7	12.8
Max Depth (m)	19.9	4.7	25.3
Surface Area (ha)	87.4	139.6	3937.7
Groundwater	Groundwater Flowthrough	Groundwater Flowthrough	Groundwater Discharge
Surface Water	Seepage	Drainage	Drainage
Groundwater Input (%)	6	35	30

Figure 3-1 shows the location and bathymetry of three morphometrically different lakes, Fish Lake, Lake Wingra, and Lake Mendota, located in Madison, Wisconsin, United States of America (USA). Table 3-1 lists the morphology and hydrology of the three study lakes. These lakes are chosen for (i) their morphology differences, (ii) their proximity to one another, and (iii) the availability of long-term limnological records, which are used for model calibration.

Fish Lake (43°17'N, 89°39'W) is a dimictic, eutrophic, shallow seepage lake located in

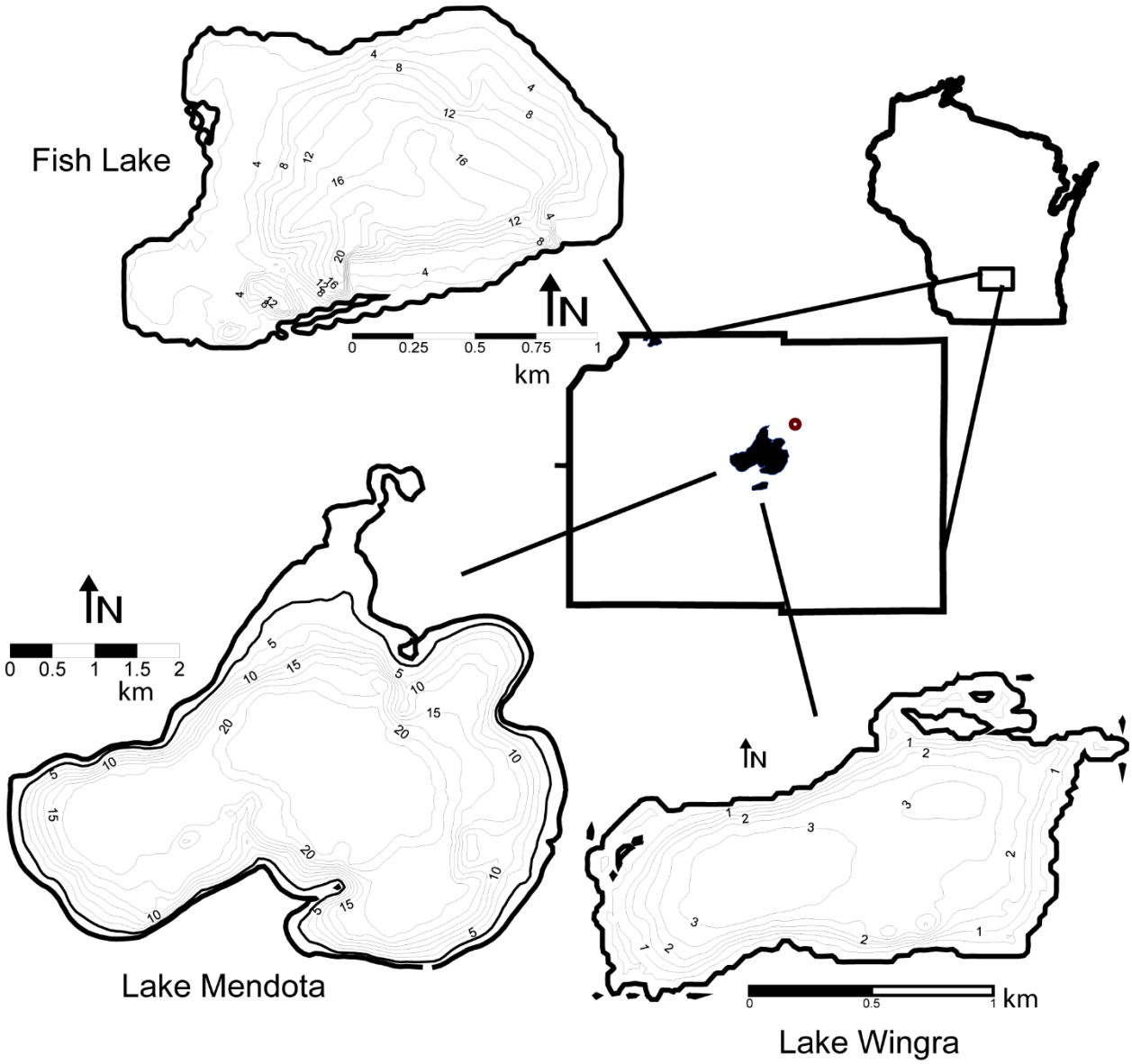

Figure 3-1: Location of three study lakes and bathymetric maps of Fish Lake, Lake Wingra, and Lake Mendota. Circle represents the location of meteorological station.

northwestern Dane County. There are no outlets or inlets for Fish Lake, although during flooding conditions, the nearby Mud Lake may overflow into Fish Lake. Fish Lake has a surface area of 87.4 ha, a mean depth of 6.6 m, a maximum depth of 19.9 m, a shoreline length of 4.3 km, and a fetch of 2 km. Fish Lake has a small watershed and has a shoreline development that is classified as high. During the period from 1966-2001, the average water level of the lake rose by approximately 2.75 meters (Krohelski et al. 2002).

Lake Wingra (43°3' N, 89°26' W) is a very shallow, eutrophic lake. Wingra is a drainage lake that has multiple inflowing streams and one outflow stream, Wingra Creek. Lake Wingra has a surface area of 140 ha, a mean depth of 2.7 m, a maximum depth of 4.3 m, a shoreline length of 5.9 km, and a fetch of 2 km. Like Fish Lake, Wingra is located high in the landscape, and the development along the shoreline is characterized as high. Lake Wingra is the shallowest of the three study lakes.

Lake Mendota (43°6'N, 89°24'W), is a dimictic, eutrophic lake in an urbanizing agricultural watershed (Carpenter and Lathrop 2008). Mendota is a drainage lake, with multiple inlets and one main outlet, the Yahara River. Lake Mendota has a surface area of 3,940 ha, a mean depth of 12.8 m, a maximum depth of 25.3 m, a shoreline length of 33.8 km, and a maximum fetch of 9.8 km (Robertson and Ragotzkie 1990). The lake is located low in the landscape, and development along the shoreline is classified as high. Lake Mendota is both the deepest and largest (by surface area) of the three study lakes.

3.3.2 Model description

In this study, a previously-developed one-dimensional hydrodynamic lake-ice model, DYRESM-WQ-I (Hamilton et al. *in review*; Magee et al. 2016; Appendix A), is used to simulate vertical water temperature profiles and ice cover thickness in Fish Lake, Lake Wingra, and Lake Mendota. This model adds an ice and snow cover sub-model to the earlier DYRESM-WQ (Hamilton and Schladow 1997). DYRESM-WQ-I simulates vertical water temperature, salinity, and density by using discrete horizontal Lagrangian layers of uniform properties that vary in thickness. More information on the hydrodynamic model simulation of water temperature and mixing can be found in Imberger and Patterson (1981), (Yeates and Imberger 2003), and Hamilton and Schladow (1997). Specifically, the ice-snow model is based upon the MLI model

of Rogers et al. (1995) with alterations to two-way coupling of the water-column dynamics to the ice model and the addition of a time-dependent sediment heat flux for all horizontal layers. Coupling between the hydrodynamic and ice models is in both directions, with the hydrodynamic model determining heat flux at the ice-water interface and ice cover characteristics providing boundary conditions for the hydrodynamic model. Ice-snow model equations are embedded into DYRESM-WQ-I in the subroutine that performs thermal transfers at the surface, with ice, snow, and water temperature determined by fluxes at the surface and at the ice-water interface. Water temperature under ice is driven by heat fluxes between the ice-water interface and radiative fluxes through the ice layer into the water column. Light extinction coefficients are calculated as a function of Secchi depth using the equation, $k = 1.1/z_s^{0.73}$ (Williams et al. 1980). Detailed description of model development may be found in Appendix A.

Input for the model includes lake morphometry (lake volume and surface area as a function of elevation), initial vertical profiles for water temperature and salinity, Secchi depth, meteorological variables, and inflows/outflows, discussed in detail next. The model calculates the surface heat fluxes using measured meteorological variables: total daily shortwave radiation, daily cloud cover (used to estimate longwave radiation), air vapor pressure, daily average wind speed, air temperature, and precipitation. During the entire simulation period, all parameters/coefficients in the model are kept constant. The time step in the model for calculating water temperature, water budget, and ice thickness is 1 hr. Snow ice compaction, snowfall, and rainfall components are updated at a daily time step, corresponding to the frequency of meteorological data input. Cloud cover, air pressure, wind speed, and temperature are assumed constant throughout the day, and precipitation is assumed uniformly distributed. The distribution of measured shortwave radiation throughout the day is computed based on the lake latitude and

Table 3-2: Parameter values for both hydrodynamic and ice cover portions of the DYRESM-WQ-I model. Asterisks (*) indicate calibration values

Hydrodynamic Model Parameters	**Value**	**Source**
Albedo	0.08	Antenucci and Imerito, 2003; Tanentzap et al., 2007
bulk aerodynamic momentum transport coefficient	0.00139	Fischer et al., 1979
Critical wind speed (m s^{-1})	4.3	Tanentzap et al., 2007
effective surface area coefficient (m^2)	$1x10^7$	Yeates and Imberger, 2003
emissivity of water surface	0.96	Imberger and Patterson, 1981
potential energy mixing efficiency	0.2	Antenucci and Imerito, 2003; Tanentzap et al., 2007
shear production efficiency	0.06	Antenucci and Imerito, 2003; Yeates and Imberger, 2003; Tanentzap et al., 2007
vertical mixing coefficient	200	Yeates and Imberger, 2003
wind stirring efficiency	0.8	Tanentzap et al., 2007
minimum layer thickness	0.125*	calibration parameter
maximum layer thickness	0.6	Tanentzap et al., 2007
vertical light attenuation coefficient	variable*	Williams et al., 1980

Ice Model Parameters	**Value**	**Source**
Waveband 1, snow ice light extinction (m^{-1})	3.8	Rogers et al., 1995
Waveband 2, snow ice light extinction (m^{-1})	20	Patterson and Hamblin, 1988; Rogers et al., 1995
Waveband 1, blue ice light extinction (m^{-1})	1.5	Patterson and Hamblin, 1988; Rogers et al., 1995
Waveband 2, blue ice light extinction (m^{-1})	20	Patterson and Hamblin, 1988; Rogers et al., 1995
Waveband 1, snow light extinction (m^{-1})	6	Patterson and Hamblin, 1988; Rogers et al., 1995
Waveband 2, snow light extinction (m^{-1})	20	Patterson and Hamblin, 1988; Rogers et al., 1995
Distance of heat transfer, ice-water (m)	0.039	Vavrus et al., 1996
Density, snow ice (kg m^{-3})	890	Rogers et al., 1995
Density, blue ice (kg m^{-3})	917	Patterson and Hamblin, 1988; Rogers et al., 1995
Density, snow (kg m^{-3})	variable	McKay, 1968
Compaction coefficient	variable	Rogers et al., 1995
Thermal conductivity, snow ice (W m^{-1} °C^{-1})	2.0	Rogers et al., 1995
Thermal conductivity, blue ice (W m^{-1} °C^{-1})	2.3	Patterson and Hamblin, 1988; Rogers et al., 1995
Thermal conductivity, snow (W m^{-1} °C^{-1})	variable	Ashton, 1986
Thermal conductivity, sediment (W m^{-1} °C^{-1})	1.2	Rogers et al., 1995
Thermal conductivity, water (W m^{-1} °C^{-1})	0.57	Patterson and Hamblin, 1988; Rogers et al., 1995

the Julian day. DYRESM-WQ-I is calibrated and validated to minimize error in water level, temperature profiles, ice thickness measurements, and ice on and ice off dates. The overall simulation period for all three lakes is 104 years, starting on 7 April 1911 and ending on 31 October 2014 without termination. Parameters used in DYRESM-WQ-I are listed in Table 3-2.

3.3.3 Model input data

The long-term data are compiled from various sources including the NTL-LTER (2012a), unpublished data from E. Birge, University of Wisconsin, unpublished data from D. Lathrop, Wisconsin Department of Natural Resources; Robertson (1989); Stewart (1965); and USGS (2010). The frequency of data available varies widely, from daily to annually.

Meteorological data includes daily solar radiation, air temperature, vapor pressure, wind speed, cloud cover, rainfall, and snowfall. Meteorological data for Madison, Wisconsin have been recorded continuously since 1869, although the station locations and specific techniques have changed during this period. A continuous daily meteorological dataset from 1884 to 1988 was constructed by Robertson (1989) by adjusting for changes in site location, observation time, and changes in surface roughness. These data are appended with recent data from the National Climate Data Center weather station located at the Dane County Regional Airport. All data appended meteorological data was obtained from http://www.ncdc.noaa.gov, except solar radiation, which was obtained from http://www.sws.uiuc.edu/warm/weather/ for St. Charles, Illinois. Further adjustments are made to wind data due to changes in observational techniques occurring in 1996 (McKee et al. 2000). To address this issue, data from the Dane County Airport are compared with those collected from the tower of the Atmospheric and Oceanic Science Building at the University of Wisconsin-Madison. Detailed comparison and adjustment can be found in (Magee et al. 2016) and will not be shown here for brevity. In this study, we assume

that the three lakes experience the same daily meteorological forcing for the duration of the model.

Seasonal Secchi depths are used to determine the light extinction coefficient in DYRESM-WQ-I. For Lake Wingra and Fish Lake, Secchi depths are obtained from the NTL – LTER (2012a) from 1995 to the present. For years with no Secchi data, the long-term mean seasonal Secchi depth was used to estimate light extinction. For Lake Mendota, Lathrop et al. (1996) compiled Secchi depth data between 1900 and 1993 (1701 daily Secchi depth readings from 70 calendar years), and summarized the data for six seasonal periods: winter (ice-on to ice-out), spring turnover (ice-off to 10 May), early stratification (11 May to 29 June), summer (30 June to 2 September), destratification (3 September to 12 October), and fall turnover (13 October to ice-on). After 1993, Secchi depths are obtained from the NTL-LTER (2012a) .

Hydrology data are daily inflow and outflow measurements at stream gauging stations. Collected measurements are used to estimate daily inflow and outflow for the three study lakes. In cases where inflow and outflow measurements are not available, the water budget approach of balancing inflow/outflow, precipitation, evaporation, and lake level changes is employed. Water level at Fish Lake was recorded almost daily from 1966-2003 (www.waterdata.usgs.gov). Water level in Lake Wingra was recorded sporadically during the period of interest. For Lake Mendota, water level has been recorded since 1916 (http://waterdata.usgs.gov/wi/nwis/dv). For instances where lake level information and inflow/outflow measurements are not available, the long-term mean lake level is assumed and used for water budget calculations. Air temperatures are used to estimate the water temperature of inflowing streams (Magee et al. 2016), and an average of groundwater temperature measurements is used for groundwater heat fluxes.

3.3.4 Observation data

For model calibration and validation, observation data are from a variety of sources. Ice thickness and water temperature data were collected for Fish lake from the NTL-LTER (2012b; c) program only from 1996-2014. For Lake Wingra, ice cover data were collected from the NTL-LTER (1996, 2012c). Ice-on is defined as the first date on which the water body is observed to be completely ice covered, and ice-off is the date of the last breakup observed before the open water phase. The dates were not fixed until the lakes remained closed at least a full day and ice persisted into a second day. In some years, observations show more than one ice-covered period; under these situations, observed ice dates are defined by the longest continuous period of ice cover duration. Water temperature information is available from the NTL-LTER (2012b) program from 1996-2014 with bi-weekly temperature profiles during open water seasons and two temperature profiles during ice cover periods. For Lake Mendota, ice thickness readings were gathered from: 1911-1916 data from E. Birge (unpublished data, University of Wisconsin); 1961-1964 (Stewart 1965), 1975-1995 (unpublished data, D. Lathrop. Wisconsin Department of Natural Resources); and 1995-2014 data from the NTL-LTER program (2012c). Ice date information is obtained from the NTL-LTER ((1996)). For Lake Mendota, ice-on date is assigned if the lake has solid ice across the southwest-northeast transect of the lake (from Picnic Point to Maple Bluff) and total ice cover is greater than 50 %. Ice-off is determined if the lake is ice-free across the same transect and total ice cover is less than 50%. Long term water temperature records for Lake Mendota are from Robertson (1989) and the NTL-LTER (2012b).

3.3.5 Model calibration and evaluation

Using known inflow and outflows and water elevations, the water balance was closed for the duration of the model simulation using the method described in Section. 3.3.3. Evaporative

water and heat flux from the lake is included in DYRESM-WQ-I. We assumed that the evaporative fluxes were properly parameterized in the model, but modeled evaporation rates were not validated. With the exception of balancing the water budget and estimation of light extinction coefficient from measured Secchi depths (see Section 3.3.4), water temperature in the model was calibrated only through the adjustment of minimum layer thickness. Calibration was performed for years 1995-2000 for all three lakes. To calibrate minimum layer thickness, values ranging from 0.05 m to 0.5 m at 0.025 m intervals were evaluated for the least amount of deviation between predicted and observed volumetrically-averaged temperature values for the three lakes. A minimum layer thickness of 0.125 m is chosen as the best setting to predict water temperature at all depths. Other parameters assumed in the model were derived from literature values, and are provided in Table 3-2.

Model performance was evaluated over the remaining years of data: 1911-1994 and 2001-2014 using three metrics, absolute mean error (AME), root-mean square error (RMSE), and Nash-Sutcliffe efficiency (NS), for ice cover and water temperature variables on all three lakes. Simulated and observed values are compared directly, with the exception of aggregation of water temperature measurements to daily intervals where sub-daily intervals are available.

3.3.6 Air temperature perturbations

Air temperature plays a significant role in influencing changes in ice cover in the Madison Area. Studies (IPCC 2007; Wisconsin Initiative on Climate Change Impacts (WICCI) 2011) suggest that the air temperatures will continue to increase. To examine potential changes to ice cover (maximum ice thickness and ice cover duration) under future warmer or colder temperatures, we perform temperature perturbations by increasing and decreasing daily air temperature values for the first 100 years of the simulation period in 1°C intervals, bounded at

−10°C and +10°C. For each scenario, meteorological inputs remained the same as for the original simulations but with snowfall (rainfall) conversions if the air temperature scenarios increase (decrease) above 0°C. Groundwater and surface water inflow temperatures were similarly adjusted to account for changes in air temperatures. Groundwater temperatures were perturbed in the same method as air temperatures and surface water temperatures were recalculated based on the perturbed air temperature scenarios. Additionally, the water balance is maintained so that the long-term water levels in all three lakes match the historical record.

3.3.7 Analysis

Two statistical methods are used to analyze the model results. First a linear regression is used to determine the trend of long-term changes of lake variables. Second, a Pearson correlation coefficient (Baron and Caine 2000) is used to determine the coherence of lake variables (Magnuson et al. 1990) between winter climate variables and between lake pairs, allowing for comparison of correlation of the lake variables to each other.

3.4 Results

3.4.1 Long-term trend of air temperature and wind speed

Figure 3-2 shows the yearly average air temperature and wind speed at the Madison area over the study period from 1911 to 2014. Historic measurements show that there has been a trend of increasing air temperature and decreasing wind speed over the last 104 years. Using the regression analysis, the air temperature has an increasing linear trend of approximately 1.45°C century^{-1} from 1911-2014. For wind speed, the decreasing linear trend has been 0.73 m s^{-1} century^{-1} over the same period. December to March changes in air temperature and wind speed are larger than the annual change at 2.25°C century^{-1} and -0.83 m s^{-1} century^{-1}, respectively. In

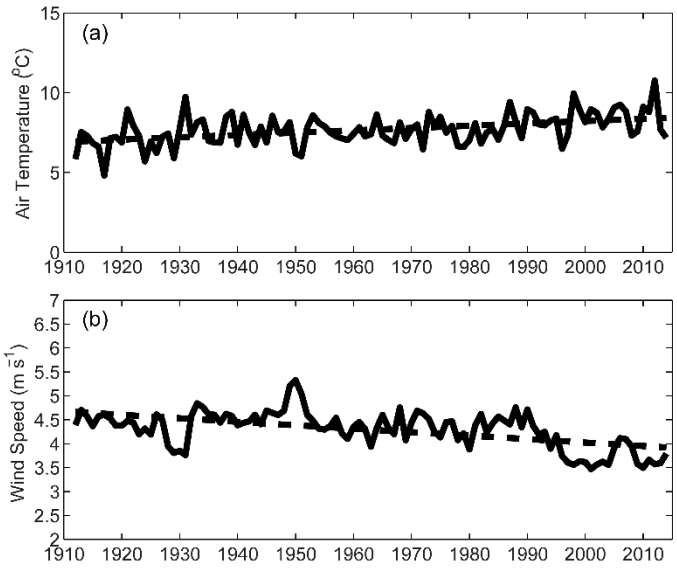

Figure 3-2: Yearly average (a) air temperature and (b) wind speed for Madison, Wisconsin. Dashed lines denote the trendline for climate variables over the period 1911 – 2014

Madison, WI, the urban heat island (UHI) has a significant effect on air temperature values (Schatz and Kucharik 2014). To determine any effect on trend from UHI, we compare Madison air temperatures with a nearby station at the Arlington Agricultural Research Station, 20 km north of Madison. The trend in yearly average air temperature at the station from NOAA (http://w2.weather.gov/climate/xmacis.php?wfo=mkx), available starting in 1963, shows a trend toward increasing air temperature of 0.314 °C decade^{-1} for 1963-2014 compared to 0.397°C decade^{-1} for Madison using the same measurement techniques. This is approximately a 20% difference, implying that the change in trend in Madison, WI may be partially due to increases in urbanization in the region, but the driving force of change is likely global increases in air temperature. Similarly, urbanization can lead to reductions in wind speed (Li et al. 2011; Grawe et al. 2013). To determine effect of urbanization on wind speed declines, we compare measured Madison wind speed to wind speed trends from Freeport, IL (~100 km south of Madison) and St. Charles, IL (~150 km southeast of Madison), which are significantly less urbanized than Madison (populations 25,000-33,000). Wind speed data for both cities is collected from http://www.sws.uiuc.edu/warm/weather/ and is available starting in 1990 for Freeport and 1988 for St. Charles. From 1990-2014, Freeport yearly average wind speed trend is −0.30 m s^{-1} decade^{-1}, while Madison is −0.23 m s^{-1} decade^{-1}. Similarly, St. Charles trend in

yearly average wind speed is −0.33 m s^{-1} $decade^{-1}$ from 1988-2014, while Madison is −0.29 m s^{-1} $decade^{-1}$. Higher decreasing trend for the less urbanized cities indicate that the trend in decreasing wind speeds in Madison, WI is not significantly impacted by urbanization in the area.

3.4.2 Model errors and statistics

Figure 3-3 compares simulations by the DYRESM-WQ-I model and observations of ice covers and water temperatures over long-term (104-year) simulations. Discrepancies between modeled and measured values come from several sources. Average daily air temperatures and wind speeds are used in the model, and average daily values are output from the model. Figure 3-4 compares simulated and observed total ice cover for all three lakes during the winter of 2009-2010. In general, thermocline depths are within 1 m between observed and simulated, but some years differ by as much as 2.5 m, significantly impacting the fit of the model near the thermo-cline for Lakes Mendota and Fish. Table 3-3 lists absolute mean error (AME), root-mean-square error (RMSE), and Nash-

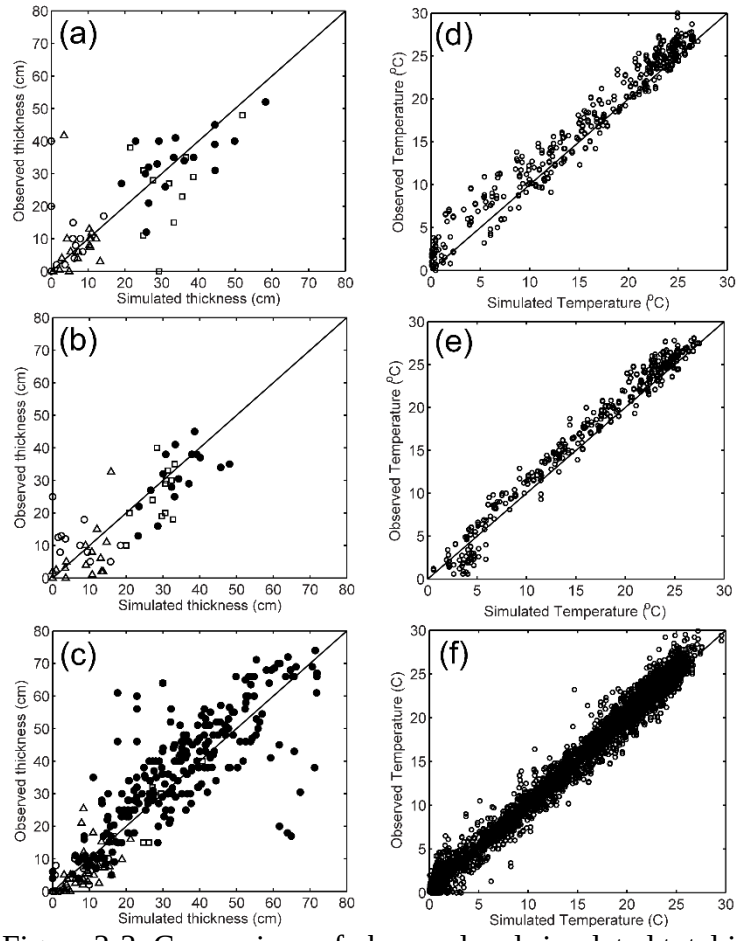

Figure 3-3: Comparison of observed and simulated total ice (●), snow cover (Δ), white ice (○), and blue ice (□) for (a) Fish Lake, (b) Lake Wingra, and (c) Lake Mendota. Comparison of observed and simulated lake surface water temperatures (°C) for (d) Fish Lake, (e) Lake Wingra, and (f) Lake Mendota.

Table 3-3: Absolute mean error (AME), root-mean square error (RMSE), and Nash-Sutcliff efficiency (NS) for ice cover and water temperature variables on Fish Lake, Lake Wingra, and Lake Mendota. n = number of measurements, N/A represents errors that cannot be determined due to availability of measurement data.

Variable	Fish Lake				Lake Wingra				Lake Mendota			
	n	AME	RMSE	NS	n	AME	RMSE	NS	n	AME	RMSE	NS
Total ice thickness (cm)	19	4.83	5.83	0.98	18	5.73	5.98	0.92	251	7.8	7.9	0.97
Blue ice thickness (cm)	19	7.11	10.1	0.95	18	5.31	5.84	0.93	21	5.5	3.3	0.96
White ice thickness (cm)	19	6.92	7.20	0.97	18	2.54	6.72	0.92	21	1.99	2.3	0.99
Snow thickness (cm)	19	4.23	4.75	0.98	18	4.42	4.75	0.93	49	4.0	3.7	0.94
Ice-on date (day)	N/A	N/A	N/A	N/A	59	2.00	3.08	0.97	103	1.80	2.43	0.99
Ice-off date (day)	N/A	N/A	N/A	N/A	61	2.29	3.48	0.97	103	2.52	3.30	0.98
Ice duration (day)	N/A	N/A	N/A	N/A	54	3.56	4.88	0.95	103	2.82	3.75	0.98
Epilimnetic temperature (°C)	263	1.23	1.45	0.95	N/A	N/A	N/A	N/A	3,239	0.69	0.3	0.99
Hypolimnetic temperature (°C)	263	1.63	1.94	0.92	N/A	N/A	N/A	N/A	3,239	1.04	0.53	0.96
Temperature at 1m interval (°C) overall range of values for depths	5,522	0.85-1.93	1.98-2.42	0.85-0.91	1,897	0.63-0.85	0.41-0.96	0.99	85,566	0.5-1.56	0.25-0.75	0.95-0.99

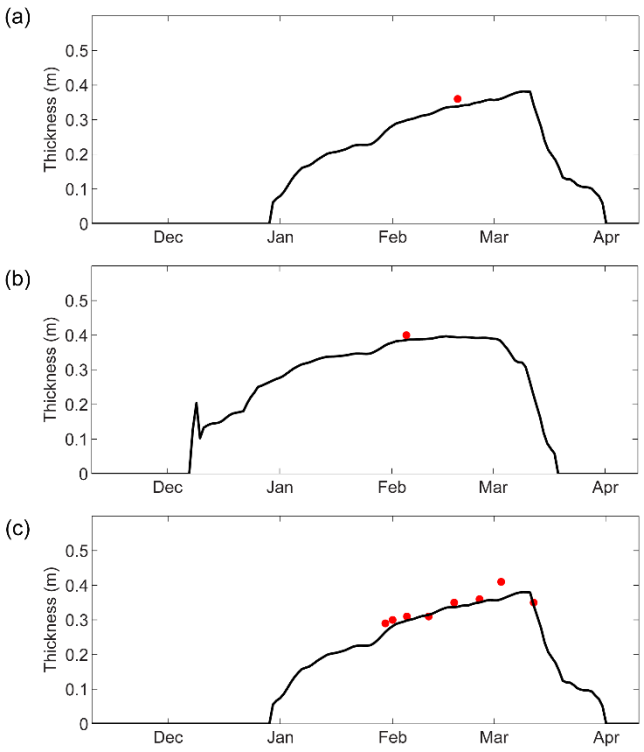

Figure 3-4: Simulated (solid black lines) and observed (red dots) total ice thickness for (a) Fish Lake, (b) Lake Wingra, and (c) Lake Mendota for the winter of 2009-2010.

Suttcliffe (NS) efficiencies for all validation parameters. AME and RMSE for all variables are low and less than standard deviations for variables. Nash-Suttcliffe efficiencies are high (>0.85) and most above 0.90, indicating high model accuracy.

3.4.3 Ice-on and ice-off dates

Figure 3-5 shows the simulated (filled circles) and observed (open circles) ice-on and ice-off dates for Fish Lake, Lake Wingra, and Lake Mendota, respectively, over the 104-year period. Modeled ice dates are defined by the dates between which the longest continuous frozen period for that winter occurred. In general, the model accurately simulated the ice-on and ice-off dates for both Lake Wingra (AME=6.1 days ice on, 4.6 days ice off; RMSE = 8.2 days ice on, 6.0 days ice off) and Lake Mendota (AME = 2.6 days ice on, 5.7 days ice off; RMSE = 4.0 days ice on, 7.4 days ice off). Table 3-4 shows the trend (days century^{-1}), mean, standard deviation (SD), and range of ice-on and ice-off dates over the period 1911-2014. All three lakes experience trends of later ice-on, earlier ice-off, and shorter ice cover duration. Trends in ice dates are significant for all three lakes

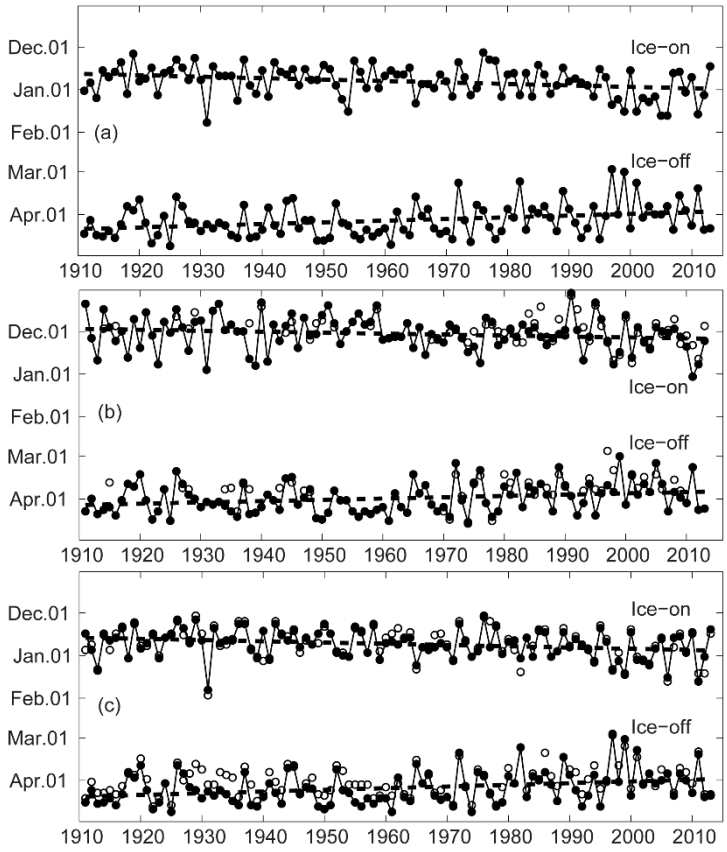

Figure 3-5: Ice-on and ice-off dates for (a) Fish Lake, (b) Lake Wingra, and (c) Lake Mendota. Filled circles are modeled ice-on and ice-off dates, while open circles are observed ice dates. Dashed lines denote the trendline for ice dates over the period 1911 – 2014

(p<0.05). Fish Lake and Lake Mendota have similar means and standard deviations of ice cover dates. Trends in ice on dates are slightly smaller than standard deviations (5% for Fish Lake; 13% for Lake Mendota); trends in ice-off dates are approximately equal to standard deviations; and trends in total ice cover duration are larger than standard deviations (25% Fish Lake; 19.5% Lake Mendota). For Lake Wingra, the mean for ice-on dates and ice-off dates are earlier than those of Fish Lake and Lake Mendota. Nevertheless, the ice duration is longer than that of Fish Lake and Lake Mendota. The trends in ice-on, ice-off, and ice duration are smaller than standard deviations (43% ice on; 15% ice off; 8.4% duration), suggesting that the shallower lake is more resilient to climate changes.

Table 3-4: Trends, means, standard deviations (SD), and range in lake ice cover variables from 1911 – 2014.

	Fish Lake				Lake Wingra				Lake Mendota			
	Trend (century^{-1})	Mean	SD	Range	Trend (century^{-1})	Mean	SD	Range	Trend (century^{-1})	Mean	SD	Range
Ice On (days)	10.6 days later*	23 Dec.	11.2	51	7.0 days later*	30 Nov.	12.3	61	9.0 days later*	21 Dec.	10.4	53
Ice Off (days)	12.2 days earlier*	3 Apr	12.0	51	9.4 days earlier*	29 Mar	11.1	48	12.3 days earlier*	4 Apr	12.0	55
Ice Duration (days)	22.9 fewer days*	100.0	18.3	85	16.4 fewer days*	119.1	17.9	89	21.4 fewer days*	104.0	17.9	87
Maximum Ice Thickness (cm)	11.8 cm less*	48.3	10.8	50.0	7.6 cm less*	44.0	9.65	45.0	12.8 cm less*	47.2	11.0	51.9

*indicates significant to p<0.05

3.4.4 Evolution of ice cover and lake surface temperature

Figures 3-6 a and b show the ice growth and decay evolution and lake surface temperature for the three lakes under the air temperatures with an extremely warm (1997-1998) and cold (1935-1936) January – March wintertime period, respectively. During the wintertime from December 1997 to March 1998, the air temperatures varied from -18.3°C to 17.8°C, with an

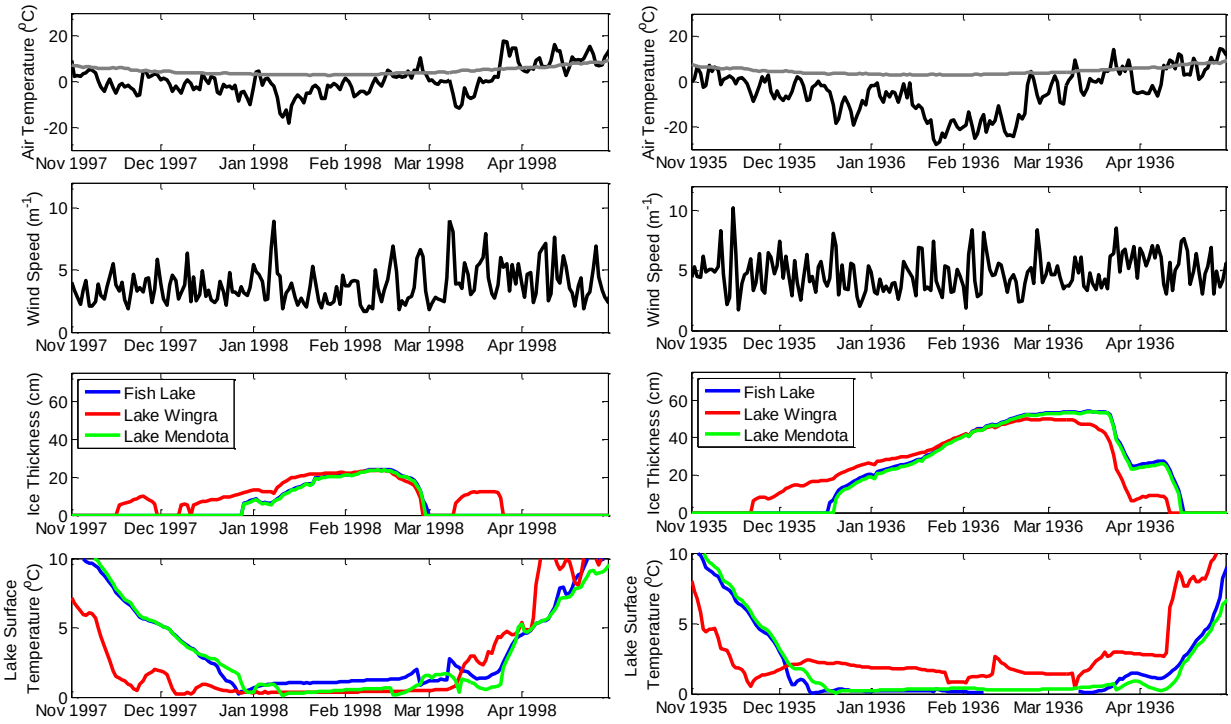

Figure 3-6: Evolution of ice thickness and lake surface temperature for (a) extreme maximum wintertime air temperature year 1997-1998 and (b) for extreme minimum wintertime air temperature year 1935-1936. Top plots show the daily average air temperature (black line) and the long-term daily average air temperature (grey line). Second plots are the daily average wind speed. Third plots and forth plots show the ice thickness evolution and lake surface temperature for Fish Lake (blue), Lake Wingra (red), and Lake Mendota (green).

average temperature of -1.6 °C. Due to the shallow depth of Lake Wingra, the lake cooled down rapidly, allowing ice formation as early as 16 November 1997 and disappeared shortly after. The complete ice cover started on 8 December1997, and the lake continuously froze over for the winter-time period until 27 February 1998. After 12 days, ice was formed again due to a sudden drop of the air temperature and the ice was off on 26 March 1997.This feature of intermittent ice on and ice off in Lake Wingra was strongly correlated with the air temperature. In contrast, both Fish Lake and Lake Mendota, which are significantly deeper than Lake Wingra, did not have ice cover until 28 December 1997 (Fish Lake) and 27 December 1997 (Lake Mendota) and the ice was off approximately the same day as Lake Wingra. Afterwards, the sudden drop in air temperature did not prompt ice growth, indicating lake morphometry, specifically water depth,

plays an important factor in ice formation. For the extremely cold wintertime from November 1935 to April 1936, the air temperatures varied from -27°C to 14.4°C, with an average temperature of -7.8ºC. All three lakes experienced early ice-on dates and late ice-off dates. Specifically, the earliest ice cover for Lake Wingra was on 21 November 1935. The ice cover for Fish Lake occurred on 18 December 1935 and for Lake Mendota on 19 December 1935.1935 The ice-off dates were as late as 13 April for Lake Wingra, and 16 April for Lake Mendota and Fish Lake. The results show that ice-on dates are earlier for shallower lakes and ice-off dates are later for deeper lakes.

Overall, the ice cover formation process consists of an initial rapid growth, increasing ice thickness responding to below-freezing air temperatures, and reaching a maximum thickness in lake wintertime (Ashton, 1986). Ice formation is preceded by intense radiative and convective heat loss from the warmer lake surface to the colder atmosphere (Kirillin et al. 2012) and follows the date that air temperature falls below freezing with a slight delay. For all three study lakes under both extreme temperature years, the ice cover, once formed, follows a fairly similar progression of growth. In the later stage, ice growth is independent of lake characteristics and instead depends primarily on air temperatures (Brown and Duguay 2010). Eventually the ice growth plateaus at the maximum ice thickness, with maximum ice thickness occurring around the same time in all three lakes. In the majority of years, ice decay occurs quickly (<2 weeks) and each lake follows a similar pattern of ice decay with ice-off dates in all three lakes occurring within a few days. However, differences are observed in cold years, as shown in the winter 1935-1936. Ice-off occurs slightly later in the deeper Lake Mendota and Fish Lake than the shallower Lake Wingra, possibly due to the decreased ice thickness in Wingra. Furthermore, later periods

of below freezing air temperatures may result in an anomalous period of late ice growth in all three lakes.

3.4.5 Maximum ice thickness

Figure 3-7 shows the maximum ice thickness for the three lakes over the period 1911-2014., and Table 3-4 lists the trend (cm century^{-1}), mean (cm), standard deviation (cm), and range (cm) of thein maximum ice thickness. The magnitude of trend is larger than the standard deviation for Fish Lake (9%) and Lake Mendota (16%) but smaller for Lake Wingra (21%). Fish Lake and Lake Mendota have a greater magnitude change in the trend of maximum ice thickness than does the shallower Lake Wingra.

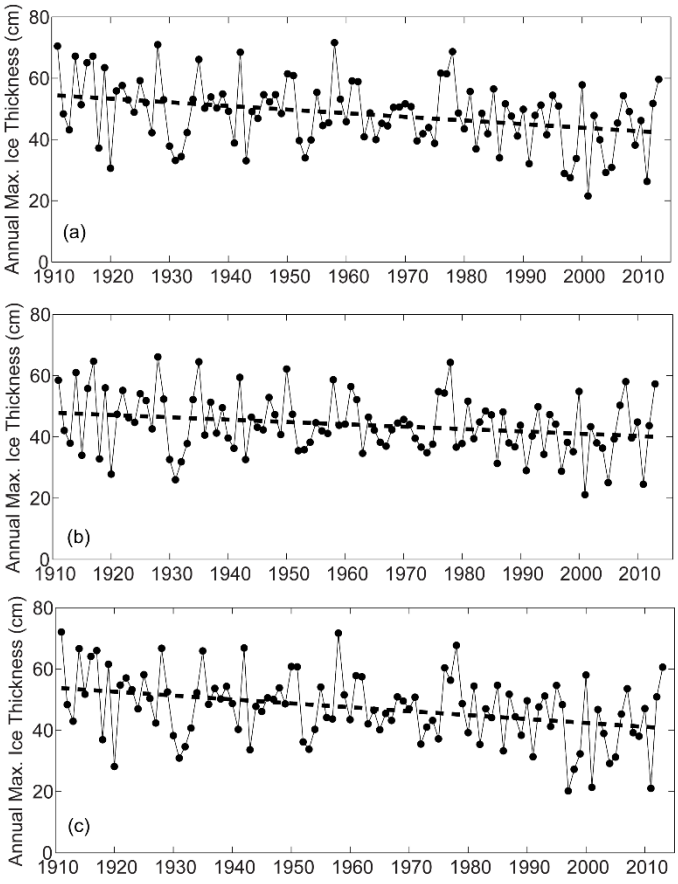

Figure 3-7: Yearly maximum ice thickness (in cm) for (a) Fish Lake, (b) Lake Wingra, and (c) Lake Mendota. Dashed lines denote the trendline for maximum ice thickness.

3.4.6 Ice cover under air temperature perturbations

Figure 3-8 shows colorplots of maximum ice thickness for each of 100 model years under air temperature perturbations. Black color indicates no ice cover during that model year − perturbation combination Results show multiple years of no ice cover for both Fish Lake and Lake Mendota at air temperature increases as small at +4°C but only four instances of no ice cover for Lake Wingra at air temperature increases of +10°C. Figure 3-9 shows the results of air

temperature perturbations (increases only) on ice growth for 1916-1917, an example of a cold year. Model results show decreasing ice thickness, later ice-on, and earlier ice-off as air temperature perturbations increase. For air temperature increases of +10°C, Lake Wingra maintains longer ice cover duration than Fish Lake and Lake Wingra.

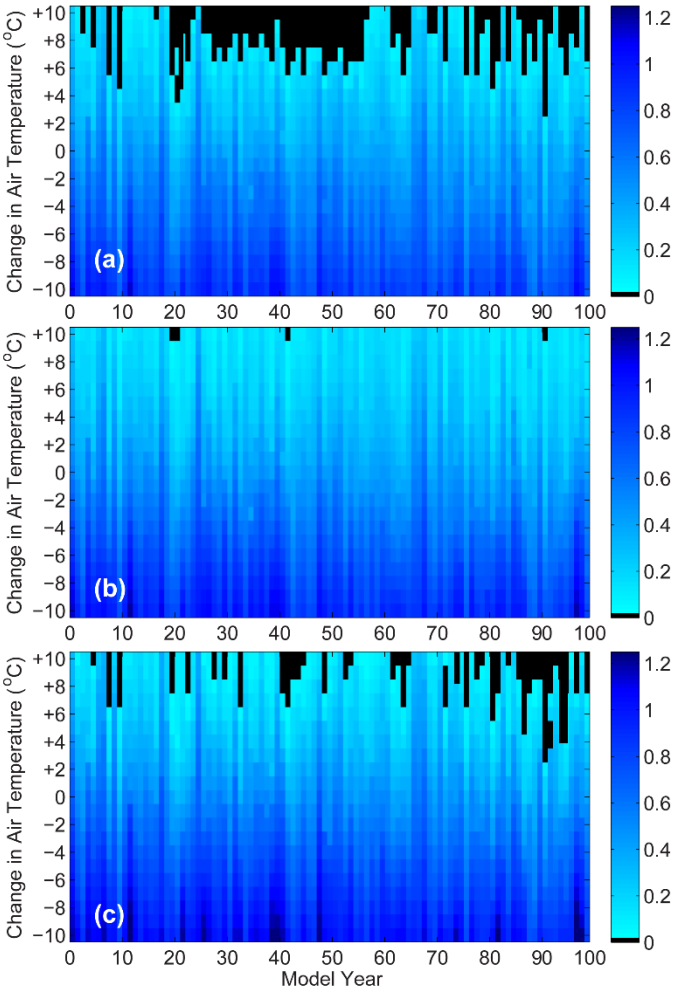

Figure 3-8: Maximum ice thickness (in m) for (a) Fish Lake (b) Lake Wingra, and (c) Lake Mendota as the air temperature is changed by intervals of 1°C.

3.5 Discussion

3.5.1 Model performance and evaluation

Discrepancies between modeled and observed ice thicknesses can be partially attributed to differences in location and timing of ice observations. Ice measurements made at multiple locations in Lake Mendota (Hsieh 2012, 2013) showed inhomogeneity in ice thickness, with ice in the middle of the lake approximately 12 cm thicker than at littoral locations. This finding is consistent to the finding by Bengtsson (1986), who showed spatial variations in ice and snow depths for a medium-to-large lake (as those in this study). As a result, the discrepancy between model and measured ice values may be expected in years when ice thickness varied spatially. Errors in water temperature (Figure 3-3) are predominantly a result of differences between simulated and

observed thermocline depth over some years, and some slight mismatches in timing of stratification onset and overturn.

The performance of the DYRESM-WQ-I model is similar to that of other studies in the literature. Using Minnesota lake model (Minlake), Fang and Stefan (1996) gave standard errors of water temperature of 1.37°C for the open water season and 1.07°C for the total simulation

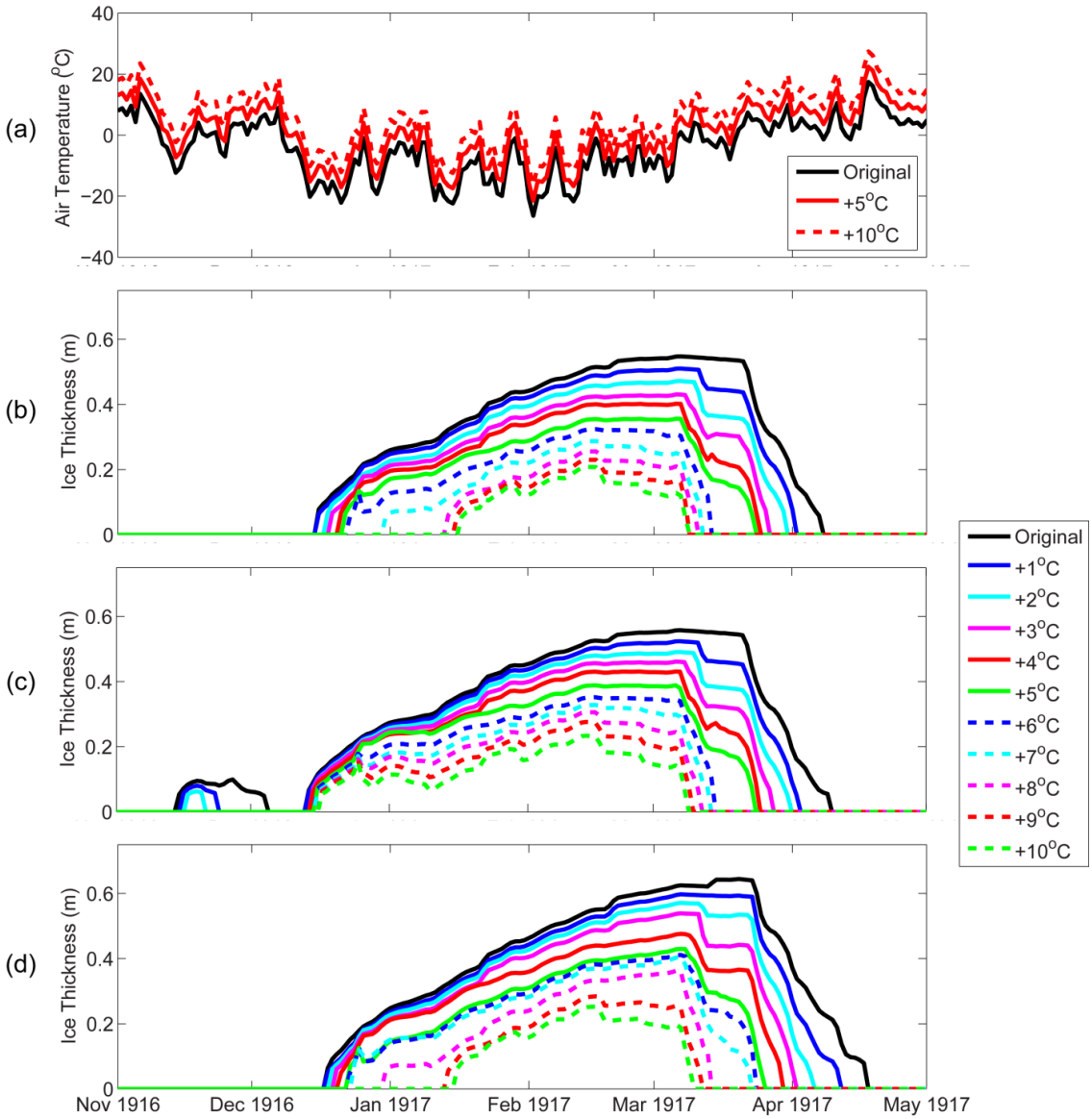

Figure 3-9: (a) Air temperatures under the original simulation and +5°C and +10°C air temperature perturbations and ice growth for (b) Fish Lake, (c) Lake Wingra, and (d) Lake Mendota perturbations for the cold winter of 1916-1917. Each line in (b) - (d) represent a one degree (C) increase in air temperature.

period for Thrush Lake, MN and errors of 6 cm for snow thickness and 11 cm for ice thickness. Perroud et al. (2009) simulated water temperature on Lake Geneva and compared RMSE using several one-dimensional lake models: 1.7°C for DYRESM (Tanentzap et al. 2007), 2°C for the Hostetler model (Hostetler and Bartlein 1990), 2°C for a k-epsilon type turbulence SIMSTRAT model (Perroud et al. 2009), and 4°C for a Freshwater Lake (Flake) model (Golosov et al. 2007; Kirillin et al. 2012). For all four models, errors were lower in the upper layers and larger in the bottom of the water column, similar to errors found in this study. On Baker Lake, Nunavut, Canada, the model, MyLake, produced mean absolute differences between model and observations of 11 cm in ice thickness (Dibike et al. 2011). Other models including LIMNOS (Vavrus et al. 1996) on Lake Mendota, Wisconsin; MLI (Rogers et al. 1995) on Harmon Lake, British Columbia, and CLIMo (Duguay et al. 2003) on lakes in Alaska and Manitoba produced similar errors between modeled and observed ice thickness and snow covers. Recent study by Yao et al. (2014) show that ice cover over a 16-year period can be reasonably modeled using the four models, i.e. Minlake, Simple Lake Model (Jöhnk et al. 2008) SIM, Hostetler, and General Lake Model (GLM, (Hipsey et al. 2014). In our study, results of Nash-Sutcliff efficiency coefficients for all three study lakes are significantly improved over the Minlake, SIM, Hostetler, and GLM lake models for all ice cover variables (i.e., ice-on dates, ice-off dates, and ice thickness) using the DYRESM-WQ-I model. Nevertheless, future efforts should be devoted to increase model accuracy and predictability of lake ice dynamics.

3.5.2 Coherence among lakes

Temporal coherence can be described as the correlation between two signals over time, i.e., the similarity of lake responses over time. Previous research showed that spatially close lakes respond coherently to climate (Magnuson et al. 1990; Thompson et al. 2005), but those

with comparable physical features exhibit substantially higher coherence than lakes with different physical properties (Novikmec et al. 2013). Large correlation coefficients indicate high temporal coherence between lakes, thus exhibiting synchronous patterns in the lake variables (Magnuson et al. 1990) that are largely driven by climate (Palmer et al. 2014). In this study, the three lakes are formed into three distinct pairs for comparison. Pair 1, Fish Lake and Lake Mendota, has deep depths but different surface areas, illustrating the effects of surface area differences. Pair 2, Lake Wingra and Fish Lake, has similar surface areas, but shallow and deep water depths, addressing the effects of lake depth. Pair 3, Lake Mendota and Lake Wingra, has both differing surface areas and water depths. The coherence of ice cover variables for the three pairs is discussed in the following.

For the ice cover variables, correlation coefficients of pairs of lakes are high, e.g. ice on dates (Fish-Mendota: $r = 0.99$, Wingra-Fish: $r = 0.99$, Mendota-Wingra: $r = 0.99$) ice-off dates (Fish-Mendota: $r = 0.99$, Wingra-Fish: $r = 0.99$, Mendota-Wingra: $r = 0.99$), and maximum ice thickness Fish-Mendota: $r = 0.98$, Wingra-Fish: $r = 0.93$, Mendota-Wingra: $r = 0.90$). The results suggest that morphometry does not play a significant role in the coherence of ice cover among the three study lakes. Similar results were reported in Alaska, where the average degree of coherence of ice-out within lake districts was 0.74 (Arp et al. 2013). The range of within-district coherence appeared similar among lakes within a district with varying elevations, lake size, and other morphometric and physiographic attributes (Arp et al. 2013), indicating that ice cover loss in lakes is driven primarily by air temperature. Nevertheless, previous studies showed the actual rate of decay and development of ice-free conditions do vary greatly among lakes within a region, depending on a number of factors, particularly lake morphometry and landscape setting (Gao and Stefan 1999; Williams et al. 2004; Brown and Duguay 2010).

3.5.3 Sensitivity to changes in air temperature change

Under the warmer air temperatures, Fish Lake has the most occurrences of no ice cover (indicated by black color in Figure 3-8). Lake Mendota has fewer ice-free occurrences because the larger lake surface area facilitates greater overall heat input, which allows the lake to adjust to isothermal conditions and form ice more quickly. In contrast, almost all the ice cover remains in Lake Wingra as the shallow lake has lower heat storage and responds to air temperature changes more quickly. Overall, the results indicate that deeper lakes are more at risk for thin or no ice conditions than are shallow lakes. Under cooler air temperatures (i.e. the bottom half of the colorplots), Fish Lake, Lake Wingra, and Lake Mendota all show similar increases in maximum ice thickness.

To examine how each lake responds to the increasing air temperature we perform simulations of air temperature perturbations from −10°C to +10°C (Figure 3-9). As air temperature increases, ice growth starts to more closely resemble that of a warm air temperature year. Ice-on dates for Fish Lake and Lake Mendota occur later with some extreme differences of 30 days under changes of +7°C and +8°C in Fish Lake and +8°C and +9°C in Lake Mendota. In contrast, ice on dates for Lake Wingra remain fairly consistent through all temperature scenarios, suggesting that cooling in a shallow lake is not sensitive to increasing air temperature. However, very early, short ice cover periods (November 15 to December 6, 1916) on Lake Wingra no longer occur after an air temperature increase of +3°C. The ice-off dates, different from ice-on dates, show consistently earlier break up for all three of the study lakes. The maximum ice thickness dramatically decreases for all three lakes, and the timing of the date of maximum ice occurs earlier in the season. Interestingly, under an extreme air temperature increase of 9-10°C,

the timing of ice off among the three lakes seems to occurs at the same time since ice melting in the spring may be mainly governed by solar radiation (Kirillin et al. 2012).

3.5.4 Role of lake morphometry

The influence of lake morphometry in terms of three attributes (i.e. lake geometry ratio, lake surface area, and lake depth) on lake ice cover are discussed in the following.

3.5.4.1 Role of lake geometry ratio

For characterizing lake stratification, Stefan et al. (1996) proposed a lake geometry ratio $A_s^{0.25}$: H_{max} , where A_s is lake surface area and H_{max} is the maximum depth. The ratio was originally obtained from a criterion as $H_{max} = 0.34A_s^{0.25}$ (Gorham and Boyce 1989). Geometry ratios above 6 generally represent lakes that are polymictic and geometry ratios below 4 denote lakes that are strongly stratified (Fang and Stefan 1997). In this study, the geometry ratios for Fish Lake, Lake Mendota, and Lake Wingra, are 1.62, 3.13, and 7.31, respectively. The large geometry ratio for Lake Wingra indicates the lake is polymictic, and it cools down quickly in the autumn enabling earlier ice formation. Under historical and perturbation scenarios, Lake Wingra has a smaller change in ice cover, indicating that lakes with larger geometry ratios may be more resilient to changes in air temperature than lakes with smaller ratios.

3.5.4.2 Role of lake surface area

While air temperature is the most significant driver for ice cover, lake surface area can also play a role in the timing and trend of ice cover formation and thickness (Williams and Stefan 2006). Stronger winds break up initial skim ice and slightly delay the formation of continuous ice cover, leading to later ice-on dates as lake surface area (fetch) increases due to increased wind shear (Williams et al. 2004; Brown and Duguay 2010). Due to Lake Mendota's

larger fetch, decreasing wind speed in Madison, Wisconsin would cause a smaller relative change in wind shear across Lake Mendota than in Fish Lake, explaining the slightly larger change in ice-on dates in Fish Lake than in Lake Mendota, as shown in Table 3-4.

The trend of ice-off dates for Fish Lake and Lake Mendota are similar, which is in agreement with previous findings of low correlation between lake surface area and ice-off dates (Williams et al. 2004; Brown and Duguay 2010). However, differences are evident in the extreme air temperature perturbations (Figure 3-9). Ice decay takes place at the top and bottom of the ice column and along the lateral edges due to both decaying and mechanical disintegration (Woo and Heron; Brown and Duguay 2010). Field data (Jakkila et al. 2009; Leppäranta 2010) show that bottom, internal, and surface melting are of the same magnitude, but an increasing air temperature elevates the effects of lateral ice decay (Arp et al. 2013), making the smaller lakes decrease in ice cover more rapidly than the larger Lake Mendota. The effect may explain the smaller ice duration in Fish Lake under extreme warm temperatures.

3.5.4.3 Role of lake depth

Water depth is an important morphological aspect of a lake in regards to ice cover (Korhonen 2006; Kirillin et al. 2012). A lake larger in volume (or depth) will need more time to cool down (or heat up) than a lake of similar area but with smaller volume (or shallow depth). Specifically, the ice-on dates for Fish Lake and Lake Mendota are significantly later than Lake Wingra (see Figure 3-5). Under extreme warm air temperatures (10°C warmer), model results show that Lake Wingra rarely experiences ice-free winters while Lake Mendota and Fish Lake have many ice-free winters (Figure 8). Brown and Duguay (2010) indicated that lake depth determines the amount of heat storage in the water and hence the time needed for the lake to cool and freeze. Deeper lakes require a longer period with air temperature below 0°C before they

freeze over since larger heat storage requires longer times to cool to a freezing temperature (Jensen et al. 2007; Kirillin et al. 2012). Under increased air temperatures, increased heat storage and slower temperature response in deeper lakes will delay ice-on dates more than in shallower lakes. In other words, deeper lakes are more sensitive than shallow lakes to the increasing air temperature trend. Furthermore, during the historical climate, maximum ice thickness decreased at a much slower rate in the shallow Lake Wingra than the deeper Lake Mendota and Fish Lake (Table 3-4). This trend still holds under the extreme warm air temperature perturbations (Figure 3-8). Interestingly, while more resilient to changes in air temperature, Lake Wingra has experienced thinner average ice cover, compared with Fish Lake and Lake Mendota (see Table 3-4). This may be explained by the higher sediment heat storages and heat flux in winter in shallow lakes (Ellis et al. 1991; Fang and Stefan 1996; Golosov et al. 2007), which can increase under-ice water temperatures and thus decrease ice thickness.

3.5 Conclusion

In this study, an ice model is added to one-dimensional hydrodynamic model. The DYRESM-WQ-I model is employed to simulate the ice cover of three lakes with differing morphometry, Fish Lake, Lake Wingra, and Lake Mendota, from 1911-2014. The model reliably reproduces the interannual variations and long term trends in ice cover for the three lakes. To our knowledge, this study presents the first attempt to model ice cover of three lakes with differing morphometries over a period of as long as a century. Simulated ice cover over the century has changed dramatically, with all three lakes experiencing later freezing, earlier breakup, shorter ice cover duration, and thinner maximum ice thickness. These results agree with the observational data and previous studies. Perturbation simulations show that a small increase in air temperature (3 - 4°C) may inhibit ice cover of the deeper lakes during some years, while the shallow Lake

Wingra may experience ice cover even under the +10°C air temperature perturbation. Analysis of ice cover on three different study lakes indicates that shallower lakes, such as Lake Wingra, are more resilient to changes in air temperature than their deeper counterparts. Additionally, lakes with larger surface areas can cool more quickly through wind mixing, which allows for easier ice formation on those lakes compared to lakes of similar depth with smaller surface areas. Shallower lakes with larger surface areas appear more resilient to changes in ice cover caused by warmer air temperatures.

3.6 Acknowledgements

The research funding was provided in part by the U.S. National Science Foundation Long-Term Ecological Research Program, NOAA-Ocean and Human Health, University of Wisconsin (UW) Water Resources Institute USGS 104(B) Research Project, and UW Office of Sustainability SIRE Award Program. In addition, funding support for the first author by the College of Engineering Grainer Wisconsin Distinguished Graduate Fellowship is acknowledged. We would like to specifically thank David Hamilton for providing the DYRESM-WQ model (Hamilton and Schladow, 1997) and Yi-Fang Hsieh for further developing an ice module into the DYRESM-WQ model in work that was initiated by Brett Wallace. We also acknowledge that Yi-Fang Hsieh collected ice data for our model calibration and validation of Lake Mendota. Finally, the authors would like to thank John Magnuson at the Center of Limnology for his insightful suggestions and valuable comments regarding climate change on ice, and Dale Robertson at Wisconsin USGS and Richard (Dick) Lathrop at the Center of Limnology for providing valuable long-term observation data.

3.7 References

Adams, W. 1976. Diversity of lake-cover and its implications. Musk-Ox **18**: 86–98.

Adrian, R., C. M. O'Reilly, H. Zagarese, and others. 2009. Lakes as sentinels of climate change. Limnol. Oceanogr. **54**: 2283–2297.

Arp, C. D., B. M. Jones, and G. Grosse. 2013. Recent lake ice-out phenology within and among lake districts of Alaska, U.S.A. Limnol. Oceanogr. **58**: 2013–2028. doi:10.4319/lo.2013.58.6.2013

Ashton, G. D. 1986. River and lake ice engineering, Water Resources Publications.

Austin, J. A., and S. M. Colman. 2007. Lake Superior summer water temperatures are increasing more rapidly than regional air temperatures: A positive ice-albedo feedback. Geophys. Res. Lett. **34**: L06604. doi:10.1029/2006GL029021

Baron, J., and N. Caine. 2000. Temporal coherence of two alpine lake basins of the Colorado Front Range, U.S.A. Freshw. Biol. **43**: 463–476. doi:10.1046/j.1365-2427.2000.00517.x

Bengtsson, L. 1986. Spatial Variability of Lake Ice Covers. Geogr. Ann. Ser. Phys. Geogr. **68**: 113–121. doi:10.2307/521182

Bernhardt, J., C. Engelhardt, G. Kirillin, and J. Matschullat. 2011. Lake ice phenology in Berlin-Brandenburg from 1947–2007: observations and model hindcasts. Clim. Change **112**: 791–817. doi:10.1007/s10584-011-0248-9

Brown, L. C., and C. R. Duguay. 2010. The response and role of ice cover in lake-climate interactions. Prog. Phys. Geogr. **34**: 671–704. doi:10.1177/0309133310375653

Butcher, J. B., D. Nover, T. E. Johnson, and C. M. Clark. 2015. Sensitivity of lake thermal and mixing dynamics to climate change. Clim. Change **129**: 295–305. doi:10.1007/s10584-015-1326-1

Carpenter, S. R., and R. C. Lathrop. 2008. Probabilistic Estimate of a Threshold for Eutrophication. Ecosystems **11**: 601–613. doi:10.1007/s10021-008-9145-0

Dibike, Y., T. Prowse, T. Saloranta, and R. Ahmed. 2011. Response of Northern Hemisphere lake-ice cover and lake-water thermal structure patterns to a changing climate. Hydrol. Process. n/a-n/a. doi:10.1002/hyp.8068

Duguay, C. R., G. M. Flato, M. O. Jeffries, P. Ménard, K. Morris, and W. R. Rouse. 2003. Ice-cover variability on shallow lakes at high latitudes: model simulations and observations. Hydrol. Process. **17**: 3465–3483. doi:10.1002/hyp.1394

Ellis, C. R., H. G. Stefan, and R. Gu. 1991. Water Temperature Dynamics and Heat Transfer Beneath the Ice Cover of a Lake. Limnol. Oceanogr. **36**: 324–335.

Fang, X., and H. G. Stefan. 1996. Dynamics of heat exchange between sediment and water in a lake. Water Resour. Res. **32**: 1719–1727. doi:10.1029/96WR00274

Fang, X., and H. G. Stefan. 1997. Simulated climate change effects on dissolved oxygen characteristics in ice-covered lakes. Ecol. Model. **103**: 209–229. doi:10.1016/S0304-3800(97)00086-0

Fang, X., and H. G. Stefan. 2000. Projected Climate Change Effects on Winterkill in Shallow Lakes in the Northern United States. Environ. Manage. **25**: 291–304.

Fang, X., and H. G. Stefan. 2009. Simulations of climate effects on water temperature, dissolved oxygen, and ice and snow covers in lakes of the contiguous U.S. under past and future climate scenarios. Limnol. Oceanogr. **54**: 2359–2370. doi:10.4319/lo.2009.54.6_part_2.2359

Gao, S., and H. G. Stefan. 1999. Multiple Linear Regression for Lake Ice and Lake Temperature Characteristics. J. Cold Reg. Eng. **13**: 59–77. doi:10.1061/(ASCE)0887-381X(1999)13:2(59)

Golosov, S., O. A. Maher, E. Schipunova, A. Terzhevik, G. Zdorovennova, and G. Kirillin. 2007. Physical background of the development of oxygen depletion in ice-covered lakes. Oecologia **151**: 331–340. doi:10.1007/s00442-006-0543-8

Gorham, E., and F. Boyce. 1989. influence of lake surface area and depth upon thermal stratification and the depth of the summer thermocline. J. Gt. Lakes Res. **15**: 233–245.

Grawe, D., H. L. Thompson, J. A. Salmond, X.-M. Cai, and K. H. Schlünzen. 2013. Modelling the impact of urbanisation on regional climate in the Greater London Area. Int. J. Climatol. **33**: 2388–2401. doi:10.1002/joc.3589

Hamilton, D. P., and S. G. Schladow. 1997. Prediction of water quality in lakes and reservoirs. Part I — Model description. Ecol. Model. **96**: 91–110. doi:10.1016/S0304-3800(96)00062-2

Hipsey, M. R., L. C. Bruce, and D. P. Hamilton. 2014. GLM - General Lake Model: Model overview and user information. AED Report #26. AED Report #26 The University of Western Perth.

Hostetler, S. W., and P. J. Bartlein. 1990. Simulation of lake evaporation with application to modeling lake level variations of Harney-Malheur Lake, Oregon. Water Resour. Res. **26**: 2603–2612. doi:10.1029/WR026i010p02603

Hsieh, Y. 2012. Modeling ice cover and water temperature of Lake Mendota. PhD Thesis. University of Wisconsin-Madison.

Hsieh, Y.-F. 2013. Lake Mendota at North Temperate Lakes LTER: Snow and Ice Depth 2009-2010.

IPCC. 2007. Summary for Policymakers, p. 18. *In* S. Solomon, D. Qin, M. Manning, Z. Chen, M. Marquis, K.B. Averyt, M. Tignor, and H.L. Miller [eds.], Climate Change 2007: The Physical Science Basis. Contribution of Working Group 1 to the Fourth Assessment Report of the Intergovernmental Panel on Climate Change. Cambridge University Press.

Jakkila, J., M. Leppäranta, T. Kawamura, K. Shirasawa, and K. Salonen. 2009. Radiation transfer and heat budget during the ice season in Lake Pääjärvi, Finland. Aquat. Ecol. **43**: 681–692. doi:10.1007/s10452-009-9275-2

Järvinen, M., M. Rask, J. Ruuhijärvi, and L. Arvola. 2002. Temporal coherence in water temperature and chemistry under the ice of boreal lakes (Finland). Water Res. **36**: 3949–3956. doi:10.1016/S0043-1354(02)00128-8

Jeffries, M. O., and K. Morris. 2007. Some aspects of ice phenology on ponds in central Alaska, USA. Ann. Glaciol. **46**: 397–403.

Jensen, O. P., B. J. Benson, J. J. Magnuson, V. M. Card, M. N. Futter, P. A. Soranno, and K. M. Stewart. 2007. Spatial analysis of ice phenology trends across the Laurentian Great Lakes region during a recent warming period. Limnol. Oceanogr. **52**: 2013–2026. doi:10.4319/lo.2007.52.5.2013

Jöhnk, K. D., J. Huisman, J. Sharples, B. Sommeijer, P. M. Visser, and J. M. Stroom. 2008. Summer heatwaves promote blooms of harmful cyanobacteria. Glob. Change Biol. **14**: 495–512. doi:10.1111/j.1365-2486.2007.01510.x

Kirillin, G. 2010. Modeling the impact of global warming on water temperature and seasonal mixing regimes in small temperate lakes. Boreal Environ. Res. **15**: 279–293.

Kirillin, G., M. Leppäranta, A. Terzhevik, and others. 2012. Physics of seasonally ice-covered lakes: a review. Aquat. Sci. **74**: 659–682. doi:10.1007/s00027-012-0279-y

Klink, K. 2002. Trends and Interannual Variability of Wind Speed Distributions in Minnesota. J. Clim. **15**: 3311–3317. doi:10.1175/1520-0442(2002)015<3311:TAIVOW>2.0.CO;2

Korhonen, J. 2006. Long-term trends in lake ice cover in Finland. *Proceedings of the 18th IAHR international symposium on ice*. 71–78.

Krohelski, J. T., Y.-F. Lin, W. J. Rose, and R. J. Hunt. 2002. Simulation of Fish, Mud, and Crystal Lakes and the shallow ground-water system, Dane County, Wisconsin. USGS Numbered Series 2002–4014. 2002–4014 U.S. Geological Survey.

Lathrop, R. C., S. R. Carpenter, and L. G. Rudstam. 1996. Water clarity in Lake Mendota since 1900: responses to differing levels of nutrients and herbivory. Can. J. Fish. Aquat. Sci. **53**: 2250–2261. doi:10.1139/f96-187

Leppäranta, M. 2010. Modelling the Formation and Decay of Lake Ice, p. 63–83. *In* G. George [ed.], The Impact of Climate Change on European Lakes. Springer Netherlands.

Leppäranta, M., A. Reinart, A. Erm, H. Arst, M. Hussainov, and L. Sipelgas. 2003. Investigation of Ice and Water Properties and Under-ice Light Fields in Fresh and Brackish Water Bodies. Hydrol. Res. **34**: 245–266.

Li, Z., Z. Yan, K. Tu, W. Liu, and Y. Wang. 2011. Changes in wind speed and extremes in Beijing during 1960–2008 based on homogenized observations. Adv. Atmospheric Sci. **28**: 408–420. doi:10.1007/s00376-010-0018-z

Livingstone, D. M. 1993. Lake Oxygenation: Application of a One-box Model with Ice Cover. Int. Rev. Gesamten Hydrobiol. Hydrogr. **78**: 465–480. doi:10.1002/iroh.19930780402

MacKay, M. D., P. J. Neale, C. D. Arp, and others. 2009. Modeling lakes and reservoirs in the climate system. Limnol. Oceanogr. **54**: 2315–2329. doi:10.4319/lo.2009.54.6_part_2.2315

Magee, M. R., C. H. Wu, D. M. Robertson, R. C. Lathrop, and D. P. Hamilton. 2016. Trends and abrupt changes in 104 years of ice cover and water temperature in a dimictic lake in response to air temperature, wind speed, and water clarity drivers. Hydrol Earth Syst Sci **20**: 1681–1702. doi:10.5194/hess-20-1681-2016

Magnuson, J. J., B. J. Benson, and T. K. Kratz. 1990. Temporal coherence in the limnology of a suite of lakes in Wisconsin, U.S.A. Freshw. Biol. **23**: 145–159. doi:10.1111/j.1365-2427.1990.tb00259.x

Magnuson, J. J., T. K. Kratz, B. J. Benson, and K. E. Webster. 2006. Coherent Dynamics among Lakes, p. 89–106. *In* J.J. Magnuson, T.K. Kratz, and B.J. Benson [eds.], Long-term Dynamics of Lakes in the Landscape: Long-term Ecological Research on North Temperate Lakes. Oxford University Press.

Magnuson, J. J., D. M. Robertson, B. J. Benson, and others. 2000. Historical Trends in Lake and River Ice Cover in the Northern Hemisphere. Science **289**: 1743–1746. doi:10.1126/science.289.5485.1743

Magnuson, J. J., K. E. Webster, R. A. Assel, and others. 1997. Potential Effects of Climate Changes on Aquatic Systems: Laurentian Great Lakes and Precambrian Shield Region. Hydrol. Process. **11**: 825–871. doi:10.1002/(SICI)1099-1085(19970630)11:8<825::AID-HYP509>3.0.CO;2-G

McKee, T. B., N. J. Doesken, C. A. Davey, and Pielke, Sr. 2000. Climate data continuity with ASOS. Report for period April 1996 through June 2000. Climno Report 00-3. Climno Report 00-3 Colorado Climate Center, Department of Atmospheric Science, Colorado State University.

Novikmec, M., M. Svitok, D. Kočický, F. Šporka, and P. Bitušík. 2013. Surface Water Temperature and Ice Cover of Tatra Mountains Lakes Depend on Altitude, Topographic Shading, and Bathymetry. Arct. Antarct. Alp. Res. **45**: 77–87. doi:10.1657/1938-4246-45.1.77

NTL LTER. 1996. North Temperature Lakes TLER: Ice Duration - Madison Lakes Area 1853 - current.

NTL LTER. 2012a. North Temperate Lakes LTER: Secchi Disk Depth; Other Auxiliary Base Crew Sample Data 1981 - current.

NTL LTER. 2012b. North Temperature Lakes LTER: Physical Limnology of Primary Study Lakes 1981-current.

NTL LTER. 2012c. North Temperate Lakes LTER: Snow and Ice Depth 1982 - current.

Palmer, M. E., N. D. Yan, and K. M. Somers. 2014. Climate change drives coherent trends in physics and oxygen content in North American lakes. Clim. Change **124**: 285–299. doi:10.1007/s10584-014-1085-4

Perroud, M., and S. Goyette. 2010. Impact of warmer climate on Lake Geneva water-temperature profiles. Boreal Environ. Res. **15**: 255–278.

Perroud, M., S. Goyette, A. Martynov, M. Beniston, and O. Anneville. 2009. Simulation of multiannual thermal profiles in deep Lake Geneva: A comparison of one-dimensional lake models. Limnol. Oceanogr.-Methods **54**: 1574–1594.

Phillips, K. A., and M. W. Fawley. 2002. Winter phytoplankton community structure in three shallow temperate lakes during ice cover. Hydrobiologia **470**: 97–113. doi:10.1023/A:1015667803372

Pryor, S. C., R. J. Barthelmie, and E. Kjellström. 2005. Potential climate change impact on wind energy resources in northern Europe: analyses using a regional climate model. Clim. Dyn. **25**: 815–835. doi:10.1007/s00382-005-0072-x

Pryor, S. C., R. J. Barthelmie, D. T. Young, and others. 2009. Wind speed trends over the contiguous United States. J. Geophys. Res. Atmospheres **114**: D14105. doi:10.1029/2008JD011416

Read, J. S., D. P. Hamilton, A. R. Desai, and others. 2012. Lake-size dependency of wind shear and convection as controls on gas exchange. Geophys. Res. Lett. **39**: L09405. doi:10.1029/2012GL051886

Robertson, D. M. 1989. The use of lake water temperature and ice cover as climatic indicators. PhD Thesis. University of Wisconsin-Madison.

Robertson, D. M., and R. A. Ragotzkie. 1990. Changes in the thermal structure of moderate to large sized lakes in response to changes in air temperature. Aquat. Sci. **52**: 360–380. doi:10.1007/BF00879763

Robertson, D. M., R. A. Ragotzkie, and J. J. Magnuson. 1992. Lake ice records used to detect historical and future climatic changes. Clim. Change **21**: 407–427. doi:10.1007/BF00141379

Rogers, C. K., G. A. Lawrence, and P. F. Hamblin. 1995. Observations and numerical simulation of a shallow ice-covered midlatitude lake. Limnol. Oceanogr. **40**: 374–385. doi:10.4319/lo.1995.40.2.0374

Schatz, J., and C. J. Kucharik. 2014. Seasonality of the Urban Heat Island Effect in Madison, Wisconsin. J. Appl. Meteorol. Climatol. **53**: 2371–2386. doi:10.1175/JAMC-D-14-0107.1

Stefan, H. G., X. Fang, and J. G. Eaton. 2001. Simulated Fish Habitat Changes in North American Lakes in Response to Projected Climate Warming. Trans. Am. Fish. Soc. **130**: 459–477. doi:10.1577/1548-8659(2001)130<0459:SFHCIN>2.0.CO;2

Stefan, H. G., M. Hondzo, X. Fang, J. G. Eaton, and J. H. McCormick. 1996. Simulated long term temperature and dissolved oxygen characteristics of lakes in the north-central United States and associated fish habitat limits. Limnol. Oceanogr. **41**: 1124–1135. doi:10.4319/lo.1996.41.5.1124

Stewart, K. M. 1965. Physical limnology of some Madison lakes. PhD Thesis. University of Wisconsin-Madison.

Tanentzap, A. J., D. P. Hamilton, and N. D. Yan. 2007. Calibrating the Dynamic Reservoir Simulation Model (DYRESM) and filling required data gaps for one-dimensional thermal profile predictions in a boreal lake. Limnol. Oceanogr. Methods **5**: 484–494. doi:10.4319/lom.2007.5.484

Thompson, R., C. Kamenik, and R. Schmidt. 2005. Ultra-sensitive Alpine lakes and climate change. J. Limnol. **64**: 139–152.

Tonn, W. M., and J. J. Magnuson. 1982. Patterns in the Species Composition and Richness of Fish Assemblages in Northern Wisconsin Lakes. Ecology **63**: 1149–1166. doi:10.2307/1937251

United States Geological Survey (USGS). 2010. USGS 05406050, Lake State Data, Fish Lake, WI.

Vavrus, S. J., R. H. Wynne, and J. A. Foley. 1996. Measuring the sensitivity of southern Wisconsin lake ice to climate variations and lake depth using a numerical model. Limnol. Oceanogr. **41**: 822–831. doi:10.4319/lo.1996.41.5.0822

Voutilainen, A., T. Huttula, J. Juntunen, M. Rahkola-Sorsa, K. Rasmus, and M. Viljanen. 2014. Diverging site-specific trends in the water temperature of a large boreal lake in winter and summer due to mixed effects of local features and climate change. Boreal Environ. Res. **19**: 104–114.

Weyhenmeyer, G. A., T. Blenckner, and K. Pettersson. 1999. Changes of the plankton spring outburst related to the North Atlantic Oscillation. Limnol. Oceanogr. **44**: 1788–1792. doi:10.4319/lo.1999.44.7.1788

Weyhenmeyer, G. A., D. M. Livingstone, M. Meili, O. Jensen, B. Benson, and J. J. Magnuson. 2011. Large geographical differences in the sensitivity of ice-covered lakes and rivers in the Northern Hemisphere to temperature changes: GLOBAL CHANGE ON LAKE AND RIVER ICE-COVER. Glob. Change Biol. **17**: 268–275. doi:10.1111/j.1365-2486.2010.02249.x

Weyhenmeyer, G. A., M. Meili, and D. M. Livingstone. 2004. Nonlinear temperature response of lake ice breakup: Patterns of lake ice breakup. Geophys. Res. Lett. **31**: n/a-n/a. doi:10.1029/2004GL019530

Williams, D. T., G. R. Drummond, D. E. Ford, and D. L. Robey. 1980. Determination of light extinction coefficients in lakes and reservoirs. *Proceedings of the Symposium on Surface Water Impoundments*. Proceedings of the Symposium on Surface Water Impoundments. 1329–1335.

Williams, G., K. L. Layman, and H. G. Stefan. 2004. Dependence of lake ice covers on climatic, geographic and bathymetric variables. Cold Reg. Sci. Technol. **40**: 145–164. doi:10.1016/j.coldregions.2004.06.010

Williams, G. P. 1965. Correlating Freeze-Up and Break-Up with Weather Conditions. Can. Geotech. J. **2**: 313–326. doi:10.1139/t65-047

Williams, S. G., and H. G. Stefan. 2006. Modeling of Lake Ice Characteristics in North America Using Climate, Geography, and Lake Bathymetry. J. Cold Reg. Eng. **20**: 140–167. doi:10.1061/(ASCE)0887-381X(2006)20:4(140)

Wisconsin Initiative on Climate Change Impacts (WICCI). 2011. Wisconsin's Changing Climate: Impacts and Adaptation. Nelson Institute for Environmental Studies, University of Wisconsin - Madison and the Wisconsin Department of Natural Resources.

Woo, M., and R. Heron. Freeze-up and break-up of ice cover on small Arctic lakes, p. 56–62. *In* W. Mackay [ed.], Northern lakes and rivers. Boreal Institute for Northern Studies.

Yao, H., N. R. Samal, K. D. Joehnk, X. Fang, L. C. Bruce, D. C. Pierson, J. A. Rusak, and A. James. 2014. Comparing ice and temperature simulations by four dynamic lake models in Harp Lake: past performance and future predictions. Hydrol. Process. **28**: 4587–4601. doi:10.1002/hyp.10180

Yeates, P. S., and J. Imberger. 2003. Pseudo two-dimensional simulations of internal and boundary fluxes in stratified lakes and reservoirs. Int. J. River Basin Manag. **1**: 297–319. doi:10.1080/15715124.2003.9635214

Chapter 4 Meteorological and water quality factors influencing cisco oxythermal habitat in Lake Mendota, WI, USA.

The following is in preparation for submission to the *Canadian Journal of Fisheries and Aquatic Sciences*

Magee MR, PB McIntyre, PC Hanson, CH Wu. Meteorological and water quality factors influencing cisco oxythermal habitat in Lake Mendota, WI, USA.

4.1 Abstract

Using a one-dimensional hydrodynamic-water quality model, we investigate whether climate-caused reductions in oxythermal fish habitat can be mitigated through phosphorus loading reductions. Temperature at dissolved oxygen of 3 mg L^{-1} (TDO3) is used to characterize oxythermal habitat of cisco (*Coregonus artedi*) in Lake Mendota, WI, USA over the period 1976 – 2013 and we determine that summer (Jun – Aug) air temperatures, spring (Mar – May) phosphorus load, and spring inflow influence maximum summer TDO3 values in the lake. Air temperature has the greatest influence on TDO3 values, but increases can be offset through reductions in phosphorus load. Under the A1B air temperature scenario, a 25% reduction in phosphorus load at a cost as low as US$16.9 could ensure TDO3 values remain at current levels, while a 75% reduction in phosphorus load at an estimated cost of US$155 million – US$167 million would improve oxythermal habitat over the current conditions and potentially enable the promotion and maintenance of the cisco population in a vulnerable lake.

4.2 Introduction

Cisco (*Coregonus artedi*) are a cold-water fish species and an important forage fish for many top predators in Canada and the northern United States (Jacobson et al. 2010; Van Zuiden et al. 2016). Physiologically, cisco require cold, well-oxygenated water to survive and reproduce (Cahn 1927; Frey 1955; Jacobson et al. 2008), and are normally found in large, deep inland lakes (Rudstam and Magnuson 1985; Jacobson et al. 2008). These physiological requirements and susceptibility to oxythermal mortality make cisco a good indicator of ecological stressors that reduce cold-water habitat (Jacobson et al. 2008). During the summer months, cisco find refuge in the hypolimnion, but they are forced to move to warmer, potentially unsuitable waters when hypolimnetic oxygen levels decrease during the stratified season (Aku et al. 1997; Ficke et al. 2007; Jacobson et al. 2008). In Wisconsin, cisco are near the southern edge of their range (Becker 1983; Lyons et al. 2000) and are at considerable risk due to both global climate change (Sharma et al. 2011; Herb et al. 2014; Van Zuiden et al. 2016) and cultural eutrophication (Jacobson et al. 2010).

Cultural eutrophication can reduce cisco habitat (Evans et al. 1996; Jacobson et al. 2010; Honsey et al. 2016) because increased primary production (Carpenter 2005) and organic material decomposition depletes hypolimnetic oxygen (Nürnberg 1995; Ito and Momii 2015). Cisco habitat is reduced as dissolved oxygen (DO) concentrations in the hypolimnion are depleted to lethal levels, forcing cisco to search for refuge habitat in the warmer epilimnion. Jacobson et al. (2010) found that phosphorus (P) plays a pivotal role in availability of cold-water fish habitat in Minnesota lakes., and Latta (1995) found that ciscoes have been extirpated from at least 14 % of Michigan lakes as a result of eutrophication. In Indiana, near the southern extent of the cisco range (Frey 1955), appropriate habitat is scarce (Clingerman et al. 2013), and cisco are limited to

the least eutrophic lakes (Honsey 2014; Honsey et al. 2016), suggesting that nutrient loading is an important driver of cisco extirpations (Honsey et al. 2016). Further exacerbating the impacts of cultural eutrophication are changes in climate (De Stasio et al. 1996; Jacobson et al. 2010; Herb et al. 2014).

Global climate change significantly alters lake water temperatures (Perroud and Goyette 2010; O'Reilly et al. 2015; Magee et al. 2016) and lake stability (Livingstone 2003; Hetherington et al. 2015), further reducing the availability of cold-water fish habitat (Sharma et al. 2011; Lynch et al. 2015; Santiago et al. 2016; Van Zuiden et al. 2016). The majority of P inputs into lake ecosystems occur as the result of extreme loading events (Gonzalez-Hidalgo et al. 2013; Duan et al. 2013; Carpenter et al. 2015). Heavy rain events, which are expected to increase with climate change (Kucharik et al. 2010; IPCC 2013) can wash P-rich soil from open ground onto surface waters (Lathrop 2007; Carpenter et al. 2015). Increasing air temperature has been shown to increase water temperatures (Kirillin 2010; O'Reilly et al. 2015; Magee et al. 2016), which can reduce cisco habitat and increase lake stability (Hadley et al. 2014; Ito and Momii 2015). This inhibits upwelling and mixing events that can increase hypolimnetic DO, further exacerbating the effects of cultural eutrophication. Warmer air temperatures and decreasing wind speeds increase stratification duration (Gerten and Adrian 2000; Cahill et al. 2005; Kerimoglu and Rinke 2013; Magee et al. 2016), isolating the hypolimnion from atmospheric exchange, making it more likely that hypolimnion DO levels will reduce to stressful or lethal levels (De Stasio et al. 1996; Stefan et al. 2001; Fang et al. 2012). The combination of warmer water and lower dissolved oxygen concentrations under climate and cultural eutrophication scenarios in lakes historically suitable for cold-water fishes could result in cisco extirpation.

Lake Mendota, a lake near the southern edge of cisco range (Lyons et al. 2000) has experienced significant summer cisco mortalities throughout its history and the population started declining after 1987 (Brock 1985; Lathrop et al. 1992; McDermot and Rose 2000). Historically, temperature and DO thresholds for the species have restricted the fish to a narrow "cisco layer" (Frey 1955; Rudstam and Magnuson 1985; Lathrop et al. 1992). In Lake Mendota, this layer historically allows cisco to occupy a 4 m depth range in the lower epilimnion and survive in most summers (Rudstam and Magnuson 1985; Lathrop et al. 1992); however declines (Lathrop et al. 1992), including a mass mortality event in 1987 (Lathrop et al. 1992; McDermot and Rose 2000), where the population declined by over 90% (Lathrop et al. 1992; Johnson and Kitchell 1996; Kitchell 2012) have significantly reduced the population. Cisco have not recovered since this time. During this same period, average air temperatures have increased significantly (Kucharik et al. 2010; Magee et al. 2016), and extensive management efforts have been undertaken to control the eutrophication problem in the lake (Lathrop et al. 1998; Lathrop 2007; Lathrop and Carpenter 2014). Since Lake Mendota has a small, but sustained cisco population (NTL LTER 2012a), with historical summer fish mortalities (Lathrop et al. 1992) it represents an ideal site to investigate the relative role of climate changes and cultural eutrophication in year-to-year variability in cisco habitat. Additionally, the small sustained population indicates that management efforts (e.g. P loading reductions) and fish stocking could potentially be utilized to restore a larger population in the lake.

The goal of this study is three-fold. First, using a modeling approach to more accurately determine cisco habitat over a long time period (38 years), we want to determine the meteorological and water quality parameters associated year-to-year changes in cisco habitat within a single lake. Second, we want to analyze the effectiveness of a simple multiple linear

regression model in place of a complicated hydrodynamic-water quality model for characterizing year-to-year variability in available habitat. Finally, we wish to determine how cisco oxythermal habitat in Lake Mendota might change in the future and estimate P loading reductions that are necessary to offset climate changes and improve cisco habitat in Lake Mendota.

4.3 Methods

4.3.1 Site description

Lake Mendota (43°6' N; 89°24'W; Figure 2-1; Table 2-1) was chosen for this study because of its status as a cisco lake near the range-edge, eutrophic status, extensive historical datasets, and frequent water quality observations. It is a dimictic, eutrophic, drainage lake in an urbanizing agricultural watershed (Carpenter and Lathrop, 2008). Mendota has three main inflows and a single outflow, the Yahara River, which connects Mendota to the downstream Madison Chain of Lakes – Lake Monona, Lake Waubesa, and Lake Kegonsa. The lake is the most upstream in the chain, and a large portion of the watershed is agricultural, which has largely contributed to the lake's eutrophic status (Brock 1985) and Mendota's phosphorus dynamics have important implications for the downstream lakes (Walsh et al. 2016). Lake Mendota has a surface area of 3,940 ha, a mean depth of 12.8 m, a maximum depth of 25.3 m, a shoreline length of 33.8 km, and a maximum fetch of 9.8 km (Robertson and Ragotzkie 1990). The mean flushing rate is 0.23 yr^{-1} (Lathrop and Carpenter 2014). The lake stratifies during the summer, and typical stratification periods lasts from May to September. Mean summer (Jun – Aug) surface temperature is 22.4 °C, and hypolimnetic temperatures range in value from 11°C to 15 °C. Normal secchi depth during the summer is 3.0 meters (Lathrop et al., 1996).

4.3.1 Observation data

4.3.1.1 Meteorological data

Meteorological data used to drive the model includes total daily solar radiation, mean daily air temperature, mean daily vapor pressure, mean daily wind speed, mean cloud cover, total rainfall, and total snowfall. Meteorological data was collected as in Magee et al. (2016) based on a continuous daily meteorological dataset for Madison, Wisconsin from 1884 to 1988 that accounted for adjustments to site location, observation time, and surface roughness (Robertson 1989). Recent solar radiation data was gathered from http://www.sws.uiuc.edu/warm/weather, and other data was appended from the National Climate Data Center weather station at the Dane County Regional Airport (Truax Field; http://www.ncdc.noaa/gov). Wind speeds were adjusted based on changes in observational techniques in 1996 (McKee et al. 2000) as described in Magee et al. (2016).

4.3.1.2 Inflow and discharge data

Volumetric flow rates of three major inflows (Yahara River, Station #05427850; Pheasant Branch, Station #05427948; and Spring Harbor, Station #05427965) were acquired from USGS stream gage data (http://waterdata.usgs.gov/wi/nwis/sw/) at a daily frequency for the duration of the model period. Daily discharge from 1975 to 1997 were calculated from gate/lock/bypass pipe USGS ratings and local governmental daily operational records. From 1998 to 2003, daily outflow was estimated from downstream Lake Waubesa and Mendota outlet data from earlier years, and after 2003 daily outflow measurements were obtained from the USGS stream gage data (http://waterdata.usgs.gov/wi/nwis/uw/?site_no=05428000).

River water temperatures have been recorded at the Yahara River inlet since 2002, and are assumed to be the same for all three inflowing streams. Prior to 2002, daily river

temperatures were estimated from air temperatures (Hsieh 2012). River temperatures and weekly average air temperatures from 2002-2009 were correlated using a linear regression for air temperatures above freezing ($r^2 = 0.86$) and a polynomial regression for air temperatures below freezing ($r^2 = 0.68$).

Daily P loadings were estimated from 1976 – 1990 using the method from Lathrop et al. (1998). From 1990 – 2013, the Yahara River at the Windsor Site (usgs.gov) was used as a proxy for loading into the lake using the equation: total load = 4.5 x Yahara River at Windsor load ($r^2 = 0.97$) (Walsh et al. 2016). Total nitrogen (N) loads were estimated by assuming an approximately constant mass ratio of TN:TP in inflows as in Kara et al. (2012). Lake Mendota salinity is low, so inflow salinity was set to zero for this study.

4.3.1.3 Temperature and DO profiles

Long-term water temperature record were collected for 1976 – 2013 from Robertson (1989) and the NTL-LTER (2012b). Spatial resolution of temperature records was normally 1-meter, but varied from 0.5 m to 5m. The frequency of water temperature data varied from only one or two profiles per year to several profiles for a given day. DO profiles were collected from 1995 – 2013 by the NTL-LTER (2012b) at approximately 2-week temporal resolution and 1-meter spatial resolution during the open water season and once per year during ice cover.

4.3.2 DYRESM-WQ-I

In this study, a physically-based, one-dimensional hydrodynamic, lake-ice and water quality model is used to obtain daily temperature and DO profiles for Lake Mendota for the duration of the study period. A modeling approach is employed to estimate oxythermal habitat for cisco in the lake because long-term daily temperature and DO observational data are not available for the lake. Additionally, using a modeling approach allows us to more suitably test

sensitivity of oxythermal habitat in response to meteorological and water quality drivers. Since the projected climate scenarios are not found within the observed driver data, extrapolation of results beyond the observational data space is more reliable when a mechanistic model rather than empirical model is used (Loucks et al. 2005).

The model used in this paper is DYRESM-WQ-I (Magee et al. 2016; Hamilton et al. *in review*; Appendix A), which is based on the DYRESM-WQ model (Dynamic Reservoir Simulation Model – Water Quality model; Hamilton and Schladow 1997) with an additional ice model included that enables simulation of water temperature, ice cover, and water quality parameters year – round. The lake is represented by horizontal Lagrangian layers with uniform properties that may change in thickness. The hydrodynamic component includes algorithms for mixed layer processes, inflow, outflow, and hypolimnetic mixing (Hamilton and Schladow 1997). The ice model is a three-component ice and snow model based on the MLI model of Rogers et al. (1995) with alterations to two-way coupling of the water and ice components and the addition of a time-dependent sediment heat flux for all horizontal layers. A full description of the hydrodynamic and ice model can be found in Magee et al. (2016). The water quality model simulates phytoplankton production and loss, nutrient cycling, and the DO budget. Detailed descriptions of the phytoplankton and nutrient subroutines are found in Hamilton and Schladow (1997). The model is configured for three functional groups of phytoplankton: a non-nitrogen fixing genus represented by *Microsystis*, chlorophytes and chrysophytes, and diatoms. Phytoplankton mortality is incorporated into the phytoplankton parameters, which allows for regulation without enabling the zooplankton model. Bacteria is not specifically included in the model, but bacterial respiration processes in the hypolimnion are captured through the sediment oxygen demand. The model was initialized on 8 April, 1976 and run until 31 December 2013.

Simulation period was chosen based on available input and observation data, specifically, P loading data, which was available starting in 1976. Initial conditions were based on observed water temperatures at that time and an average of April chemical and biological observations collected from NTL-LTER (2012b).

4.3.3 Model parameterization and calibration

The hydrodynamic and ice cover components of the model were previously calibrated for Lake Mendota in Magee et al (2016). The model was calibrated for the period 2010-2013 by varying the minimum layer thickness with final layer thickness values chosen based on the least amount of deviation between predicted and observed temperature values for Lake Mendota. A detail of this analysis can be found in Magee et al. (2016) along with final hydrodynamic and ice model parameters (Table 1 in Magee et al. 2016). Evaporative flux is included in DYRESM-WQ-I and we assume that these are properly parameterized by the wind-driven equations in the model, although we did not independently validate modeled evaporation rates. DO was calibrated for Lake Mendota through trial – and – error adjustment of chemical and phytoplankton parameters within the bounds of available published literature values and assigned ranges and values for DYRESM-WQ-I until a satisfactory performance was achieved based on traditional goodness – of – fit metrics. Initial phytoplankton and chemical parameters before calibration were obtained from Kara et al. (2012) and Snortheim (2015), who similarly calibrated Lake Mendota using DYRESM-CAEDYM and GLM-FABM-AED, respectively with appropriate conversions between model units. Final calibrated chemical and phytoplankton parameters are provided in Table 4-1 and Table 4-2. Parameters not specifically listed are taken as default values from DYRESM-WQ (Hamilton and Schladow 1997).

Table 4-1: Assigned chemical parameters for DYRESM-WQ-I model

Parameter	Units	Assigned value
Light extinction coefficient of pure water	m^{-1}	0.25[A]
Fraction of incoming solar radiation which is photosynthetically active		0.45[A]
Oxygen demand of sub-euphotic sediments	g m^{-2} day^{-1}	2.25[C]
Decomposition rate of BOD	day^{-1}	0.02[D]
Rate constant for denitrification	day^{-1}	0.05[A]
Half saturation constant for effect of DO on denitrification	g DO m^{-3}	0.4[A]
Nitrification rate	day^{-1}	0.10[A]
Rate of conversion of organic phosphorus to DRP	day^{-1}	0.03[A]
Rate of conversion of organic nitrogen to ammonia	day^{-1}	0.04[C]
Density of TN and TP for settling	g cm^{-3}	1.02[D]
Diameter of TN/TP	µm	16[D]
Density of BOD for settling	g cm^{-3}	1.01[D]
BOD diameter	µm	16[D]
Half saturation constant for DO effect on nitrification	g DO m^{-3}	0.4[A]
Half saturation constant for DO effect on BOD decay	g DO m^{-3}	0.5[A]
Half saturation constant for DO effect on SOD decay	g DO m^{-3}	1.5[A]
Nitrification temperature multiplier		1.08[A]
Organic decomposition temperature multiplier		1.08[C]
Base release rate of phosphorus from sediments	mg m^{-2} day^{-1}	1.1[C]
Base release rate of ammonia from sediments	mg m^{-2} day^{-1}	12.5[C]
Temperature multiplier for sediment nutrient release		1.065[B]

Sources: [A] Kara et al. 2012; [B] Snortheim 2015; [C] calibration parameter; [D] default DYRESM-WQ-I parameter

4.3.4 Model evaluation

We used three goodness – of – fit measures to statistically evaluate model output against observational data: Spearman's rank correlation coefficient (Rho), normalized mean absolute error (NMAE), and root-mean squared error (RMSE). Statistics were calculated for observed and predicted data at times and depths when observations were made.

Table 4-2: Assigned phytoplankton parameters for DYRESM-WQ-I model

Parameter	**Unit**	**Assigned value**		
		Diatoms	**Chlorophytes**	***Microcystis***
Maximum algal growth rate	day^{-1}	1.25[A]	0.2[A]	0.6[A]
Maximum algal respiratory rate	day^{-1}	0.17[D]	0.17[D]	0.17[D]
Maximum algal mortality rate	day^{-1}	0.055[C]	0.055[C]	0.055[C]
Temperature multiplier for growth, respiration, death		1.08[A]	1.08[A]	1.07[A]
Light saturation for phytoplankton	$\mu E\ m^{-2}\ s^{-1}$	20[A]	170[A]	250[A]
Specific attenuation coefficient for chl*a*	m^2 (mg chl*a*)$^{-1}$	0.02[D]	0.02[D]	0.02[D]
Minimum phosphorus to chlorophyll mass ratio	mg P (mg chl*a*)$^{-1}$	0.24[C]	0.28[C]	0.25[C]
Minimum nitrogen to chlorophyll mass ratio	mg N (mg chl*a*)$^{-1}$	1.8[C]	1.4[C]	1.8[C]
Maximum phosphorus to chlorophyll mass ratio	mg P (mg chl*a*)$^{-1}$	2.5[C]	7.0[C]	7.0[C]
Maximum nitrogen to chlorophyll mass ratio	mg N (mg chl*a*)$^{-1}$	5.0[C]	2.4[C]	2.4[C]
Maximum uptake rate of phosphorus	mg P (mg chl*a*)$^{-1}$ day^{-1}	0.18[A]	0.05[A]	0.05[A]
Maximum uptake rate of nitrogen	mg N (mg chl*a*)$^{-1}$ day^{-1}	1.5[A]	0.7[A]	0.8[A]
Half saturation constant for phosphorus update	mg m-3	5.0[A]	10.0[A]	1.8[A]
Half saturation constant for nitrogen uptake	mg m-3	6.0[A]	3.0[A]	20.0[A]
Density of phytoplankton for settling	$g\ cm^{-3}$	1.06[D]	1.01[D]	1.14[D]
Phytoplankton diameter	µm	10[A]	10[A]	10[A]

Sources: [A] Kara et al. 2012; [B] Snortheim 2015; [C] calibration parameter; [D] default DYRESM-WQ-I parameter

4.3.3 Oxythermal habitat parameter

To quantify the oxythermal niche of cisco in Lake Mendota, we use the temperature at 3 mg L^{-1} of DO (TDO3; Jacobson et al. 2010) as an easily calculable variable that quantifies oxythermal habitat for cold-water fish species. This TDO3 variable is derived by interpolating

the water temperature at a benchmark DO concentration of 3 mg L^{-1} from temperature and DO profiles generated from the mechanistic model for each day of the summer stratified season, as used for field data in (Jacobson et al. 2010). A 3 mg L^{-1} DO concentration was chosen by Jacobsen et al. (2010) and used here because it is the concentration that is most likely lethal or nearly lethal for cold-water fish species, including cisco (Frey 1955; US EPA 1986). Originally, TDO3 was developed for use in presence-absence models for multiple cold-water fish species across large numbers of lakes. Here, we use the TDO3 metric as a tool to look at long-term changes in habitat suitability for a single lake, representing a novel application of the metric. We choose this method over earlier, more conventional approaches (Fang and Stefan 2000; Stefan et al. 2001; Dillon et al. 2003) because it allows us to quantify to some degree the lack of available habitat (i.e. the overlap of low DO and high temperature conditions) in addition to available habitat. Lower TDO3 values represent better oxythermal habitat for cisco, while higher TDO3 values are an indication of poor oxythermal habitat. Very high values of TDO3, or those exceeding our defined threshold values indicate warm, anoxic waters that are unsuitable for cisco during the year.

While we choose to look at the range of TDO3 values to quantify habitat, it is important to note what TDO3 values represent unsuitable or poor habitat for cisco populations. In applications of TDO3 values (Jacobson et al. 2010; Jiang et al. 2012; Herb et al. 2014) for quantifying cold-water fish oxythermal habitat, TDO3 values were averaged over the course of a month during the stratified season and presence-absence data was used to determine a long-term mean TDO3 threshold value of 17°C for presence of cisco populations. However, in this study, we are interested in small changes in available habitat over the long term and whether management efforts could be performed to increase the available cisco habitat in Lake Mendota.

To this end, we choose to use the maximum TDO3 value during the stratified period rather than a longer term average TDO3 values. Based on Jacobson et al. (2008), who estimated the lethal oxythermal niche for cisco in Minnesota lakes based on known temperature and DO profiles at the time of cisco fish kills, the TDO3 temperature threshold values is chosen as 22°C, the lethal temperature at 3 mg L^{-1} DO concentration.

4.3.5 Multiple linear regression

Multiple linear regression (MLR) analysis was used to examine the relationships between the meteorological drivers and water quality drivers and the simulated maximum TDO3 value during the summer period. The first goal of the MLR analysis was to determine which meteorological and/or water quality drivers that most highly impact the oxythermal habitat of cisco. The second aim of the MLR analysis was to investigate the adequacy of using a simple MLR regression equation to represent oxythermal cisco habitat rather than the using the complex DYRESM-WQ-I model to simulate habitat changes.

Meteorological drivers investigated included: summer (June, July, August; JJA) air temperature, spring (March, April, May; MAM) air temperature, summer wind speed, spring wind speed, summer relative humidity, spring relative humidity, spring total precipitation, and summer total precipitation. Air temperature, wind speed, and relative humidity were averaged over the period and precipitation values were summed. Water quality drivers investigated included: Yearly (November – November) total P load, spring (MAM) P load, summer (JJA) P load, yearly (N-N) total inflow, spring total inflow, summer total inflow, summer water level, spring secchi depth, and summer secchi depth. P loads and inflow volumes were total values during the specified time period, while water level and secchi depths were averaged over the

period of interest. Additionally, precipitation, P load, and inflow values were analyzed using both raw values and log-normalized values before choosing the best fit.

4.3.6 Scenario development

To determine the sensitivity of TDO3 and cisco oxythermal habitat to changes in meteorological and water quality parameters, we perturbed the drivers identified through MLR analysis as having high influence on oxythermal habitat. Air temperatures were perturbed in units of 1°C from the range -2°C to +5°C. Analysis was skewed toward positive perturbations because increasing air temperatures are the likely climate future (IPCC 2013). All other parameters were perturbed in percentages from -50% to +50% in 25% increments. Drivers were perturbed individually and in combination to characterize the effect of multiple climate possibilities. For air temperature perturbations, meteorological inputs remained the same as for the original simulations, but with snowfall (rainfall) conversions if the air temperature scenarios increase (decrease) above 0°C. Groundwater and surface water inflow temperatures were similarly adjusted to account for changes in air temperatures. During all scenarios, the water balance is maintained so that the long-term water level in the lake during the simulation period matches that of the historical record by adjusting the output appropriately to account for increases or decreases in inflow.

To determine P loading reductions necessary to offset the climate-induced changes in cisco habitat, we use statistically downscaled air temperature perturbations from Wisconsin Initiative on Climate Change Impacts (WICCI; 2011) for mid-century (2055) for the Madison, WI area. The downscaled projections are based on simulations of 14 global circulation models. We choose the A1B scenario as it is considered the most-likely case for future fossil fuel use (WICCI 2011). Seasonal perturbations for this scenario are 4.4°C for winter, 3.3 °C for spring,

2.7°C for summer, and 3.6°C for autumn. As with the sensitivity scenarios, the water balance is maintained so that the long – term water level in the lake during the simulation period matches that of the historical record. Snowfall is converted to rainfall if the air temperature scenario increases above 0°C, and groundwater the surface water inflow temperatures were adjusted to account for changes in air temperatures.

4.3.7 Estimate economic cost of phosphorus loading reductions

We estimate the reduction in P load required to improve TDO3 values under the future A1B scenario by simulating the following P loading scenarios: 100%, 90%, 75%, 50%, 25%, and 10% of the historical loading. The corresponding cost of P loading reductions is estimated from the *Yahara CLEAN Engineering Report* by Strand Associates, Inc (2013). The report details a list of action items that result in a 50% P loading reduction to Lake Mendota and the cost of those items (Table 4.01-2 in Strand Associates 2013) and a maximum implementation plan representing an 86 % load reduction (97% of direct drainage sources; Table 4.05-1 in Strand Associates 2013). The report details the efficiency of each proposed reduction effort (in US dollars per lb P reduced) and nonmonetary factors that will influence prioritization of reduction efforts. Loading reduction costs are estimated as present-day value over a 20-year period. Costs of necessary loading reductions are estimated using the Table 4.05 in the *Yahara CLEAN Engineering Report* (Strand Associates 2013) by summing the most- and least-cost effective items that would achieve the desired load reduction.

4.4 Results

4.4.1 Model evaluation

The model acceptably reproduced the observed data (Table 4-3 and Figure 4-1). Observed and predicted temperature values were highly correlated and NMAE and RMSE were both small. Epilimnion temperatures had higher correlations and smaller RMSE than did hypolimnion temperatures, indicating that the model more accurately reproduces observed epilimnion values than hypolimnion values. During the year, thermocline depth and duration of stratification is accurately and reliably simulated (Figure 4-1c). Similarly, DO values were highly correlated and NMAE and RMSE were both small and within acceptable values. Unlike temperature values, hypolimnetic DO is more accurately simulated than epilimnetic values. During the course of the summer, epilimnetic DO values are under-predicted by the model (Figure 4-1 b and d). The depth of DO depletion in the water column is reproduced well, however the model simulates slightly earlier de-oxygenation of the hypolimnion than observed data and earlier re-oxygenation of the hypolimnion earlier than observations (Figure 4-1 d)

Table 4-3: Spearman's rank correlation coefficient (Spearman's rho), NMAE, and RMSE values for simulated temperature and dissolved oxygen values compared to observed values. Comparisons are evaluated for epilimnion, hypolimnion, and whole lake-depth measurements. Each observation represents a distinct lake depth and time observation point.

Variable	Number of Observations	Spearman's rho	NMAE	RMSE
Epilimnetic Temperature	5,658	0.99	0.0017	1.01
Hypolimnetic Temperature	12,259	0.92	0.0017	1.54
All Temperatures	24,518	0.97	0.0004	1.59
Epilimnetic DO	1,484	0.58	0.013	0.87
Hypolimnetic DO	2,756	0.84	0.021	0.86
All DO	5,514	0.88	0.0055	0.93

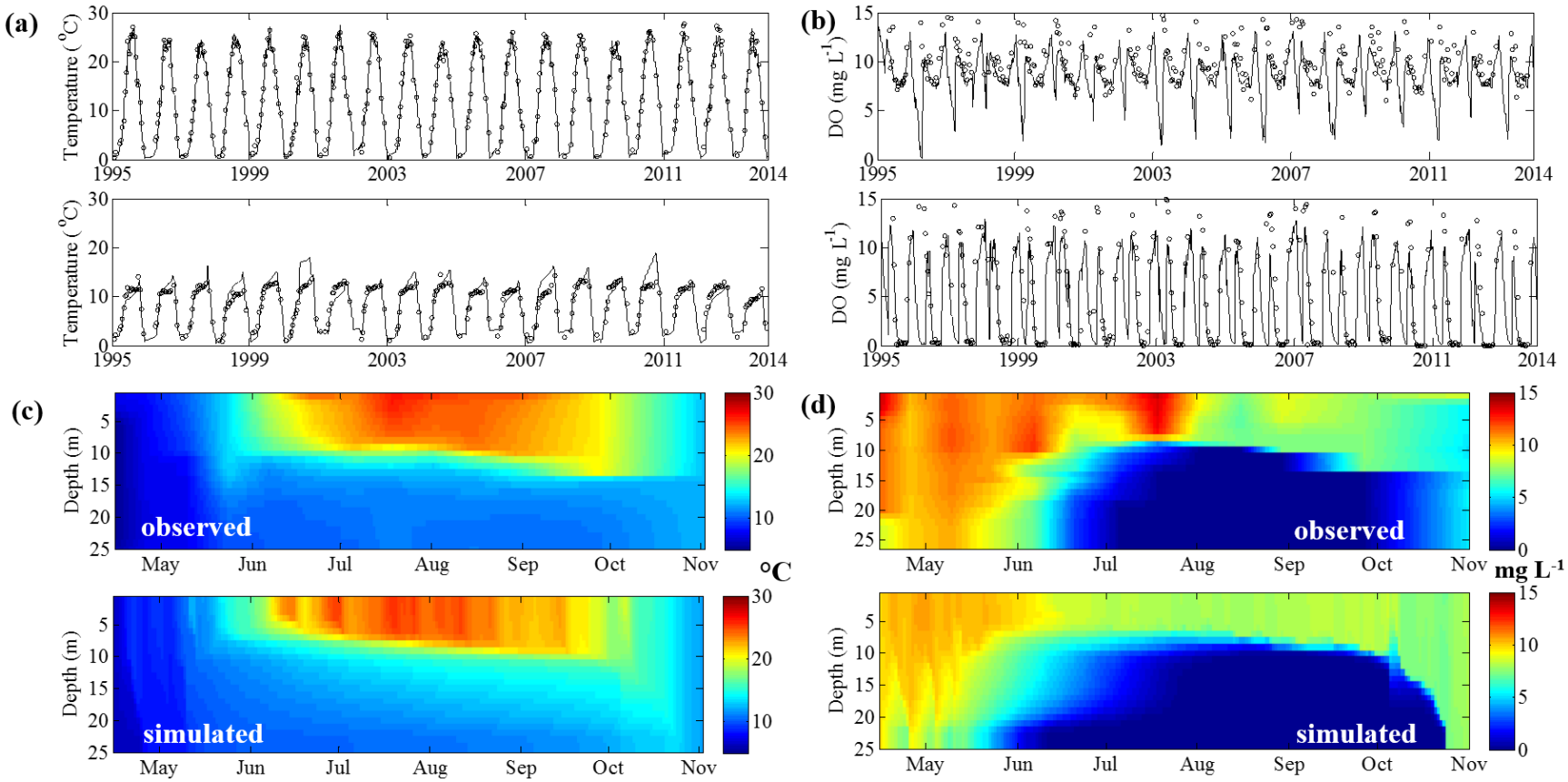

Figure 4-1: volumetrically averaged simulated (solid line) and observed (circles) epilimnion (top) and hypolimnion (bottom) (a) temperatures and (b) dissolved oxygen values for the period 1995 – 2013. Temperature comparison from 1975 – 1995 are not shown for brevity. Interpolated observed (upper) and simulated (lower) temperature (c) and dissolved oxygen (d) profiles for depths 0 – 25 m from 15 April to 1 November 2005 are shown in bottom plots.

4.4.2 Historical characterization of oxythermal niche

Maximum TDO3 for each year from 1976 – 2013 are shown in Figure 4-2 a. The mean TDO3 value was 23.59°C, the maximum was 26.60 °C, and the minimum value was 19.80°C, and the distribution is shown in Figure 4-2 b. During the study period, the yearly maximum TDO3 value has increased significantly (p=1.45x10-5) at a rate of 0.92°C decade-1 (Figure 4-2 a), and 32 of the 38 study years (84 %) experienced maximum TDO3 values that exceeded the death threshold of 22°C. As there is a small population of cisco present in the lake currently, this indicates that the population may be regularly stressed and finding an oxythermal refuge in only a small area of the lake. Under these conditions, it is unlikely that a population of cisco could be sustained in the lake at the present time without extensive management efforts.

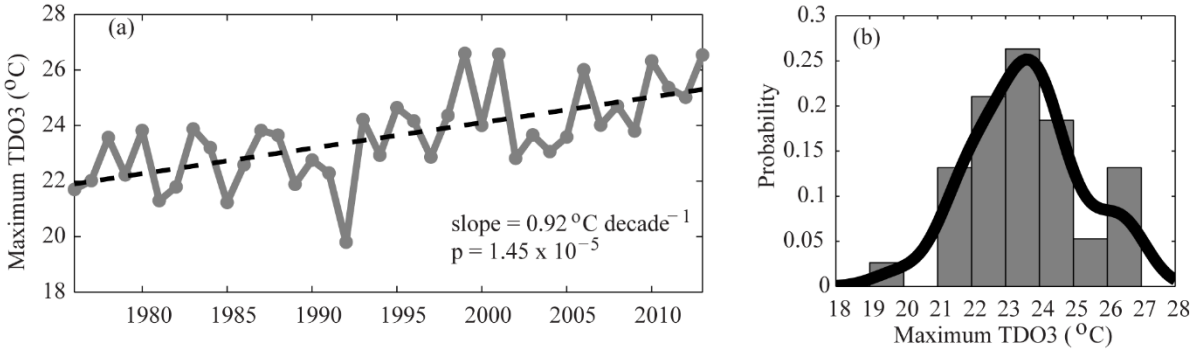

Figure 4-2: (a) calculated TDO3 values over the period 1976 – 2013 and (b) probability plot and of TDO3 values during the historical period.

4.4.3 MLR analysis of meteorological and water quality variables

MLR analysis of the simulated TDO3 results and meteorological and water quality drivers showed that summer (JJA) air temperature, log – transformed spring (MAM) P load, and log – transformed spring (MAM) inflow were all significant predictors of the yearly maximum TDO3 value (p<0.01 for all three variables, N = 38). Together, they explain 76 % of the variance. Analysis of the residual plots for the MLR model showed linearity, normality, and

homoscedasticity, suggesting that the TDO3 response is adequately represented by a linear combination of summer air temperature, spring phosphorus load, and spring discharge. The MLR results are shown in equation 4.1

$$TDO3 = -4.26 + (0.59\pm0.26)\times\log(P) + (0.62\pm0.01) \times AT + (2.03\pm0.48) \times\log(I) \quad (4.1)$$

where TDO3 is the maximum yearly TDO3 value, P is the spring (MAM) P loading into the lake, AT is the summer (JJA) average air temperature, and I is the spring (MAM) inflow into Lake Mendota. Coefficients and standard errors are presented in parenthesis before each driver variable. The MLR model revealed that higher external P loading, higher summer air temperatures, and higher inflow values accompany higher TDO3 values. However, it is important to note that spring P load and inflow are highly correlated (r = 0.79, p=1.79×10^{-9}). Spring inflow into the lake is related to precipitation in the watershed in that increased (decreased) precipitation generally results in increased (decreased) inflow, but here spring total precipitation and spring total inflow are not correlated (r = 0.05, p = 0.76). Surprisingly, wind speed does not have a significant effect on maximum TDO3 values, although other research does suggest that it influences anoxic factor in Lake Mendota (Snortheim 2015) and lake water temperatures and stratification (Magee et al. 2016, Chapter 2)

4.4.4 Sensitivity of TDO3 to air temperature, discharge, and phosphorus load

The sensitivity of TDO3 to simultaneous perturbations in air temperature, inflow volumes, and P loads can be visualized using response surface plots (Figure 4-3). Data to create the response plots are the average maximum TDO3 value for the 38 simulation years under each scenario run (i.e. +1°C temperature + 75% of P load perturbation). The contours the first two plots (inflow + air temperature perturbation and P load + air temperature perturbations) show

some slight non-linearity in the response, while the third plot of inflow and P load perturbations are more linear. From the response plots, it is clear that multiple driver combinations result in the same TDO3 values. Changes in air temperature generally yield high changes in TDO3 values. Overall, increasing air temperatures result in higher TDO3 values; increasing P loading yields higher TDO3 values; and decreasing inflow volumes yield increasing TDO3 values if the other variables remain constant. Surface plots in Figure 4-3 a and c indicate that increases in inflow volumes result in decreases in maximum TDO3 values, which is contrary to results from the MLR regression. This may be due to the very high correlation between inflow volumes and phosphorus loadings. Generally, high inflow will have correspondingly high P load since the majority of phosphorus loadings come from high inflow events (Carpenter et al. 2015). During the sensitivity analysis, the compiled data for all

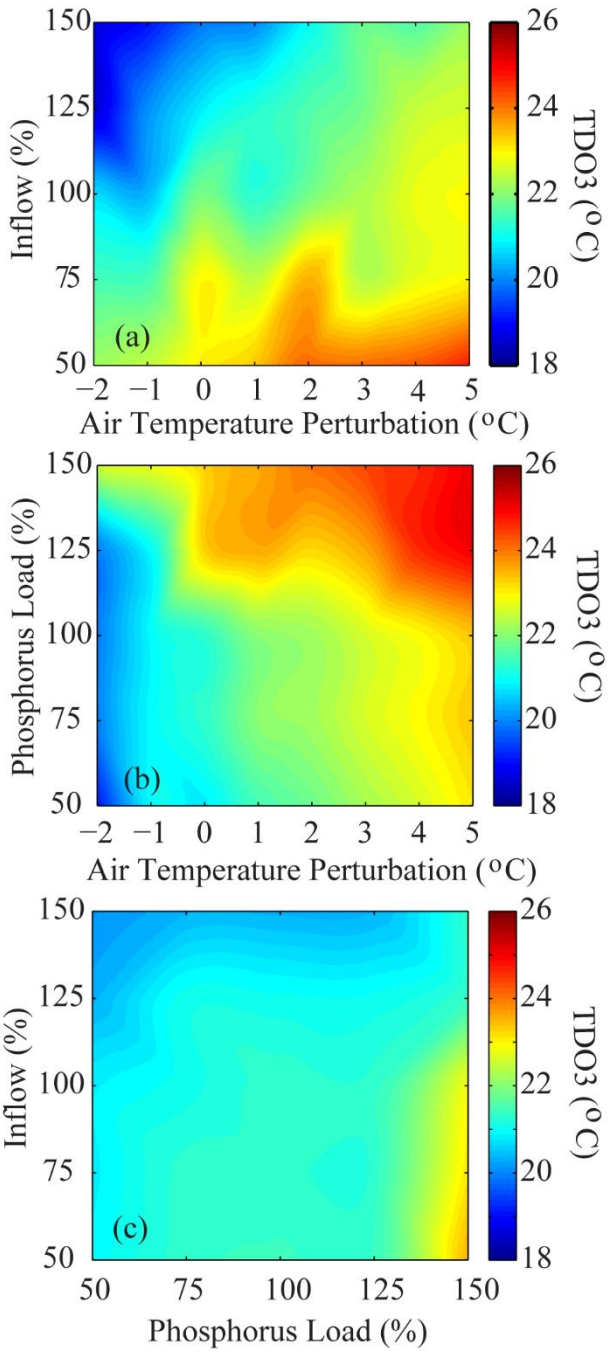

Figure 4-3: response surface plots showing sensitivity of TDO3 to changes in three drivers in combination (a) air temperature and inflow volume with P load constant; (b) air temperature and P load with inflow constant; and (c) P load and inflow volume with air temperature constant.

three model runs has a much lower correlation between inflow volume and P load (r = 0.30, p = 1.60×10^{-85}), and altering the data to keep inflow volume and/or P load constant while changing the other variable allows us to determine that when P load remains constant, increases in inflow volume will reduce TDO3. This may be due to the decreased flushing time with increased inflow volume, more quickly removing P from the lake than during low-flow scenarios.

4.4.5 Phosphorus loading reductions

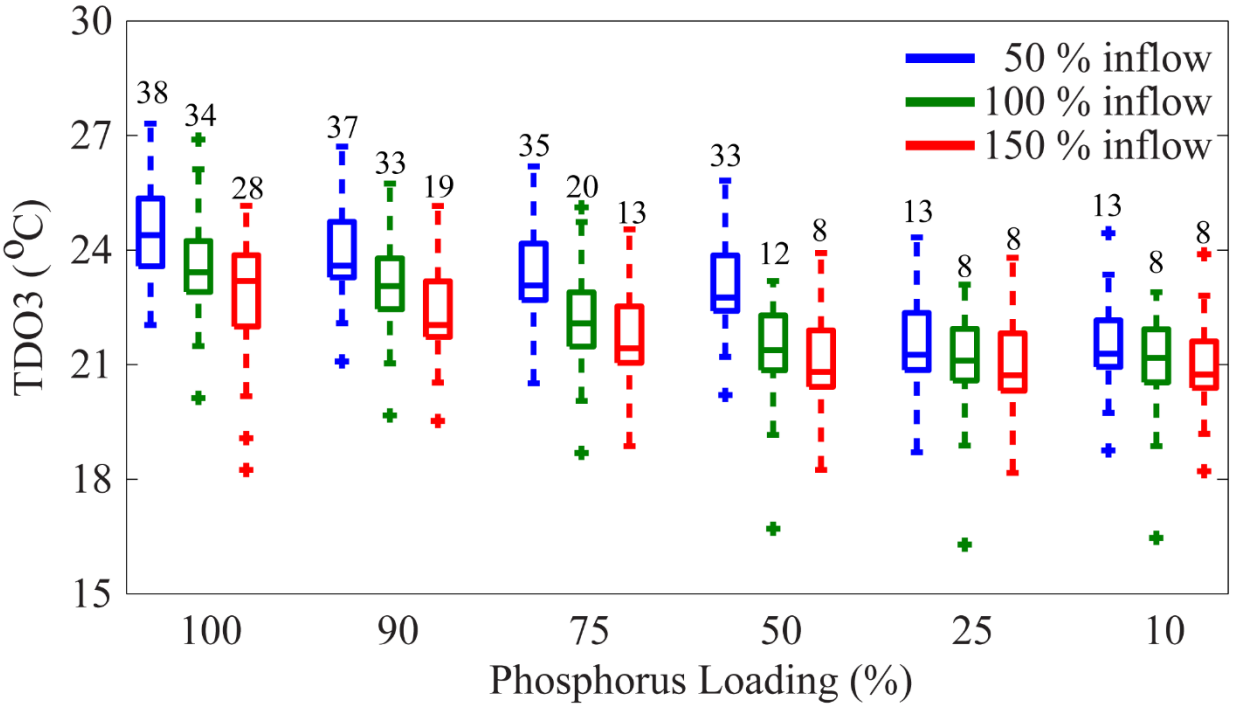

Figure 4-4: Box plot of maximum TDO3 values for the A1B temperature scenario considering three inflow volume scenarios: 50 % of historical inflow (blue), 100% of historical inflow (green), and 150% of historical inflow (red), and six P loading reduction scenarios: 100% of historical load, 90%, 75% 50%, 25%, and 10%. Central lines indicate median values, and box edges indicate 25th and 75th percentiles. Whiskers extend to the most extreme data points not considered outliers, and the outliers are plotted individually. Numbers above boxes indicate the number of years with TDO3 values above the threshold of 22°C.

TDO3 values in response to proposed P loading reductions under the A1B temperature perturbation scenario are shown in Figure 4-4. We simulated the response of TDO3 values for the duration of the 38 – year study period to loading reductions (i.e. 100%, 90%, 75%, 50%,

25%, and 10% of historical loading values) under the A1B temperature perturbations and three inflow volumes (i.e. 50%, 100%, and 150% of historical volumes). For all inflow scenarios, TDO3 values decrease as P load is decreased. Under the A1B scenario with identical inflow and P load as the present, 34 of 38 years (89.5%) have TDO3 values which exceed the specified threshold value of 22°C, while the 50% inflow scenario has every year higher than the threshold value, and the 150% inflow scenario has 28 years (74%) above the threshold. None of the scenarios presented reduced TDO3 values enough such that each year of the simulation was below the threshold value even after a 90% reduction in phosphorus load. The fewest number of years below the threshold value in any scenario is 8 years (21%), and this may be the minimum possible under the A1B scenario. To achieve this threshold value P loads need to be reduced to 25% of historical values (75% reduction) assuming past inflow, while P loads need to be reduced to 50% of historical values (50% reduction) if the 150% inflow scenario is assumed.

4.5 Discussion

4.5.1 Model evaluation and uncertainty

For the duration of the simulation, water temperatures matched quite well with observed values, as measured by Spearman's rho, NMAE, and RMSE values for epilimnion, hypolimnion, and all – depth water temperatures (Table 4-3). The timing of stratification and the thermocline depths both match well with the observed values during each year (Figure 4-1). Deviations between measured and observed temperatures can be partially attributed to the input averaging, particularly daily averaging of air temperature and wind speed, as there is evidence of diurnally asymmetric effects of air temperature and wind speed on water temperatures (Wilhelm et al. 2006), with nighttime temperatures having a greater influence on lake thermal structure (Livingstone 2003). Overall, the temperature model performed as well as those of other studies,

including (Perroud et al. 2009), who found RMSE values for water temperature ranging between 1.7°C and 4°C for a variety of models including the Hostetler model, DYRESM, SIMSTRAT, and FLake, and Fang and Stefan (1996) gave standard errors of 1.37°C for the open water season. Spearman's rho and NMAE values here are in line with those of Kara et al (2012) for Lake Mendota.

Dissolved oxygen simulations also fit well with observed data as indicated by the three goodness – of – fit metrics (Table 4-3). NMAE values compare well with those from Kara et al. (2012) and Snortheim (2015) for Lake Mendota, and are improved over NMAE dissolved oxygen values from Bruce et al. (2006) and Gal et al. (2009). Spearman's rho values here are lower than those from Gal et al. (2009) and Kara et al. (2012). During the summer, the depth of DO depletion in the water column and hypolimnetic DO values are simulated accurately (Figure 4-1). The majority of model error occurs in the epilimnion DO values; however, for the purposes of this study, hypolimnion DO accuracy is more critical to determine cisco habitat than epilimnion DO accuracy, and simulated epilimnion DO is satisfactory.

Limitations in the simulations presented here arise from the one – dimensional assumption inherent in the model, and uncertainties in the observed and model driver dataset. Generally, for small, stratified lakes, the assumption of one – dimensionality is appropriate (Imberger and Patterson 1981). However, short – term deviations in water temperature and thermocline depth do exist in larger lakes (Tanentzap et al. 2007), and there is significant spatial heterogeneity in ecological processes and DO within a lake (Hudson and Vandergucht 2015; Cavalcanti et al. 2016). Neither process is captured in a one-dimensional approach, and to fully determine available cisco habitat within the lake, three-dimensional modeling would be required. Locations and techniques of data collection and measurements have changed at various times

over the study period. Meteorological driver data was adjusted for changes in measurement techniques and locations, which leave uncertainty in those measurements and driver data. Inflow and outflow measurements were assessed for quality assurance and control by the United States Geological Survey (USGS), and can be assumed highly accurate, but uncertainty remains as a result of estimating missing data. Where possible, chemical and phytoplankton parameters were taken from previous studies to minimize both calibration time and errors in calibration parameters, but there is uncertainty in both the provided parameters and the calibration parameters. Temperature and DO were calibrated to best match the observed time series data at all depths, with equal weighting placed on all measurements to reduce bias in the simulation results. Overall, the model evaluation shows that the simulation can successfully reproduce scenarios outside of the calibration period, validating its use in this application.

4.5.2 Predictive ability of MLR

Comparison of the relationship between TDO3 values calculated from the MLR analysis and those from the DYRESM-WQ-I simulation for all simulations in the historical and sensitivity study (Figure 4-5a; Table 4-4) show that the MLR model does not accurately predict TDO3 values. The MLR model correctly predicts TDO3 values above or below the threshold value only 58% of the time. The MLR model performs similarly when predicting average TDO3 values for each simulation scenario (Figure 4-5b; Table 4-4), only correctly predicting whether the TDO3 was above or below the threshold 52% of time. These results indicate that the MLR regression does not fully capture necessary processes to be used reliably as a method to predict year-to-year variability in cisco oxythermal habitat. A longer time period of observation data with more variability in driver input may improve the model to an adequate performance. Additionally, further model perturbations prior to MLR analysis may reveal a more appropriate

regression equation. For example, research by Snortheim (2015) indicated that spring wind speed is related to the anoxic factor in Lake Mendota, but the 38-year analysis did not show significant correlation between wind speed and TDO3 values. Additional model perturbations may reveal such a correlation and account for more variability in TDO3 values. Sensitivity analysis (Figure 4-3) on the three significant drivers revealed that TDO3 values decrease with increasing inflow, which is contrary to the MLR equation, most likely caused by the high correlation between spring inflow and spring phosphorus loading in the lake.

Table 4-4: Hit and miss table showing when the MLR model successfully reproduced TDO3 values greater than or less than the threshold 22°C when compared to TDO3 values estimated from the DYRESM-WQ-I model.

		TDO3 from DYRESM-WQ-I	
TDO3 from MLR		TDO3 < 22°C	TDO3 > 22°C
all modeled values	TDO3 < 22°C	2477	1153
	TDO3 > 22°C	1167	799
scenario-averaged values	TDO3 < 22°C	105	81
	TDO3 > 22°C	52	44

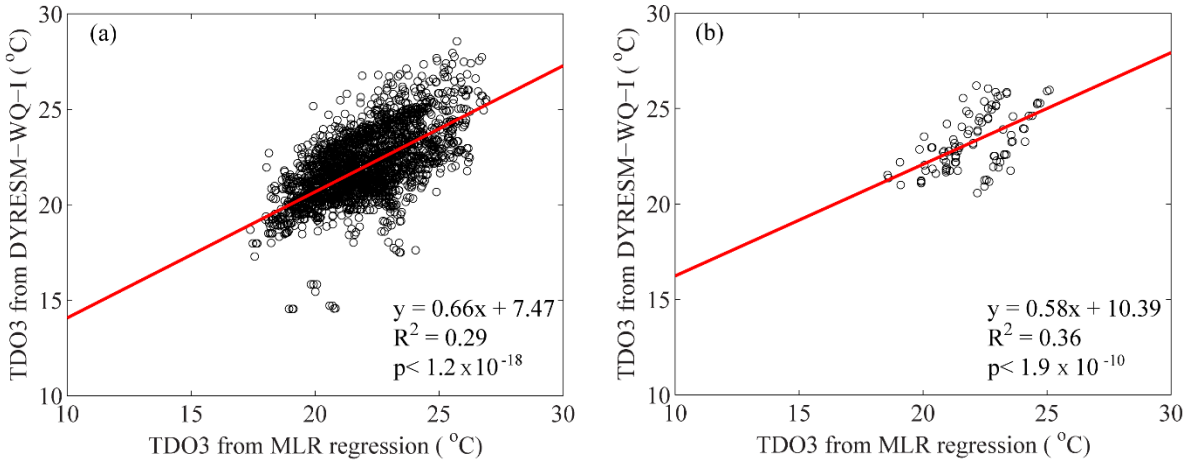

Figure 4-5: (a) comparison of the relationship between TDO3 values estimated from the DYRESM-WQ-I model and TDO3 values estimated from the MLR regression provided

4.5.3 Effect of climate and water quality changes on TDO3

Using the simulated results from sensitivity analysis, we determined that for a 1°C increase (decrease) in air temperatures, TDO3 values will increase (decrease) by approximately 0.46°C; 10% increase (decrease) in P load yields a 0.27°C increase (decrease) in TDO3; and a 10% increase (decrease) in inflow volume results in a 0.10°C decrease (increase) in TDO3 values. These results are supported in Figure 4-3, which shows larger changes for increasing air temperature and increasing P loading than for changes in inflow volumes. Climate projections vary, but generally show a +3°C change in air temperature by mid-century, which would require a roughly 50 % decrease in P loadings to offset the warmer climate and return Lake Mendota to current TDO3 distributions. Improvements in oxythermal habitat beyond that would require further decreases in P loading.

Warmer air temperatures increase TDO3 values directly through increasing water temperatures in the epilimnion (Livingstone 2003; Kirillin 2010; Magee et al. 2016) and also indirectly through increased stratification duration (Cahill et al. 2005; Magee et al. 2016). P loading increases TDO3 values through increased productivity and corresponding increased deoxygenation of the hypolimnion during the stratified season. Surprisingly, DYRESM-WQ-I model results show that increasing inflow volume yields smaller TDO3 values rather that higher values as suggested by the MLR analysis of historical data. We believe this is a result of increased flow through the lake reducing the P flushing time. While results do not suggest that precipitation drives differences in TDO3 value, lake inflow is indirectly related to overall precipitation. Changes in precipitation in the future climate may have a small effect on TDO3 values through inflow volume alterations. Wind speeds are significantly correlated to stratification onset, fall overturn, and hypolimnion water temperature (Magee et al. 2016) and

anoxic factor (Snortheim 2015) in Lake Mendota; however, in the MLR analysis, wind speed was not a significant driver of TDO3 values. Further sensitivity analysis may reveal that in combination with other factors, wind speed decreases could worsen TDO3 values in the lake.

4.5.4 P loading reductions

We chose to investigate the effect of P loading reductions because of its influence on TDO3 values as found in the MLR analysis and because there are initiatives within the Lake Mendota and larger Yahara Chain of Lakes watersheds to reduce P load into Lake Mendota to improve water quality (Lathrop et al. 1998; Lathrop and Carpenter 2014). Under the A1B scenario, the effectiveness of P loading reductions depends on the flow of water through the system (Figure 4-4). The Yahara Chain of Lakes is a highly managed system, and control of Lake Mendota's outflow impacts downstream lakes both in terms of water quality (Lathrop and Carpenter 2014) and flood control (Reimer and Wu 2016). Under current inflow conditions, to only offset changes in air temperature and return TDO3 values to those of current (1976 – 2013) conditions would require a reduction in phosphorus load of 25%. To offset air temperature changes and further reduce TDO3 values to levels that might sustain a cisco habitat, P loadings would need to be reduced by 75%. The cost of a 25% loading reduction is estimated between US$16.9 million and US$132 million. To reduce P by 75% may cost between US$155 million and US$167 million. Currently, there is a goal to reduce P loading into Lake Mendota by 50% (Jones et al. 2010; Dane County et al. 2011), at an estimated cost of US$70 million over a 20 – year period (Strand Associates 2013). This proposed loading reduction, if successful, would reduce TDO3 values under the projected climate to current conditions. The additional cost of a further 25% loading reduction is estimated at US$85million – US$90 million. However, the 50% loading reduction under the A1B scenario still represents an improvement over the historical

period, and would be at no additional cost above the already proposed management efforts for the watershed.

4.5.5 Implications

Changing climate and increasing cultural eutrophication reduce cisco habitat by increasing water temperatures, enhancing stratification and stability, and increasing productivity and hypolimnetic anoxia. Many lakes in the Midwestern United States and Canada have experienced cisco extirpations (Jacobson et al. 2008; Honsey 2014; Honsey et al. 2016) and this trend of decreasing habitat is expected to continue with increasingly warm air temperatures and eutrophication (Jacobson et al. 2010; Sharma et al. 2011; Herb et al. 2014; Van Zuiden et al. 2016). In this study, we show that summer (JJA) air temperature, spring (MAM) P load, and spring (MAM) inflow drive changes to the oxythermal habitat parameter of TDO3. While little can be done to reduce summer air temperatures or inflow of most lakes, P loading can be managed in an effort to offset climate-caused reductions in cisco oxythermal habitat. For the Lake Mendota, USA, given the most likely air temperature scenario, a reduced P load of 25% would improve TDO3 to historic values and could be accomplished through efforts costing as little at US$16.9 million over a 20-year period. P reductions of 50%, which is already a goal in the watershed to improve water clarity and decrease harmful algal blooms (Jones et al. 2010; Lathrop and Carpenter 2014) would reduce TDO3 values below current conditions (1976 – 2013), improving cisco oxythermal habitat. This estimate represents no additional cost above current reduction goals. For the Lake Mendota, it is possible to offset reduced oxythermal habitat caused by increases in air temperature through targeted P loading reductions. If management efforts are incorporated into other goals and the cost distributed among all stakeholders, cisco

and other cold-water fish populations in many at-risk lakes could be sustained for a minimal cost through targeted P loading reductions.

4.6 Acknowledgements

Financial support for authors was provided by the NSF – LTER program, University of Wisconsin Water Resources Institute USGS 10(B) Research grant, the UW Office of Sustainability SIRE Award Program, and the Northeast Climate Science Center. The authors would like to thank Dale Robertson for assistance with creating the long – term meteorological and inflow data sets. We thank Richard Lathrop and John Magnuson for helpful and insightful comments on cisco in Lake Mendota, and we thank Jake Walsh for assistance in estimating cost of phosphorus load reductions.

4.7 References

Aku, P. M. K., L. G. Rudstam, and W. M. Tonn. 1997. Impact of hypolimnetic oxygenation on the vertical distribution of cisco (Coregonus artedi) in Amisk Lake, Alberta. Can. J. Fish. Aquat. Sci. **54**: 2182–2195.

Becker, G. 1983. Fishes of Wisconsin, University of Wisconsin Press.

Brock, T. D. 1985. A eutrophic lake: Lake Mendota, Wisconsin, Springer Verlag Gmbh.

Bruce, L. C., D. Hamilton, J. Imberger, G. Gal, M. Gophen, T. Zohary, and K. D. Hambright. 2006. A numerical simulation of the role of zooplankton in C, N and P cycling in Lake Kinneret, Israel. Ecol. Model. **193**: 412–436. doi:10.1016/j.ecolmodel.2005.09.008

Cahill, K. L., J. M. Gunn, and M. N. Futter. 2005. Modelling ice cover, timing of spring stratification, and end-of-season mixing depth in small Precambrian Shield lakes. Can. J. Fish. Aquat. Sci. **62**: 2134–2142. doi:10.1139/f05-127

Cahn, A. R. 1927. An ecological study of southern Wisconsin fishes, the brook silver-side and the cisco in their relation to the region. Ill. Biol. Monogr. **11**: 1–151.

Carpenter, S. R. 2005. Eutrophication of aquatic ecosystems: Bistability and soil phosphorus. Proc. Natl. Acad. Sci. U. S. A. **102**: 10002–10005. doi:10.1073/pnas.0503959102

Carpenter, S. R., E. G. Booth, C. J. Kucharik, and R. C. Lathrop. 2015. Extreme daily loads: role in annual phosphorus input to a north temperate lake. Aquat. Sci. **77**: 71–79. doi:10.1007/s00027-014-0364-5

Cavalcanti, J. R., D. da Motta-Marques, and C. R. Fragoso Jr. 2016. Process-based modeling of shallow lake metabolism: Spatio-temporal variability and relative importance of individual processes. Ecol. Model. **323**: 28–40. doi:10.1016/j.ecolmodel.2015.11.010

Clingerman, J., T. Petty, F. Boettner, S. Letsinger, J. Strager, and E. Hansen. 2013. Midwest fish habitat partnership fish habitat modeling results: Regional assessment. Modelling report Downstream Strategies.

Dane County, Department of Natural Resoure, City of Madison, and Department of Agriculture, Trade, and Consumer Protection. 2011. Yahara Future Memorandum of Understanding Regarding Efforts to Improve Water Quality in the Yahara River Chain of Lakes.

De Stasio, B. T., D. K. Hill, J. M. Kleinhans, N. P. Nibbelink, and J. J. Magnuson. 1996. Potential effects of global climate change on small north-temperate lakes: Physics, fish, and plankton. Limnol. Oceanogr. **41**: 1136–1149. doi:10.4319/lo.1996.41.5.1136

Dillon, P. J., B. J. Clark, L. A. Molot, and H. E. Evans. 2003. Predicting the location of optimal habitat boundaries for lake trout (*Salvelinus namaycush*) in Canadian Shield lakes. Can. J. Fish. Aquat. Sci. **60**: 959–970. doi:10.1139/f03-082

Duan, W., K. Takara, B. He, P. Luo, D. Nover, and Y. Yamashiki. 2013. Spatial and temporal trends in estimates of nutrient and suspended sediment loads in the Ishikari River, Japan, 1985 to 2010. Sci. Total Environ. **461**–**462**: 499–508. doi:10.1016/j.scitotenv.2013.05.022

Evans, D. O., K. H. Nicholls, Y. C. Allen, and M. J. McMurtry. 1996. Historical land use, phosphorus loading, and loss of fish habitat in Lake Simcoe, Canada. Can. J. Fish. Aquat. Sci. **53**: 194–218. doi:10.1139/f96-012

Fang, X., S. R. Alam, H. G. Stefan, L. Jiang, P. C. Jacobson, and D. L. Pereira. 2012. Simulations of water quality and oxythermal cisco habitat in Minnesota lakes under past and future climate scenarios. Water Qual. Res. J. Can. **47**: 375. doi:10.2166/wqrjc.2012.031

Fang, X., and H. G. Stefan. 1996. Long-term lake water temperature and ice cover simulations/measurements. Cold Reg. Sci. Technol. **24**: 289–304. doi:10.1016/0165-232X(95)00019-8

Fang, X., and H. G. Stefan. 2000. Projected Climate Change Effects on Winterkill in Shallow Lakes in the Northern United States. Environ. Manage. **25**: 291–304.

Ficke, A. D., C. A. Myrick, and L. J. Hansen. 2007. Potential impacts of global climate change on freshwater fisheries. Rev. Fish Biol. Fish. **17**: 581–613. doi:10.1007/s11160-007-9059-5

Frey, D. G. 1955. Distributional ecology of the cisco (Coregonus artedii) in Indiana. Invest Indiana Lakes Streams **4**: 177–228.

Gal, G., M. R. Hipsey, A. Parparov, U. Wagner, V. Makler, and T. Zohary. 2009. Implementation of ecological modeling as an effective management and investigation tool: Lake Kinneret as a case study. Ecol. Model. **220**: 1697–1718. doi:10.1016/j.ecolmodel.2009.04.010

Gerten, D., and R. Adrian. 2000. Climate-driven changes in spring plankton dynamics and the sensitivity of shallow polymictic lakes to the North Atlantic Oscillation. Limnol. Oceanogr. **45**: 1058–1066. doi:10.4319/lo.2000.45.5.1058

Gonzalez-Hidalgo, J. C., R. J. Batalla, and A. Cerda. 2013. Catchment size and contribution of the largest daily events to suspended sediment load on a continental scale. CATENA **102**: 40–45. doi:10.1016/j.catena.2010.10.011

Hadley, K. R., A. M. Paterson, E. A. Stainsby, and others. 2014. Climate warming alters thermal stability but not stratification phenology in a small north-temperate lake. Hydrol. Process. **28**: 6309–6319. doi:10.1002/hyp.10120

Hamilton, D. P., and S. G. Schladow. 1997. Prediction of water quality in lakes and reservoirs. Part I — Model description. Ecol. Model. **96**: 91–110. doi:10.1016/S0304-3800(96)00062-2

Herb, W. R., L. B. Johnson, P. C. Jacobson, and H. G. Stefan. 2014. Projecting cold-water fish habitat in lakes of the glacial lakes region under changing land use and climate regimes. Can. J. Fish. Aquat. Sci. **71**: 1334–1348. doi:10.1139/cjfas-2013-0535

Hetherington, A. L., R. L. Schneider, L. G. Rudstam, G. Gal, A. T. DeGaetano, and M. T. Walter. 2015. Modeling climate change impacts on the thermal dynamics of polymictic Oneida Lake, New York, United States. Ecol. Model. **300**: 1–11. doi:10.1016/j.ecolmodel.2014.12.018

Honsey, A. E. 2014. The decline of Cisco Coregonus artedi at its southern range extent: stock biology and management implications. Master's Thesis. Purdue University.

Honsey, A. E., S. B. Donabauer, and T. O. Höök. 2016. An Analysis of Lake Morphometric and Land-Use Characteristics that Promote Persistence of Cisco in Indiana. Trans. Am. Fish. Soc. **145**: 363–373. doi:10.1080/00028487.2015.1125949

Hsieh, Y. 2012. Modeling ice cover and water temperature of Lake Mendota. PhD Thesis. University of Wisconsin-Madison.

Hudson, J. J., and D. M. Vandergucht. 2015. Spatial and temporal patterns in physical properties and dissolved oxygen in Lake Diefenbaker, a large reservoir on the Canadian Prairies. J. Gt. Lakes Res. **41**, **Supplement 2**: 22–33. doi:10.1016/j.jglr.2015.06.007

Imberger, J., and J. C. Patterson. 1981. Dynamic reservoir simulation model - DYRESM: 5, p. 310–361. *In* H.B. Fischer [ed.], Transport Models for Inland and Coastal Waters. Academic Press.

IPCC. 2013. Summary for Policymakers, p. 3–29. *In* T. Stocker, D. Qin, G.-K. Plattner, et al. [eds.], Climate Change 2013: The Physical Science Basis. Contribution of Working Group I to the Fifth Assessment Report of the Intergovernmental Panel on Climate Change. Cambridge University Press.

Ito, Y., and K. Momii. 2015. Impacts of regional warming on long-term hypolimnetic anoxia and dissolved oxygen concentration in a deep lake. Hydrol. Process. **29**: 2232–2242. doi:10.1002/hyp.10362

Jacobson, P. C., T. S. Jones, P. Rivers, and D. L. Pereira. 2008. Field Estimation of a Lethal Oxythermal Niche Boundary for Adult Ciscoes in Minnesota Lakes. Trans. Am. Fish. Soc. **137**: 1464–1474. doi:10.1577/T07-148.1

Jacobson, P. C., H. G. Stefan, and D. L. Pereira. 2010. Coldwater fish oxythermal habitat in Minnesota lakes: influence of total phosphorus, July air temperature, and relative depth. Can. J. Fish. Aquat. Sci. **67**: 2002–2013. doi:10.1139/F10-115

Jiang, L., X. Fang, H. G. Stefan, P. C. Jacobson, and D. L. Pereira. 2012. Oxythermal habitat parameters and identifying cisco refuge lakes in Minnesota under future climate scenarios using variable benchmark periods. Ecol. Model. **232**: 14–27. doi:10.1016/j.ecolmodel.2012.02.014

Johnson, T. B., and J. F. Kitchell. 1996. Long-term changes in zooplanktivorous fish community composition: implications for food webs. Can. J. Fish. Aquat. Sci. **53**: 2792–2803.

Jones, S., S. Josheff, D. Presser, and G. Steinhorst. 2010. A CLEAN future for the Yahara Lakes: Solutions for tomorrow, starting today.

Kara, E. L., P. Hanson, D. Hamilton, and others. 2012. Time-scale dependence in numerical simulations: Assessment of physical, chemical, and biological predictions in a stratified lake at temporal scales of hours to months. Environ. Model. Softw. **35**: 104–121. doi:10.1016/j.envsoft.2012.02.014

Kerimoglu, O., and K. Rinke. 2013. Stratification dynamics in a shallow reservoir under different hydro-meteorological scenarios and operational strategies. Water Resour. Res. **49**: 7518–7527. doi:10.1002/2013WR013520

Kirillin, G. 2010. Modeling the impact of global warming on water temperature and seasonal mixing regimes in small temperate lakes. Boreal Environ. Res. **15**: 279–293.

Kitchell, J. F. 2012. Food Web Management: A Case Study of Lake Mendota, Springer Science & Business Media.

Kucharik, C. J., S. P. Serbin, S. Vavrus, E. J. Hopkins, and M. M. Motew. 2010. Patterns of Climate Change Across Wisconsin From 1950 to 2006. Phys. Geogr. **31**: 1–28. doi:10.2747/0272-3646.31.1.1

Lathrop, R. C. 2007. Perspectives on the eutrophication of the Yahara lakes. Lake Reserv. Manag. **23**: 345–365.

Lathrop, R. C., S. R. Carpenter, C. A. Stow, P. A. Soranno, and J. C. Panuska. 1998. Phosphorus loading reductions needed to control blue-green algal blooms in Lake Mendota. Can. J. Fish. Aquat. Sci. **55**: 1169–1178. doi:10.1139/f97-317

Lathrop, R. C., S. B. Nehls, C. L. Brynildson, and K. R. Plass. 1992. The Fishery of the Yahara Lakes. Technical Bulletin Technical Bulletin No. 181. Technical Bulletin No. 181 Wisconsin Department of Natural Resources.

Lathrop, R., and S. Carpenter. 2014. Water quality implications from three decades of phosphorus loads and trophic dynamics in the Yahara chain of lakes. Inland Waters **4**: 1–14. doi:10.5268/IW-4.1.680

Latta, W. C. 1995. Distribution and abundance of the lake herring (Coregonus artedi) in Michigan. Fisheries division research report 2014. 2014 Michigan Department of Natural Resources.

Livingstone, D. M. 2003. Impact of Secular Climate Change on the Thermal Structure of a Large Temperate Central European Lake. Clim. Change **57**: 205–225. doi:10.1023/A:1022119503144

Loucks, D. P., E. van Beek, J. R. Stedinger, J. P. M. Dijkman, and M. T. Villars. 2005. Water Resources Systems Planning and Management: An Introduction to Methods, Models and Applications, Paris : UNESCO.

Lynch, A. J., W. W. Taylor, T. D. Beard Jr., and B. M. Lofgren. 2015. Climate change projections for lake whitefish (Coregonus clupeaformis) recruitment in the 1836 Treaty Waters of the Upper Great Lakes. J. Gt. Lakes Res. **41**: 415–422. doi:10.1016/j.jglr.2015.03.015

Lyons, J., P. A. Cochran, and D. Fago. 2000. Wisconsin Fishes 2000: Status and Distribution. WISCU-B-00-001. WISCU-B-00-001 University of Wisconsin Sea Grant Institute.

Magee, M. R., C. H. Wu, D. M. Robertson, R. C. Lathrop, and D. P. Hamilton. 2016. Trends and abrupt changes in 104 years of ice cover and water temperature in a dimictic lake in response to air temperature, wind speed, and water clarity drivers. Hydrol Earth Syst Sci **20**: 1681–1702. doi:10.5194/hess-20-1681-2016

McDermot, D., and K. A. Rose. 2000. An individual-based model of lake fish communities: application to piscivore stocking in Lake Mendota. Ecol. Model. **125**: 67–102.

McKee, T. B., N. J. Doesken, C. A. Davey, and Pielke, Sr. 2000. Climate data continuity with ASOS. Report for period April 1996 through June 2000. Climno Report 00-3. Climno Report 00-3 Colorado Climate Center, Department of Atmospheric Science, Colorado State University.

NTL LTER. 2012a. North Temperature Lakes LTER: Fish Abundance 1981-current.

NTL LTER. 2012b. North Temperature Lakes LTER: Physical Limnology of Primary Study Lakes 1981-current.

Nürnberg, G. K. 1995. Quantifying anoxia in lakes. Limnol. Oceanogr. **40**: 1100–1111.

O'Reilly, C. M., S. Sharma, D. K. Gray, and others. 2015. Rapid and highly variable warming of lake surface waters around the globe. Geophys. Res. Lett. **42**: 2015GL066235. doi:10.1002/2015GL066235

Perroud, M., and S. Goyette. 2010. Impact of warmer climate on Lake Geneva water-temperature profiles. Boreal Environ. Res. **15**: 255–278.

Perroud, M., S. Goyette, A. Martynov, M. Beniston, and O. Anneville. 2009. Simulation of multiannual thermal profiles in deep Lake Geneva: A comparison of one-dimensional lake models. Limnol. Oceanogr.-Methods **54**: 1574–1594.

Reimer, J. R., and C. H. Wu. 2016. Development and Application of a Nowcast and Forecast System Tool for Planning and Managing a River Chain of Lakes. Water Resour. Manag. **30**: 1375–1393. doi:10.1007/s11269-016-1228-7

Robertson, D. M. 1989. The use of lake water temperature and ice cover as climatic indicators. PhD Thesis. University of Wisconsin-Madison.

Robertson, D. M., and R. A. Ragotzkie. 1990. Changes in the thermal structure of moderate to large sized lakes in response to changes in air temperature. Aquat. Sci. **52**: 360–380. doi:10.1007/BF00879763

Rogers, C. K., G. A. Lawrence, and P. F. Hamblin. 1995. Observations and numerical simulation of a shallow ice-covered midlatitude lake. Limnol. Oceanogr. **40**: 374–385. doi:10.4319/lo.1995.40.2.0374

Rudstam, L. G., and J. J. Magnuson. 1985. Predicting the vertical distribution of fish populations: analysis of cisco, Coregonus artedii, and yellow perch, Perca flavescens. Can. J. Fish. Aquat. Sci. **42**: 1178–1188.

Santiago, J. M., D. García de Jalón, C. Alonso, J. Solana, J. Ribalaygua, J. Pórtoles, and R. Monjo. 2016. Brown trout thermal niche and climate change: expected changes in the distribution of cold-water fish in central Spain. Ecohydrology **9**: 514–528. doi:10.1002/eco.1653

Sharma, S., M. J. Vander Zanden, J. J. Magnuson, and J. Lyons. 2011. Comparing Climate Change and Species Invasions as Drivers of Coldwater Fish Population Extirpations H. Browman [ed.]. PLoS ONE **6**: e22906. doi:10.1371/journal.pone.0022906

Snortheim, C. A. 2015. Meteorological drivers of oxygen depletion in Lake Mendota. University of Wisconsin-Madison.

Stefan, H. G., X. Fang, and J. G. Eaton. 2001. Simulated Fish Habitat Changes in North American Lakes in Response to Projected Climate Warming. Trans. Am. Fish. Soc. **130**: 459–477. doi:10.1577/1548-8659(2001)130<0459:SFHCIN>2.0.CO;2

Strand Associates. 2013. Yahara CLEAN Engineering Report. Strand Associates.

Tanentzap, A. J., D. P. Hamilton, and N. D. Yan. 2007. Calibrating the Dynamic Reservoir Simulation Model (DYRESM) and filling required data gaps for one-dimensional thermal profile predictions in a boreal lake. Limnol. Oceanogr. Methods **5**: 484–494. doi:10.4319/lom.2007.5.484

US EPA. 1986. Ambient water quality criteria for dissolved oxygen. 440/5-86-003. 440/5-86-003 US Environmental Protection Agency (EPA).

Van Zuiden, T. M., M. M. Chen, S. Stefanoff, L. Lopez, and S. Sharma. 2016. Projected impacts of climate change on three freshwater fishes and potential novel competitive interactions. Divers. Distrib. **22**: 603–614. doi:10.1111/ddi.12422

Walsh, J. R., S. R. Carpenter, and M. J. V. Zanden. 2016. Invasive species triggers a massive loss of ecosystem services through a trophic cascade. Proc. Natl. Acad. Sci. **113**: 4081–4085. doi:10.1073/pnas.1600366113

Wilhelm, S., T. Hintze, D. M. Livingstone, and R. Adrian. 2006. Long-term response of daily epilimnetic temperature extrema to climate forcing. Can. J. Fish. Aquat. Sci. **63**: 2467–2477. doi:10.1139/f06-140

Wisconsin Initiative on Climate Change Impacts (WICCI). 2011. Wisconsin's Changing Climate: Impacts and Adaptation. Nelson Institute for Environmental Studies, University of Wisconsin - Madison and the Wisconsin Department of Natural Resources.

Chapter 5 : Oxythermal fish stress in response to changing air temperature using a cumulative dosage approach

The following is in preparation for submittal to *Journal of Environmental Management*

Magee MR, and CH Wu. Oxythermal fish stress in response to changing air temperature using a cumulative dosage approach.

5.1 Abstract

Assessing the impact of increasing air temperature on cool-water fish populations is important to fisheries and lake ecosystem management, and developing an appropriate measure to quantify both temperature and oxygen (oxythermal) stress is imperative to that goal. To address this need, we develop a novel metric, Cumulative Oxythermal Stress Dosage (COSD) to quantify oxythermal stress and corresponding habitat loss for a cool-water fish species in Fish Lake, Wisconsin, USA. Results indicate that for yellow perch (*Perca flavescens*), the COSD method is a better predictor of fish declines than a method previously developed for cold-water fish. The main advantage of the COSD method in comparison to previous metrics is the ability to account for both stress duration and stress magnitude. Simulations of historical climate data reveal a COSD increase driven largely by increased values occurring after 1996. Daily air temperature perturbation scenarios reveal a 22.55°C increase in the COSD metric for each 1°C increase in July – September average air temperature and the possibility of yellow perch extirpation from the lake after summer air temperature increases of 3.0°C.

5.2 Introduction

In lakes, water temperature and dissolved oxygen (DO) availability significantly affect the survival and growth of fish (Fry 1971; Magnuson et al. 1979; Coutant 1990; Jacobson et al. 2010), with species from lower thermal guilds requiring well-oxygenation water of cooler temperatures to survive (Cahn 1927; Frey 1955; Rudstam and Magnuson 1985). Water temperatures control metabolism, feeding, and growth (Brett 1971; Elliott 2010), impact reproduction and recruitment (Farmer et al. 2015; Feiner et al. 2016), affect predator and prey availability (Hinz and Wiley 1998; Sharma et al. 2011), and drive competitive interactions (De Stasio and Rahel 1994; Reese and Harvey 2002). At the southern edge of species' ranges, temperature requirements of cool-and cold-water fish species are met within the hypolimnion and metalimnion of dimictic lakes during the summer stratified season. However, increased rates of organic material deposition and decay can reduce the available suitable habitat for species in lower thermal guilds to lethal levels (Nürnberg 1995), leading to oxythermal stress conditions where low-temperature and high-DO requirements are not met in the same location. Cool- and cold-water fish populations are especially vulnerable to the effects of increasing air temperatures (Sharma et al. 2011; Jiang et al. 2012; Van Zuiden et al. 2016).

Warmer air temperatures negatively impact cool- and cold-water fish species directly through lake warming and indirectly through changes in stratification patterns (Stefan et al. 2001; Casselman 2002; Fang and Stefan 2009). As air temperature increases, water temperatures are expected to increase (Fang and Stefan 2009; O'Reilly et al. 2015; Magee et al. 2016), threatening the oxythermal habitat of cool- and cold-water fish populations near their southern ranges (Casselman 2002; Sharma et al. 2011; Herb et al. 2014). Simultaneously, stratification duration is also expected to increase, isolating deep waters from atmospheric exchange, reducing

DO concentrations in the hypolimnion and metalimnion to stressful or lethal levels (Fang and Stefan 2009; Ito and Momii 2015). The combination of warmer water temperatures and lower DO concentrations under new climate conditions may result in increased fish stress or fish kills in lakes that have historically been suitable for cool-water fish, particularly those at range edges.

Understanding the effect of air temperature increases on fish populations is critical for lake managers; however, predicting how and when fish populations will respond to increases in air temperature is difficult. Temperature-only considerations ignore the effect of air temperature changes on DO levels and may not be informative enough in lakes near range edges. Regression techniques (Sharma et al. 2011; Van Zuiden et al. 2016) are useful for looking at a broad suite of lakes, but important processes may be neglected, resulting in misclassification or mis-management of some lakes. Earlier models predict water volume or layer thickness between thermal and oxygen boundaries (Stefan et al. 2001; Dillon et al. 2003). However, these methods consider neither chronic effects of sub-lethal temperature (Selong et al. 2001; Wehrly et al. 2007) nor behavioral thermal regulation (Snucins and Gunn 1995). Newer methods, such as the TDO3 method (temperature at 3 mg L^{-1} of DO) and its variations (Jacobson et al. 2010; Jiang et al. 2012; Herb et al. 2014) attempt to generalize the measure of cold, oxygenated water availability to allow for direct comparisons across taxa, simplify modeling efforts (Jacobson et al. 2010). While they have proven useful for cold-water fish species on a regional scale (Jiang et al. 2012; Herb et al. 2014), they have not been applied to cool-water species or as a method of assessing stress variability and changes on a single lake through time. Accurately assessing oxythermal stress of cool-water fish species is integral for proper management of lake ecosystems under increasing air temperatures.

The goal of this paper is to develop a novel metric for quantifying oxythermal stress in a cool-water fish species and apply this metric to investigate the effects of air temperature increases on a cool-water fish species, yellow perch (*Perca flavescens*). To address this goal, we utilize a one-dimensional hydrodynamic-water quality model to simulate temperature and DO in dimictic Fish Lake, Wisconsin, USA. We build upon a previously developed metric to create a new metric for quantifying oxythermal stress in cool-water fish and apply it to both historical air temperature simulations and daily air temperature perturbation simulations to investigate how oxythermal stress of yellow perch is affected by changes in air temperatures.

5.3 Methods

In this study, we develop an oxythermal habitat variable, cumulative oxythermal stress dosage (COSD) to define suitable cool-water fish habitat and compare the method to the previously developed TDO3 method (Jacobson et al. 2010; Jiang et al. 2012; Herb et al. 2014). COSD and TDO3 values are calculated from simulated daily temperature and dissolved oxygen profiles obtained from a mechanistic model.

5.3.1 Study site

Fish Lake (43°17'N, 89°39'W) is a dimictic, eutrophic seepage lake located in northwestern Dane County, Wisconsin, USA. There are no stream inlets or outlets, although the nearby Mud Lake may overflow into Fish Lake during large storm events. Fish Lake has a surface area of 87.4 ha, mean depth of 6.6 m, maximum depth of 18.9 m, and a shoreline length of 4.3 km. The lake is classified as a groundwater flow-through lake with only 6 percent of the annual water budget input due to groundwater inflow. During the period 1996-2001, the water level of the lake rose by approximately 2.75 m due to increased groundwater flow to the lake

(Krohelski et al. 2002). The lake was chosen as a study site because of its yellow perch population, long term (20-year) water temperature and DO data, appropriate data availability to extend model simulations past 20 years, and the isolated nature of the lake, which removes issues of fish movement upstream or downstream during undesirable conditions.

5.3.2 Oxythermal stress parameters

5.3.2.1 Cumulative oxythermal stress dosage

The oxythermal habitat variable developed in this study, cumulative oxythermal stress dosage (COSD) builds off the TDO3 approach, developed by Jacobsen et al. (2010), by accounting for the cumulative dosage of TDO3 temperature above a threshold value. TDO3 is the water temperature at DO concentrations of 3 mg L^{-1} as defined by Jacobsen et al. (2010) and further refined in Jiang et al. (2012). TDO3 is calculated from simulated daily temperature and DO profiles for every simulated day (see Jacobsen et al. (2010), Figure 1). Following the Jiang et al. (2012) method, TDO3 is determined for each day of the year (Figure 5-1a). Next, a daily temperature dosage that is in exceedance of a threshold value is determined (Figure 5-1b). Finally, a cumulative total of TDO3 exceedance dosage is determined for the year (Figure 5-1c). This final variable, COSD, is equal to the total yearly TOD3 dosage that exceeds a temperature threshold. COSD may be determined for each year during the study period. Advantages are the combined cumulative effects of both high stress situations as determined by the TDO3 method (Jacobson et al. 2010) and the duration of stress situations as in other approaches (Stefan et al. 2001; Dillon et al. 2003; Fang et al. 2004). Additionally, this method may be easily applied to study the effects of long exposure times and situations in which temperatures fluctuate above and below threshold values.

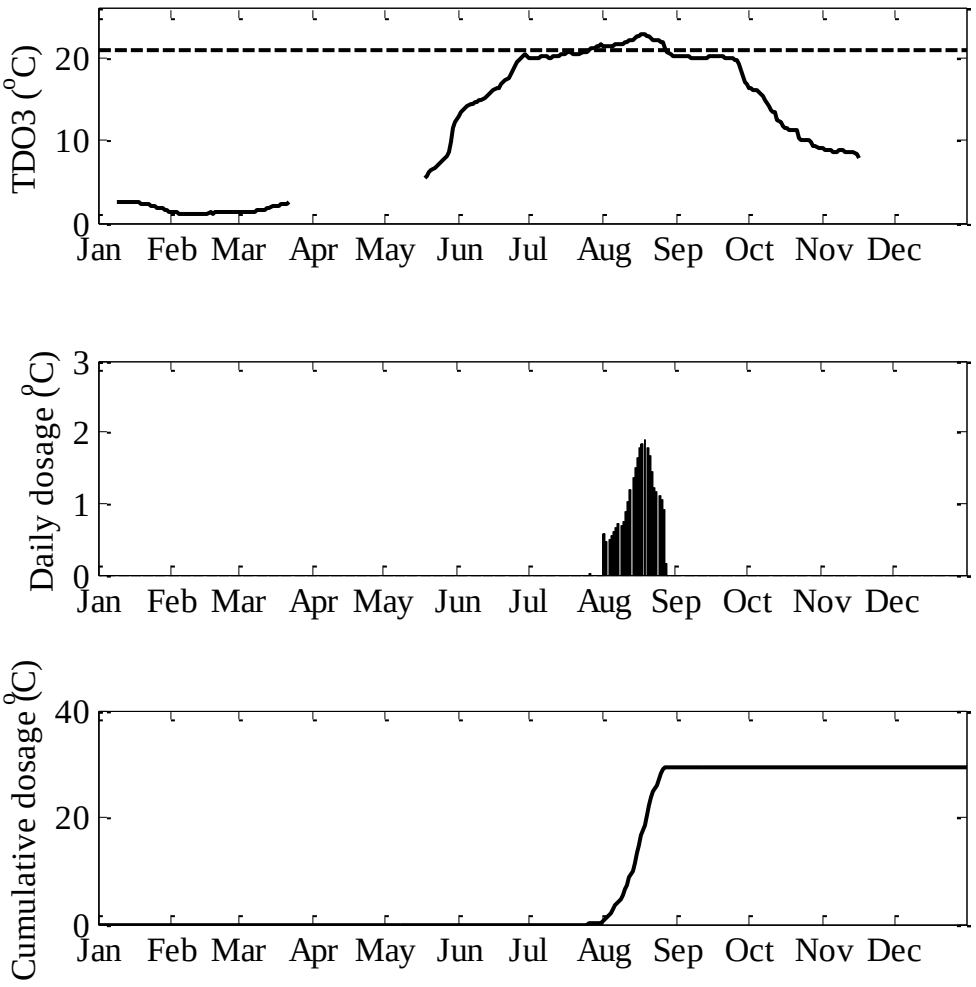

Figure 5-1: Schematic showing cumulative dosage approach for the year 2009 on Fish Lake. (a) Shows daily TDO3 values (solid line) as described in Jacobsen et al. (2010) and Jiang et al. (2012), while the dashed line shows the temperature threshold value of 21°C for yellow perch. (b) shows the daily TDO3 dosage during the summer season. (c) shows the cumulative total of daily TDO3 dosage during the year.

5.3.2.2 Temperature and DO thresholds

Suitable fish habitat in the water column is determined by water temperature and DO values falling within suitable ranges. Laboratory investigations on the temperature preference of yellow perch show that the final referendum during the summer appears to depend on the size of the fish (McCauley and Read 1973). Reported values range from 21.4 to 24.2°C for young fish (McCauley and Read 1973; Neill and Magnuson 1974; Cherry et al. 1977) and from 20 to 21°C

for older fish (Ferguson 1958; McCauley and Read 1973; Reutter and Herdendorf 1974). However, these previous studies do not consider the chronic effects of temperature, and some evidence suggests that fish exposed to sub-lethal temperatures during acute tests may experience delayed mortality during longer exposure times (Selong et al. 2001). For this study, we choose to use 21°C as in Rudstam and Magnuson (1985) as the threshold TDO3 dosage in order to account for effects of mortality as a result of prolonged sub-lethal temperature exposures. The acute lethal limit for cool-water fish species is 3 mg L^{-1} (Frey 1955; US EPA 1986), which has been chosen as our threshold criteria here.

5.3.3 Model description

5.3.3.1 Temperature model

The model used in this paper is DYRESM-WQ-I, a one-dimensional hydrodynamic, lake-ice, and water quality model based on the DYRESM-WQ (Dynamic Reservoir Simulation Model – Water Quality) model (Hamilton and Schladow 1997) with an additional ice model that can simulate water temperature and ice cover year-round. Discrete horizontal Lagrangian layers of uniform properties that vary in thickness are employed to simulate vertical water temperature, salinity, and density with input including inflows, outflow, and mixing (Imberger et al. 1978). A full description of the hydrodynamic and ice models can be found in Magee et al. (2016), Chapters 2 and 3, and Appendix A.

5.3.3.2 Dissolved oxygen model

The ecological model in DYRESM-WQ-I is composed of subroutines for phytoplankton production and loss, nutrient cycling, and dissolved oxygen dynamics. Detailed descriptions of the phytoplankton and nutrient subroutines are found in Hamilton and Schladow (1997). DO concentrations in the model are determined from the sum of oxygen sources and sinks: surface

transfer, inflows and outflows, phytoplankton photosynthesis and respiration, biochemical oxygen demand, sediment oxygen demand, and nitrification. At the surface, the saturation concentration of DO is determined from the surface water layer temperature according to the equation given by Mortimer (1981) and described in Hamilton and Schladow (1997). A transfer velocity for oxygen exchange dependent on wind velocity, wave action, and water viscosity at the surface determines the oxygen flux at the surface-water interface. Phytoplankton photosynthesis and respiration affect DO concentrations similar to that of changes in chlorophyll *a*, except for a phytoplankton carbon to chlorophyll *a* conversion factor and a constant stoichiometric factor to convert changes in phytoplankton carbon to DO production or respiration (Hamilton and Schladow 1997). An additional stoichiometric factor is used to convert nitrate produced to oxygen consumed during nitrification (Wlosinski et al. 1995; Hamilton and Schladow 1997). In the euphotic zone, oxygen demand in the sediments is met through primary benthic production, and in the euphotic zone, a modification of the sediment oxygen model of Walker and Snodgrass (1986) is used (Hamilton and Schladow 1997). Biochemical oxygen demand is modeled by considering the detrital mass in terms of its equivalent oxygen consumption.

5.3.3.3 Model calibration

Calibration parameters for the model included water temperature, water level, ice cover dates, and DO. The hydrodynamic and water temperature portion of the model was previously calibrated for Fish Lake (Chapter 2 and Chapter 3), and is not discussed here for brevity. DO was calibrated for Fish Lake through trial-and-error adjustment of chemical and phytoplankton parameters within the bounds of available published literature and assigned ranges and values for DYRESM-WQ until a satisfactory performance was achieved based on traditional goodness-of-

Table 5-1: Final phytoplankton and chemical parameters used for the DYRESM-WQ-I simulations

Parameter	Units	Assigned Value
active chlorophyll groups		1
maximum algal growth rate	day^{-1}	1.3
maximum algal respiratory rate	day^{-1}	0.05
maximum algal mortality rate	day^{-1}	0.03
temperature multiplier		1.08
light saturation	$\mu E\ m^{-2}\ s^{-1}$	130
specific attenuation coefficient for Chl *a*	m^2 (mg Chl *a*)$^{-1}$	0.085
background light attenuation	m^{-1}	0.45
minimum phosphorus to chlorophyll mass ratio	mg P (mg Chl *a*)$^{-1}$	0.24
minimum nitrogen to chlorophyll mass ratio	mg N (mg Chl *a*)$^{-1}$	1.8
maximum phosphorus to chlorophyll mass ratio	mg P (mg Chl *a*)$^{-1}$	2.5
maximum nitrogen to chlorophyll mass ratio	mg N (mg Chl *a*)$^{-1}$	5.0
maximum uptake rate of P	mg P (mg Chl *a*)$^{-1}$ day^{-1}	0.18
maximum uptake rate of N	mg N (mg Chl *a*)$^{-1}$ day^{-1}	1.5
half saturation constant for P uptake	$mg\ m^{-3}$	2.0
half saturation constant for N uptake	$mg\ m^{-3}$	12.0
half saturation constant for silica uptake	$mg\ m^{-3}$	0.0
density of phytoplankton	$g\ cm^{-3}$	1.06
phytoplankton diameter	µm	10
rate constant for denitrification	day^{-1}	0.04
half saturation constant for effect of DO on denitrification	$mg\ L^{-1}$	0.2
nitrification rate	day^{-1}	0.05
oxygen demand of sub-euphotic sediments	$g\ m^{-2}\ day^{-1}$	3.1
decomposition rate of BOD	day^{-1}	0.02
rate of conversion of organic P to DRP	day^{-1}	0.04
rate of conversion of organic N to ammonia	day^{-1}	0.05
nitrification temperature multiplier		1.03
organic decomposition temperature multiplier		1.08
sediment P release	$mg\ m^{-2}\ day^{-1}$	1.1
sediment ammonia release	$mg\ m^{-2}\ day^{-1}$	5.0
temperature multiplier for sediment nutrient release		1.02

fit metrics. The model was calibrated using the period 1995-2010. Final phytoplankton and chemical parameters are provided in Table 5-1.

5.3.3.4 Model evaluation

We used three statistical measures to evaluate model output against observational data (Table 5- 1): linear coefficient of determination (R^2), Spearman's rank correlation coefficient (Rho), and the normalized mean absolute error (NMAE; Alewell and Manderscheid 1998) were used to compare simulated and observed temperature and DO values. Statistics were calculated for observed and predicted data at times and depths when observations were made. Temperature and DO measurements were obtained for Fish Lake from the NTL-LTER program (https://lter.limnology.wisc.edu/data/filter/5721). Data were collected from the deepest part of the lake at 1 m depth intervals. Sampling frequency occurs every two-weeks during the ice-free season except that sampling occurs monthly during the fall and typically only once during the winter.

Surface water level was maintained within 0.2 m (~1%) of observed elevations. Water temperature was reproduced well (Figure 5-2a). Observed and predicted temperature were highly correlated (R^2 = 0.79, Rho = 0.83, Table 5- 1) and the NMAE was small (0.022; Table 5- 1). Similarly, DO was fairly well represented through the water column (Figure 5-2b), although there were under-predictions of DO in the epilimnion layer (Figure 5-2c) and occasional under predictions of DO in the hypolimnion during mixing events in spring and fall (Figure 5-2d). During the stratified period, the hypolimnion DO was reproduced well in both magnitude and timing of hypoxic conditions. Goodness-of-fit metrics were poorer than for water temperature, but still highly correlated (R^2 = 0.67, Rho = 0.78, Table 5- 1) and NMAE was low (0.20, Table 5- 1).

Table 5- 1: Coefficient of determination (r2) from linear regression, Spearman's rank correlation coefficient (Spearman's rho), and NMAE value for temperature and dissolved oxygen simulated and observed data.

Variable	Number of observations	R^2	Spearman's rho	NMAE
Temperature	5523	0.79	0.83	0.022
DO	5466	0.62	0.78	0.20

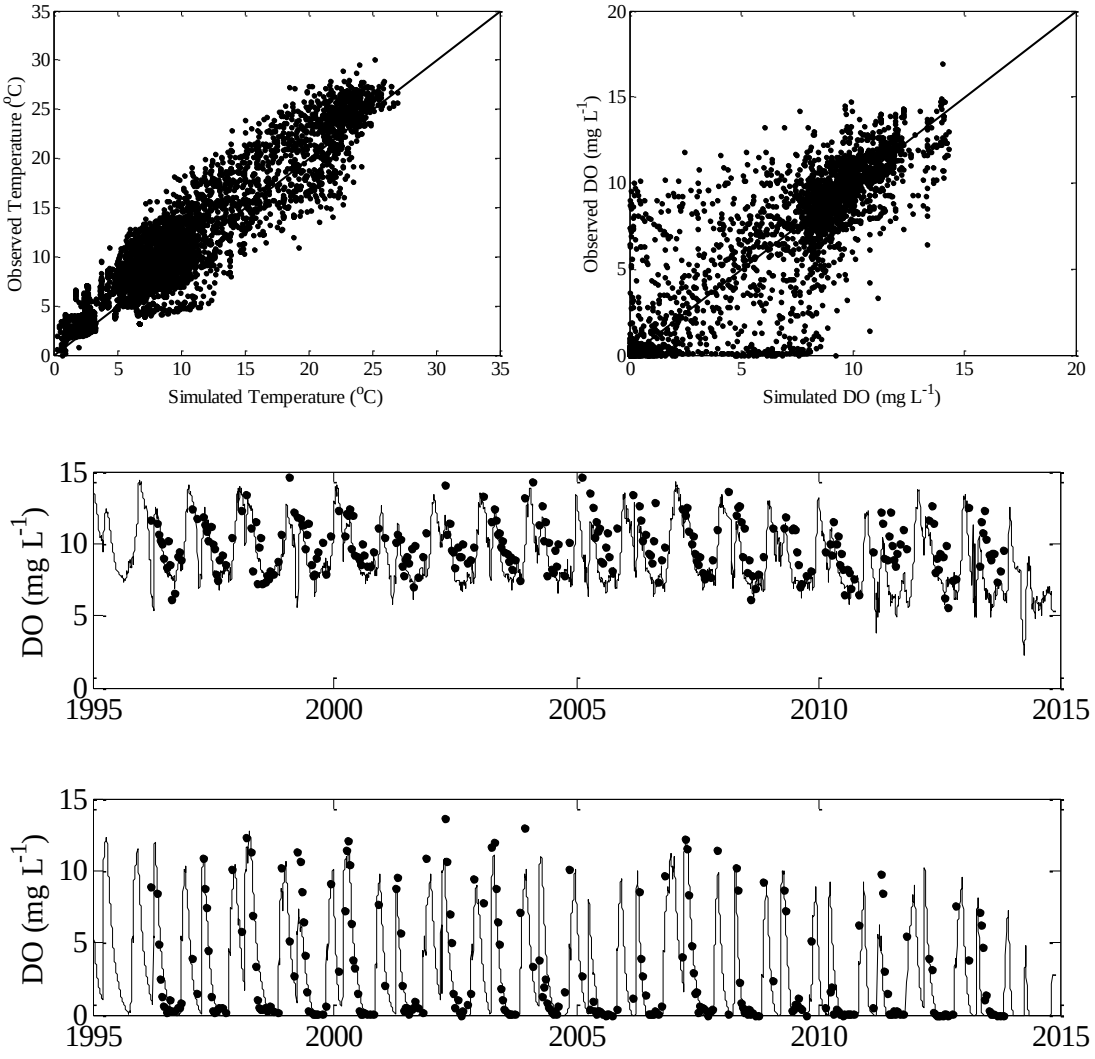

Figure 5-2: Simulated and observed (a) water temperature and (b) dissolved oxygen. Each point represents a distinct temperature or dissolve oxygen modeled and observed pair for one date and lake depth. Volumetrically-averaged simulated (solid lines) and observed (black circles) (c) epilimnion and (d) hypolimnion dissolved oxygen values are also provided.

5.3.4 Data

5.3.4.1 Meteorological data

Meteorological data used in the model input consists of daily solar radiation, air temperature, vapor pressure, wind speed, cloud cover, rainfall, and snowfall. Air temperature, wind speed, vapor pressure, and cloud cover were computed as an average of the whole day, while solar radiation, rainfall, and snowfall are the daily totals. Meteorological data was gathered from Robertson (1989), who constructed a continuous daily meteorological dataset for Madison, Wisconsin from 1884 to 1988 by adjusting for changes in site location, observation time, and surface roughness. Appended to this data was more recent data from the National Climate Data Center weather station (NCDC, NOAA) at the Dane County Regional Airport (Truax Field) in Madison. All data can be obtained from http://www.ncdc.noaa.gov/, except solar radiation, which can be gathered from http://www.sws.uiuc.edu/warm/weather/. Additional adjustments were made to wind speed data based upon changes in observational techniques occurring in 1996 (McKee et al. 2000) by comparing data from the Truax Field site to that collected from the tower of the Atmospheric and Oceanic Science Building at the University of Wisconsin-Madison (http://ginsea.aos.wisc.edu/labs/mendota/index.htm). Detail of this adjustment is in Magee et al. (2016).

5.3.4.2 Water level data

Water level in Fish Lake has increased by 2.75 m from 1966-2001 (Krohelski et al. 2002). To account for this water level increase, USGS water level data from 1996 to 2003 (www.waterdata.usgs.gov) was used to estimate inflow and outflow from surface runoff and groundwater inflow using the water budget approach of balancing inflows, outflows, precipitation, evaporation, and lake level changes. For early years of simulation, where lake level

information was not available, the long-term mean lake level was assumed for calculations. Previous research (Krohelski et al. 2002) determined that surface runoff accounted for two-thirds of inflowing water while groundwater inflow accounted for one-third of total inflow over the period 1990-1991. Using these values, we attributed two-thirds of the inflowing water as surface runoff using air temperatures to estimate the runoff temperature similar to the method for Lake Mendota in Magee et al. (2016) and one-third of inflowing water as groundwater inflow and used an average of groundwater temperature measurements (Hennings and Connelly 2008) to determine the temperature of groundwater fluxes.

5.3.4.3 Fish data

Yellow perch abundance data (Figure 5-3a) was derived from fish catch data collected by the North Temperature Lakes – Long Term Ecological Research (NTL-LTER) program (https://lter.limnology.wisc.edu/data/filter/5698). The same sampling sites are used each year and sampling occurs between the 3rd week of July and Labor Day every year. Sampling is done at six littoral zone sites with seine, minnow or crayfish traps, and fyke nets. Further information on sampling can be found at https://lter.limnology.wisc.edu/dataset/north-temperate-lakes-lter-fish-abundance-1981-current. Three years, 2002, 2005, and 2012 showed a decline in catch per unit effort of greater than 60 % compared to the prior year, and they have been identified as possible fish stress years used to compare the effectiveness of the TDO3 and COSD methods in determining fish stress and fish-kill years.

5.3.5 Air temperature perturbation scenarios

To evaluate changes in COSD and TDO3 values in response to increasing air temperatures, five additional scenarios of increased air temperature were simulated in addition to the historical period 1995-2014. The five scenarios were daily air temperature perturbations of +1°C, +2°C,

+3°C, +4°C, and +5°C. For each scenario, meteorological inputs remained the same as for the original simulations with the exception of snowfall conversion to rainfall if the air temperature scenarios increase above 0°C on the day of precipitation. Similarly, the water balance is maintained so that the long-term water levels in Fish Lake matches the historical record.

5.4 Results and discussion

5.4.1 COSD as a predictor of fish stress

Fish abundance, COSD, and TDO3 values for the period 1995-2014 are shown in Figure 5-3). The three years with possible fish stress years are identified as 2002, 2005, and 2012. These three years correspond to the three years with the highest COSD values, indicating that large COSD values are likely to be related to years of fish stress or fish declines. 2002 has the lowest COSD value of the three years (COSD = 95.65°C), while 2006 has the next-highest COSD value (89.6°C), but there is no apparent fish abundance decline during that year. There is likely a threshold COSD value between 90°C and 95°C under which yellow perch are able to survive stressful conditions and over which mortality occurs.

In comparison, the three years associated with yellow perch declines do not represent the three years with highest TDO3 values in the study. As TDO3 takes only into account the average of oxythermal stress conditions, rather than the duration of stress conditions, the TDO3 method may not adequately describe year-to-year changes in oxythermal stress. Long exposure to elevated temperatures may be an important factor determining habitat suitability and species performance (Wehrly et al. 2007), so consideration of this exposure time is vitally important when trying to evaluate future stress conditions and develop management and mitigation strategies to sustain fish populations in at-risk lakes. An advantage of the COSD method is that it

can characterize stress by considering both the cumulative effects of high stress situations and the duration of stress situations. Combining both aspects of oxythermal stress can provide a more in-depth characterization of stress during a particular year and of interannual variability in stress. Additionally, this method may easily be applied to study the effects of situations where temperatures fluctuate above and below threshold values. Based on results from this single lake, COSD appears to be a practical method for predicting fish stress years and corresponding fish population declines.

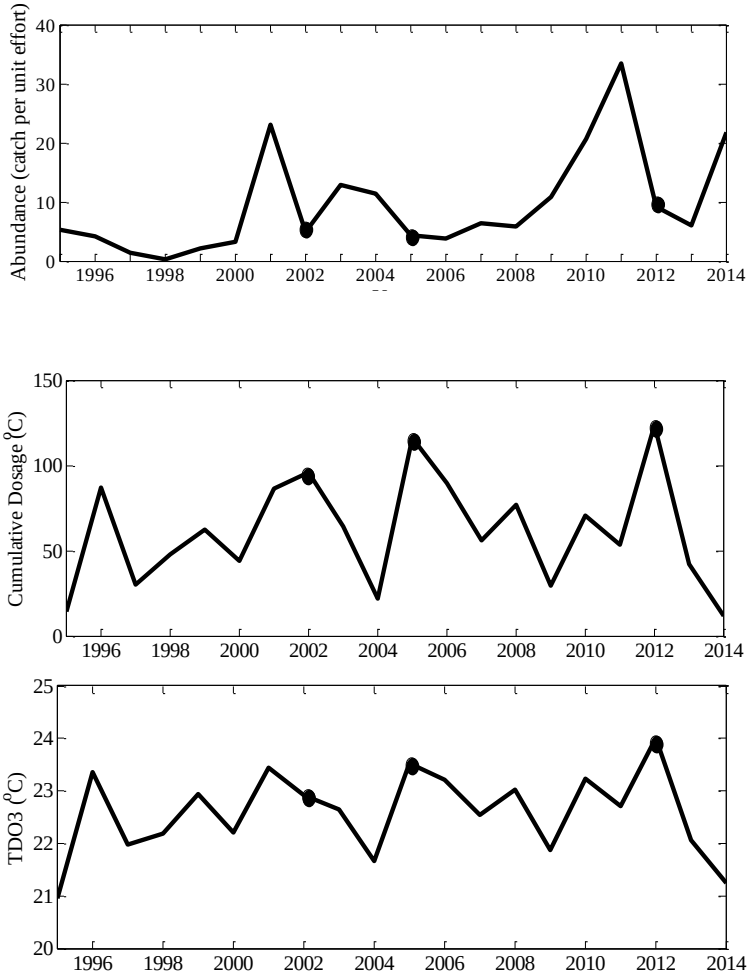

Figure 5-3: (a) yellow perch abundance in Fish Lake measured as catch per unit effort (b) maximum 30-day-averaged TDO3 values and (c) yearly total cumulative oxythermal stress dosage. Circles indicate possible fish-kill years where fish abundance data decreased significantly (>60%) from previous years.

5.4.2 Long term changes in oxythermal stress

Over the 20-year period (Figure 5-3), there is no significant trend in either COSD or TDO3 values. The mean COSD value is 61.2°C, with a standard deviation of 32.2°C, and the mean TDO3 value is 22.6°C with a standard deviation of 0.81°C. However, if we extend the model period to 1911 (shown in Figure 5-4), we are able to obtain additional long term information about changes in oxythermal stress in Fish Lake. Using the extended simulation period, long term changes in both COSD and TDO3 are apparent. First, a significant (p<0.01) trend in COSD values of 5.45°C decade^{-1} exists, largely driven by significantly higher COSD values starting after 1996. Before 1996, the majority of years have COSD values of 0°C, with only 13 of the 85 years having COSD values greater than 0°C. If we consider a COSD threshold value for yellow perch declines of between 90-95°C based on fish abundance data (see Section 5.4.1), four years in the simulation period (1955, 2002, 2005, 2012) exceed a COSD dosage of 90°C. Three of the four exceedance years occur after 2000, indicating a rise in exceedance with time, possibly due to changing climate, specifically air temperatures. Increases in air temperature are predicted to continue (IPCC 2013) and these may increase the occurrence of years with yellow perch fish kills such that a population is not sustainable in Fish Lake. For TDO3 values, there is a significant (p<0.01) increasing trend of 0.61°C decade^{-1}, and unlike for COSD, the trend is consistent over the 104-year period. Water temperature and DO measurements are unavailable before 1995, and therefore the ability of the simulation results is unknown, especially considering the large change in water level over the period. However, the longer simulation period does show that there has been a change in both COSD and TDO3 values through time, indicating that oxythermal habitat for yellow perch has decreased through time.

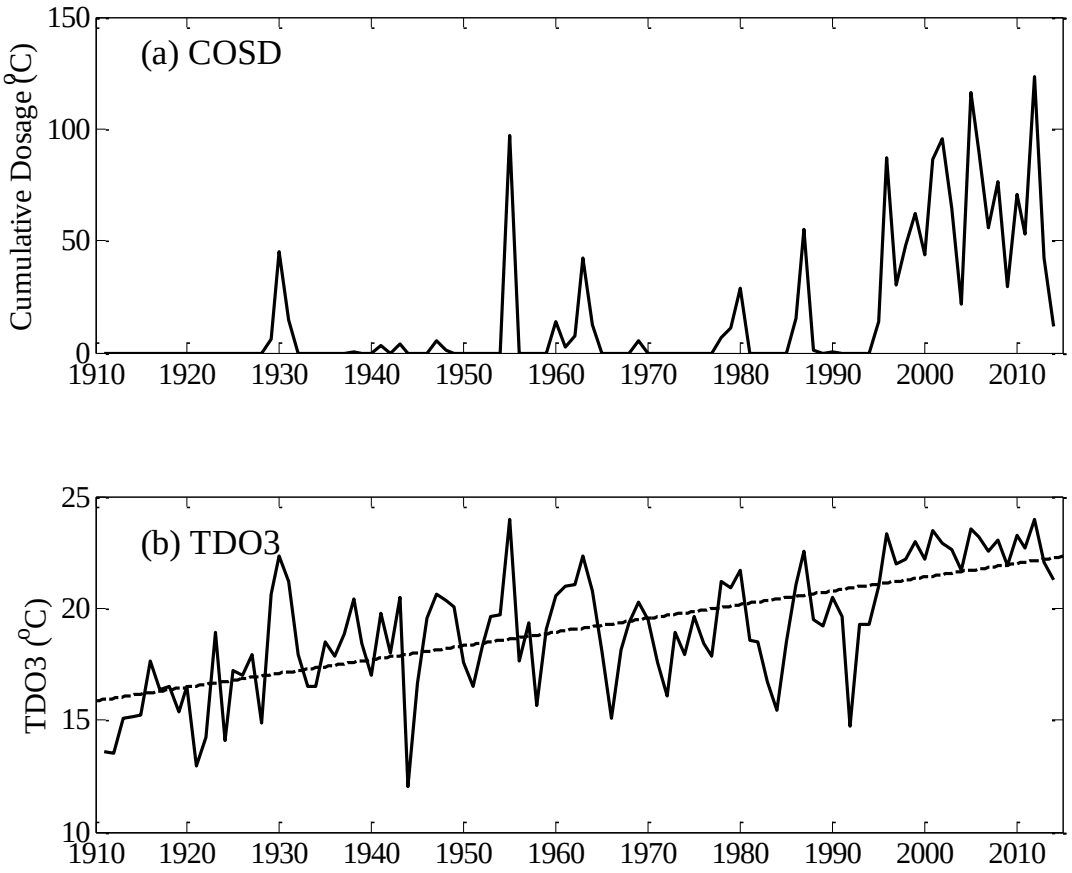

Figure 5-4: yearly (a) COSD and (b) TDO3 values from 1911 to 2014. Dashed line in (b) represents the trend of increasing TDO3.

5.4.3 Differences between COSD and TDO3

COSD and TDO3 values are highly correlated for both the 20-year study period (r = 0.95, p<0.01) and the 104-year extended period (r = 0.71, p<0.01), and in general, years with high (low) TDO3 values also have high (low) COSD values. This makes sense as COSD is an additional calculation step based upon daily TDO3 values. However, there are some years with key differences between the two values mainly due to the duration of high temperature and low DO conditions during the stratified period. For example, comparing the years 2005 and 2006, both years have similar TDO3 values (23.5°C for 2005 and 23.2°C for 2006, 1.3% difference), but different COSD values (116.2°C for 2005 and 89.6°C for 2006, 22.9% difference). As shown

in Figure 5-5 b, the majority of this difference in COSD value between the two years is due longer amount of time that TDO3 values exceed the 21°C threshold during 2005 when compared to 2006. Additionally, 2006 has a higher peak daily dosage value than 2005 (3.31°C in 2006 compared to 2.92°C in 2005), but a shorter duration of days exceeding the dosage threshold (56 days compared to 73 days). This illustrates the primary difference between, and advantage of, COSD over TDO3 – consideration of the stress duration. These stress duration differences are representative of years with similar TDO3 values but largely different COSD values. The TDO3 method only takes into account the average of 31 days of stress conditions, so the effects of stressful or near-stressful conditions lasting longer than the 31 days averaging period are not apparent. Conversely, years with short periods of high stress conditions, may be identified as low stress years by the TDO3 method even though acute temperature exposures may exceed the upper lethal limit.

While the ability of the COSD method to account for stress duration is a clear advantage over the TDO3 method, there are disadvantages. Firstly, in lakes where DO levels are generally high and water temperatures are low, COSD values do not exceed 0°C, unlike TDO3 values which are always above zero unless the lake has no anoxic conditions (i.e. DO is always above 3 mg L^{-1}). Since there is a numerical value for each year of interest, it is easier to assess trends and changes in stress values when using the TDO3 method in comparison to the COSD method. Second, the TDO3 method can be used easily to analyze stress for multiple fish species in the same lake and across lakes without any additional analysis (Jacobson et al. 2010; Jiang et al. 2012; Herb et al. 2014), whereas COSD values must be recalculated for each fish species of interest.

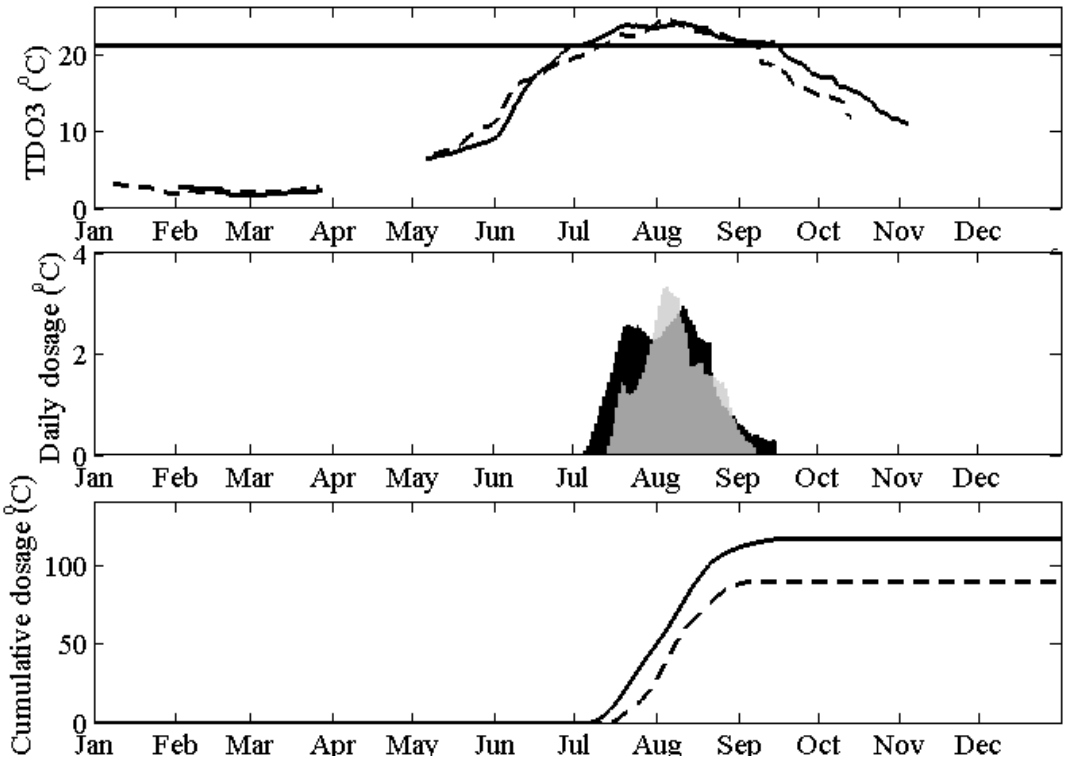

Figure 5-5: comparison of TDO3 and cumulative dosage for two consecutive years, 2005 and 2006. (a) shows the daily TDO3 values for both years with 2005 in solid black line and 2006 in dashed black line. (b) shows the daily TDO3 dosage over the threshold value with 2005 in black and 2006 in grey. (c) shows the cumulative oxythermal stress dosage for the year with 2005 as the solid black line and 2006 as the dashed black line.

5.4.4 Changing COSD and TDO3 with air temperature perturbations

To assess the impact of changing air temperature on stress conditions, simulations with daily air temperature perturbations of +1°C to +5°C were performed on the 1995-2014 simulations, totaling 120 different years of simulations with unique air temperature scenarios. July, August, September (JAS) averaged air temperatures were determined to be most highly correlated with COSD (r = 0.62, p <0.01) values and TDO3 (r = 0.53, p<0.01) values in comparison to other 3-month air temperature averages and are used for evaluation here. For the 120 years of simulation, increasing air temperature results in increasing COSD values and

increasing TDO3 values (Figure 5-6). For each 1°C increase in air temperature, COSD increases by 22.55°C (p<0.01), while TDO3 increases by 0.49°C (p<0.01). This is consistent with previous research showing increasing air temperatures increase fish stress conditions and loss of available lake habitat in temperate regions (Sharma et al. 2011; Jiang et al. 2012; Herb et al. 2014; Van Zuiden et al. 2016). Simulated COSD values become more variable as JAS air temperatures increase, while variation in TDO3 values remain fairly constant. This is a product of variability in the duration of stress conditions during the stratified period.

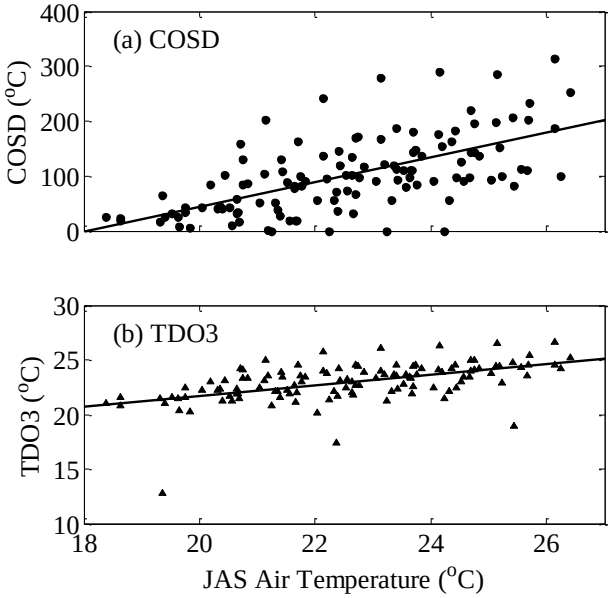

Figure 5-6: (a) COSD and (b) TDO3 values determine from the model for 120 scenarios of July, August, and September (JAS) averaged air temperatures. The first 20 years representing the air temperature conditions during the period 1995-2014 and the remaining years representing daily air temperature increases of +1°C, + 2°C, +3°C, +4°C, and +5°C. Solid lines in (a) and (b) represent the linear trend of changing oxythermal stress with increasing JAS air temperatures.

Probability distributions for the different air temperature scenarios (Figure 5-7) show that as air temperatures increase, both the average COSD value increases and the distribution shifts so that there is a larger probability of high COSD values with larger air temperatures. After air temperature perturbations of +3°C, the mean COSD value exceeds the 90°C threshold that may result in yellow perch kills, and 65% (13 of 20) years exceeded the 90°C threshold. For the +2°C perturbation scenario, only 40% of years (8 of 20) exceeded the threshold. This may indicate the likelihood of a possible extirpation of yellow perch in Fish Lake after at 3.0°C increase in summer air temperatures. Other factors may also influence temperature changes causing

extirpation. For example, juvenile perch often inhabit hypoxic pelagic zones to avoid predators (Vejřík et al. 2016), which may sustain a perch population in the lake, although shift it towards that of a younger, smaller community. Shorter, warmer winters, however, may exacerbate fish stress conditions occurring in the summer by reducing recruitment. Warmer overwinter temperatures can alter the number of females that spawn and the overall composition of egg tissue (Feiner et al. 2016) and short, warm winters are followed by failed annual recruitment events due to smaller egg production, lower hatch rates, and smaller larvae (Farmer et al. 2015). Such conditions may impact fish extirpation to an equal or greater degree than warm summer water temperatures and low DO values.

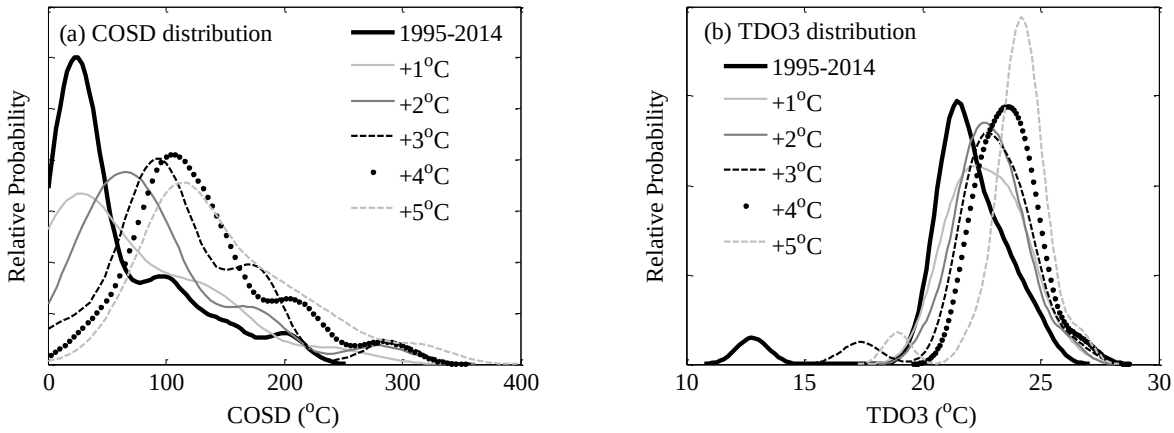

Figure 5-7: probability density functions for (a) COSD and (b) TDO3 values given six air temperature scenarios: the original daily air temperatures from 1995-2014 (solid black line), +1°C increase of daily air temperatures (solid light gray line), +2°C increase of daily air temperatures (solid dark gray line), +3°C increase of daily air temperatures (black dashed line), +4°C increase of daily air temperatures (dotted black line), and +5°C increase of daily air temperatures (dashed gray line).

5.5 Conclusion

Understanding the impact of increasing air temperatures on cool-water fish populations, particularly fish stress and fish kill years under increasing air temperature scenarios is incredibly important from both a fisheries and lake ecosystem management standpoint. Assessing the

impact of increasing air temperature involves not only simulating future air temperature scenarios, but also developing an appropriate measure to quantify conditions of oxythermal stress for low-temperature thermal guilds that require both cool- or cold-waters and high DO concentrations.

To address this problem, we developed a novel metric, Cumulative Oxythermal Stress Dosage (COSD) to quantify oxythermal stress and corresponding habitat loss in a cool-water fish species, yellow perch (*Perca flavescens*). Then we assessed the change in historical COSD and future COSD as a result of daily air temperature perturbations using the hydrodynamic-water quality model, DYRESM-WQ-I.

Results indicate that for yellow perch on Fish Lake, Wisconsin, USA, the COSD method does a better job of predicting fish declines than does the previously developed TDO3 method. The main advantage of the COSD method in comparison to previously developed metrics for quantifying stress is the capability to consider both the duration of stress conditions and the magnitude of water temperature stress conditions. Over a 20-year period (1995-2014) for which water temperature and DO data was available for direct comparison, there was no long-term trend in COSD values for the lake; however, extending the simulation period to include 104 years of simulations for which meteorological data is available, there was an increase in the COSD driven largely by increased COSD values occurring after 1996. When analyzing daily air temperature perturbations of +1°C to +5°C, results reveal that for each 1°C increase in air temperature, COSD increases by 22.55°C and COSD values become more variable as the July – September average air temperatures increase. Additionally, probability distributions indicate that as perturbation values increase there is a larger probability of high COSD values and there is a

possibility of yellow perch extirpation in Fish Lake after summer air temperature increases of 3.0°C.

5.6 Acknowledgements

Financial support for authors was provided by the NSF – LTER program, University of Wisconsin Water Resources Institute USGS 10(B) Research grant, the UW Office of Sustainability SIRE Award Program, and the Northeast Climate Science Center. The authors would like to thank Richard Lathrop, John Magnuson, Peter McIntyre, Paul Hanson, Trina McMahon, and Paul Block for helpful and insightful comments on the manuscript.

5.7 References

Alewell, C., and B. Manderscheid. 1998. Use of objective criteria for the assessment of biogeochemical ecosystem models. Ecol. Model. 107: 213–224. doi:10.1016/S0304-3800(97)00218-4

Brett, J. R. 1971. Energetic Responses of Salmon to Temperature. A Study of Some Thermal Relations in the Physiology and Freshwater Ecology of Sockeye Salmon (Oncorhynchus nerkd). Am. Zool. 11: 99–113. doi:10.1093/icb/11.1.99

Cahn, A. R. 1927. An ecological study of southern Wisconsin fishes, the brook silver-side and the cisco in their relation to the region. Ill. Biol. Monogr. 11: 1–151.

Casselman, J. M. 2002. Effects of temperature, global extremes, and climate change on year-class production of warmwater, coolwater, and coldwater fishes in the Great Lakes basin. *Fisheries in a changing climate*. Proceedings of the American Fisheries Society Symposium. 39–60.

Cherry, D., K. Dickson, J. Cairns, and J. Stauffer. 1977. Preferred, Avoided, and Lethal Temperatures of Fish During Rising Temperature Conditions. J. Fish. Res. Board Can. 34: 239–246.

Coutant, C. 1990. Temperature-Oxygen Habitat for Fresh-Water and Coastal Striped Bass in a Changing Climate. Trans. Am. Fish. Soc. 119: 240–253. doi:10.1577/1548-8659(1990)119<0240:THFFAC>2.3.CO;2

De Stasio, J. D. S., and F. J. Rahel. 1994. Influence of Water Temperature on Interactions between Juvenile Colorado River Cutthroat Trout and Brook Trout in a Laboratory

Stream. Trans. Am. Fish. Soc. 123: 289–297. doi:10.1577/1548-8659(1994)123<0289:IOWTOI>2.3.CO;2

Dillon, P. J., B. J. Clark, L. A. Molot, and H. E. Evans. 2003. Predicting the location of optimal habitat boundaries for lake trout (*Salvelinus namaycush*) in Canadian Shield lakes. Can. J. Fish. Aquat. Sci. 60: 959–970. doi:10.1139/f03-082

Elliott, A. 2010. A comparison of thermal polygons for British freshwater teleosts. *Freshwater Forum*.

Fang, X., and H. G. Stefan. 2009. Simulations of climate effects on water temperature, dissolved oxygen, and ice and snow covers in lakes of the contiguous U.S. under past and future climate scenarios. Limnol. Oceanogr. 54: 2359–2370. doi:10.4319/lo.2009.54.6_part_2.2359

Fang, X., H. G. Stefan, J. G. Eaton, J. H. McCormick, and S. R. Alam. 2004. Simulation of thermal/dissolved oxygen habitat for fishes in lakes under different climate scenarios: Part 1. Cool-water fish in the contiguous US. Ecol. Model. 172: 13–37. doi:10.1016/S0304-3800(03)00282-5

Farmer, T. M., E. A. Marschall, K. Dabrowski, and S. A. Ludsin. 2015. Short winters threaten temperate fish populations. Nat. Commun. 6: 7724. doi:10.1038/ncomms8724

Feiner, Z. S., D. P. Coulter, S. C. Guffey, and T. O. Höök. 2016. Does overwinter temperature affect maternal body composition and egg traits in yellow perch Perca flavescens? J. Fish Biol. 88: 1524–1543. doi:10.1111/jfb.12929

Ferguson, R. G. 1958. The Preferred Temperature of Fish and their Midsummer Distribution in Temperate Lakes and Streams. J. Fish. Res. Board Can. 15: 607–624. doi:10.1139/f58-032

Frey, D. G. 1955. Distributional ecology of the cisco (Coregonus artedii) in Indiana. Invest Indiana Lakes Streams 4: 177–228.

Fry, E. F. J. 1971. The Effect of Environment on the Physiology of Fish, Academic Press.

Hamilton, D. P., and S. G. Schladow. 1997. Prediction of water quality in lakes and reservoirs. Part I — Model description. Ecol. Model. 96: 91–110. doi:10.1016/S0304-3800(96)00062-2

Hennings, R. G., and J. P. Connelly. 2008. Average ground-water temperature map, Wisconsin. 1980–5. 1980–5 Wisconsin Geological and Natural History Survey.

Herb, W. R., L. B. Johnson, P. C. Jacobson, and H. G. Stefan. 2014. Projecting cold-water fish habitat in lakes of the glacial lakes region under changing land use and climate regimes. Can. J. Fish. Aquat. Sci. 71: 1334–1348. doi:10.1139/cjfas-2013-0535

Hinz, L. C., and M. J. Wiley. 1998. Growth and production of juvenile trout in Michigan streams: influence of potential ration and temperature, Michigan Department of Natural Resources, Fisheries Division.

Imberger, J., I. Loh, B. Hebbert, and J. Patterson. 1978. Dynamics of Reservoir of Medium Size. J. Hydraul. Div. 104: 725–743.

IPCC. 2013. Summary for Policymakers, p. 3–29. *In* T. Stocker, D. Qin, G.-K. Plattner, et al. [eds.], Climate Change 2013: The Physical Science Basis. Contribution of Working Group I to the Fifth Assessment Report of the Intergovernmental Panel on Climate Change. Cambridge University Press.

Ito, Y., and K. Momii. 2015. Impacts of regional warming on long-term hypolimnetic anoxia and dissolved oxygen concentration in a deep lake. Hydrol. Process. 29: 2232–2242. doi:10.1002/hyp.10362

Jacobson, P. C., H. G. Stefan, and D. L. Pereira. 2010. Coldwater fish oxythermal habitat in Minnesota lakes: influence of total phosphorus, July air temperature, and relative depth. Can. J. Fish. Aquat. Sci. 67: 2002–2013. doi:10.1139/F10-115

Jiang, L., X. Fang, H. G. Stefan, P. C. Jacobson, and D. L. Pereira. 2012. Oxythermal habitat parameters and identifying cisco refuge lakes in Minnesota under future climate scenarios using variable benchmark periods. Ecol. Model. 232: 14–27. doi:10.1016/j.ecolmodel.2012.02.014

Krohelski, J. T., Y.-F. Lin, W. J. Rose, and R. J. Hunt. 2002. Simulation of Fish, Mud, and Crystal Lakes and the shallow ground-water system, Dane County, Wisconsin. USGS Numbered Series 2002–4014. 2002–4014 U.S. Geological Survey.

Magee, M. R., C. H. Wu, D. M. Robertson, R. C. Lathrop, and D. P. Hamilton. 2016. Trends and abrupt changes in 104 years of ice cover and water temperature in a dimictic lake in response to air temperature, wind speed, and water clarity drivers. Hydrol Earth Syst Sci 20: 1681–1702. doi:10.5194/hess-20-1681-2016

Magnuson, J. J., L. B. Crowder, and P. A. Medvick. 1979. Temperature as an ecological resource. Am. Zool. 19: 331–343.

McCauley, R., and L. Read. 1973. Temperature Selection by Juvenile and Adult Yellow Perch (perca-Flavescens) Acclimated to 24 C. J. Fish. Res. Board Can. 30: 1253–1255.

McKee, T. B., N. J. Doesken, C. A. Davey, and Pielke, Sr. 2000. Climate data continuity with ASOS. Report for period April 1996 through June 2000. Climno Report 00-3. Climno Report 00-3 Colorado Climate Center, Department of Atmospheric Science, Colorado State University.

Mortimer, C. H. 1981. The oxygen content of air-saturated fresh waters over - ranges of temperature and atmospheric pressure of - limnological interest.

Neill, W., and J. Magnuson. 1974. Distributional Ecology and Behavioral Thermoregulation of Fishes in Relation to Heated Effluent from a Power-Plant at Lake-Monona, Wisconsin. Trans. Am. Fish. Soc. 103: 663–710. doi:10.1577/1548-8659(1974)103<663:DEABTO>2.0.CO;2

Nürnberg, G. K. 1995. Quantifying anoxia in lakes. Limnol. Oceanogr. 40: 1100–1111.

O'Reilly, C. M., S. Sharma, D. K. Gray, and others. 2015. Rapid and highly variable warming of lake surface waters around the globe. Geophys. Res. Lett. 42: 2015GL066235. doi:10.1002/2015GL066235

Reese, C. D., and B. C. Harvey. 2002. Temperature-dependent interactions between juvenile steelhead and Sacramento pikeminnow in laboratory streams. Trans. Am. Fish. Soc. 131: 599–606.

Reutter, J. M., and C. E. Herdendorf. 1974. Laboratory Estimates of the Seasonal Final Temperature Preferenda of Some Lake Erie Fish. Proc. Conf. Gt. Lakes Res. 17: 59–67.

Robertson, D. M. 1989. The use of lake water temperature and ice cover as climatic indicators. PhD Thesis. University of Wisconsin-Madison.

Rudstam, L. G., and J. J. Magnuson. 1985. Predicting the vertical distribution of fish populations: analysis of cisco, Coregonus artedii, and yellow perch, Perca flavescens. Can. J. Fish. Aquat. Sci. 42: 1178–1188.

Selong, J. H., T. E. McMahon, A. V. Zale, and F. T. Barrows. 2001. Effect of temperature on growth and survival of bull trout, with application of an improved method for determining thermal tolerance in fishes. Trans. Am. Fish. Soc. 130: 1026–1037.

Sharma, S., M. J. Vander Zanden, J. J. Magnuson, and J. Lyons. 2011. Comparing Climate Change and Species Invasions as Drivers of Coldwater Fish Population Extirpations H. Browman [ed.]. PLoS ONE 6: e22906. doi:10.1371/journal.pone.0022906

Snucins, E. J., and J. M. Gunn. 1995. Coping with a Warm Environment: Behavioral Thermoregulation by Lake Trout. Trans. Am. Fish. Soc. 124: 118–123. doi:10.1577/1548-8659(1995)124<0118:CWAWEB>2.3.CO;2

Stefan, H. G., X. Fang, and J. G. Eaton. 2001. Simulated Fish Habitat Changes in North American Lakes in Response to Projected Climate Warming. Trans. Am. Fish. Soc. 130: 459–477. doi:10.1577/1548-8659(2001)130<0459:SFHCIN>2.0.CO;2

US EPA. 1986. Ambient water quality criteria for dissolved oxygen. 440/5-86-003. 440/5-86-003 US Environmental Protection Agency (EPA).

Van Zuiden, T. M., M. M. Chen, S. Stefanoff, L. Lopez, and S. Sharma. 2016. Projected impacts of climate change on three freshwater fishes and potential novel competitive interactions. Divers. Distrib. 22: 603–614. doi:10.1111/ddi.12422

Vejřík, L., I. Matějíčková, T. Jůza, and others. 2016. Small fish use the hypoxic pelagic zone as a refuge from predators. Freshw. Biol. 61: 899–913. doi:10.1111/fwb.12753

Walker, R. R., and W. J. Snodgrass. 1986. Model for sediment oxygen demand in lakes. J. Hydraul. Eng. ASCE 112: 25–43.

Wehrly, K. E., L. Wang, and M. Mitro. 2007. Field-Based Estimates of Thermal Tolerance Limits for Trout: Incorporating Exposure Time and Temperature Fluctuation. Trans. Am. Fish. Soc. 136: 365–374. doi:10.1577/T06-163.1

Wlosinski, J. H., A. S. Lessem, M. S. Dortch, M. Schneider, and J. L. Martin. 1995. CE-QUAL-R1: A Numerical One-Dimensional Model of Reservoir Water Quality; User's Manual. DTIC Document.

Chapter 6 : Conclusion

6.1 Summary

The impact of climate changes on lake ecosystems is becoming better understood (Adrian et al. 2009; Heino et al. 2009; Kosten et al. 2012; Jeppesen et al. 2012; Comte et al. 2013), but there are still unanswered questions, both in understanding differences among lake responses and in developing adaptation and/or mitigation techniques to combat the effect of changing climate. In view of these knowledge gaps, the objective of this dissertation was to determine the following: (1) what role does morphometry play in the response of lake water temperature and ice cover to air temperature increases and wind speed decreases; (2) what factors drive changes in oxythermal habitat and can management efforts, specifically phosphorus loading reductions mitigate the climate effects; (3) is there a more accurate (in terms of predicting CPUE-defined population declines) metric for quantifying changes in oxythermal habitat for a cool-water fish species and how does this metric change with increasing air temperatures. To address these knowledge deficiencies, a modeling approach (DYRESM-WQ-I) is used on three lakes near Madison, WI – Lake Mendota, Lake Wingra, and Fish Lake.

In Chapter 2, we use the one-dimensional hydrodynamic lake model on the years 1911-2014 for all three lakes to elucidate the effects of increasing air temperature and decreasing wind speed on lake thermal variables (water temperature, stratification dates, strength of stratification, and surface heat fluxes). Results show that epilimnetic temperatures increased, hypolimnetic temperatures decreased, stratification duration increased due to earlier stratification onset and fall overturn, and Schmidt stability increased. Perturbation analysis revealed that increasing air temperatures promoted warmer hypolimnion water, but decreasing wind speed cooled the

hypolimnion, indicating that changing hypolimnetic temperatures may be influenced by wind speed changes rather than temperature. Overall, lake depth impacts the influences the presence of stratification and magnitude of stability, but surface area influences the trend and variability of the remaining variables.

In Chapter 3, the effects of air temperature on ice cover (ice-on, ice-off, ice cover duration, and maximum ice thickness) are modeled and compared among three different lakes, one deep lake with large surface area, one deep lake with small surface area, and one shallow lake with small surface area. Ice cover duration has decreased because of later ice-on and earlier ice-off, and maximum ice cover has decreased significantly for all three lakes. Later, a perturbation analysis is performed to see how the three lakes respond to a range of air temperature scenarios. Results of historical and perturbation analysis show that shallower lakes with larger surface areas appear more resilient to ice cover changes caused by increases in air temperature.

In Chapter 4, DYRESM-WQ-I was used to investigate the importance of meteorological and water quality drivers on oxythermal habitat of cisco in Lake Mendota, WI. We found that the oxythermal habitat metric, maximum TDO3, has been significantly increasing over the period 1976-2013, and MLR analysis revealed that these TDO3 values are most influenced by summer (Jun – Aug) air temperature, spring (Mar – May) phosphorus load and spring (MAM) inflow into the lake. Sensitivity analysis, performed using a perturbation approach of varying two variables at once in different combinations, showed that when phosphorus load and lake inflow are decoupled, increasing inflow yields decreasing TDO3 values possibly due to flushing time reductions. Air temperature is the most significant driver, followed by phosphorus loading, and then inflow volumes. When comparing MLR analysis to DYRESM-WQ-I result, the MLR model

only accurately characterizes TDO3 values above or below the threshold values 58% of the time. Analysis under the probable A1B air temperature scenario reveal that phosphorus loading reductions would offset habitat loss from air temperature increases. This supports the hypothesis that management efforts could be effective in sustaining vulnerable populations in at-risk lakes both now and in the future.

In Chapter 5 we develop a novel metric, Cumulative Oxythermal Stress Dosage (COSD) to quantify oxythermal stress and corresponding habitat loss for a cool-water fish species in Fish Lake, WI. For yellow perch (*Perca flavescens*), the COSD method is a better predictor of fish declines as determined with CPUE values than the TDO3 method, which was previously developed for cold-water fish species. COSD method is able to account for both stress duration and stress magnitude, making it more advantageous when compared to other methods. Perturbations of air temperatures revealed a large, statistically significant increase in COSD per degree (°C) increase in air temperature. It is likely that in Fish Lake, yellow perch could be extirpated from the lake with summer average air temperature increases as little as 3°C.

6.2 Conclusions

- **Morphometric differences impact the response of water temperature and ice cover to increases in air temperature and decreases in wind speed**

Simulation results from Chapter 2 and 3 reveal that lake depth and surface area do play a role in expression of climate signals in lakes. The analysis presented in Chapters 2 and 3 represents one of the first attempts to examine 100-years of changes in lakes with three different morphometry characteristics to ascertain the role of lake depth and surface area on response of water temperature and ice cover to air temperature and wind speed changes. In our study, the

three lakes were simulated under identical meteorological scenarios and model parameters, so they would show identical responses if lake morphometry had no impact on the response of water temperature and ice cover to increases in air temperature and decreases in wind speed. However, for water temperature and stratification variables, lake surface area appears to play a prominent role in response to changes in air temperature and wind speed. Larger surface area promotes more wind mixing, so they respond more quickly to decreases in wind speed and have more variability in lake response. For ice cover variables, depth more highly influences changes in ice dates and maximum ice thickness, with shallower lakes appearing to be more resilient to changes in air temperature than their deeper counterparts.

- **Wind speed is an important driver to consider in regards to water temperature and stratification variables**

While much research has investigated the physical response of lakes to climate changes (Arvola et al. 2009; Dokulil 2014; Butcher et al. 2015; Almeida et al. 2015; O'Reilly et al. 2015), the effect of changes in wind speed on lake thermal structure has largely been ignored in observational studies (Desai et al. 2009) and numerical simulation studies (MacKay et al. 2009; Kerimoglu and Rinke 2013). In Chapter 2, wind speed perturbation simulations were performed to deduce the effects of changing wind speed in addition to changing air temperatures on water temperature and stratification. Results indicate that decreasing wind speeds increase stratification duration (earlier onset and later overturn) and lake stability above that of increases in air temperatures. Increasing wind speeds, however, have a mitigating effect on lake water temperatures and stratification response to increasing air temperatures. Additionally, previous research has shown inconsistencies in hypolimnion temperature increases (Livingstone 2003)

and decreases (Bueche and Vetter 2014), but perturbation scenarios here suggest that these inconsistencies may be due to local differences in the direction of wind speed changes.

- **Phosphorus loading reductions are an effective tool to combat loss of fish habitat from increases in air temperature**

Simulation and multiple linear regression analysis in Chapter 4 show that for Lake Mendota, available cisco habitat is driven by summer (JJA) air temperature, spring (MAM) phosphorus loading, and spring (MAM) inflow volume to the lake. These results are consistent with previous studies showing that warmer air temperatures and increased phosphorus loads reduce cold-water fish habitat (Jacobson et al. 2010; Herb et al. 2014; Honsey et al. 2016). Simulation and sensitivity analysis shows that for Lake Mendota, under the future A1B air temperature scenario, available habitat for cisco could be increased to, and even improved above, current levels by reducing the phosphorus loading into the lake. This represents an opportunity to maintain cisco populations in at-risk lakes.

- **COSD may be a useful metric for quantifying oxythermal habitat changes of cool-water fish species, and increases in air temperature alter the mean of COSD values and distribution of those values**

Chapter 5 develops a novel metric, cumulative oxythermal stress dosage (COSD), and compares it to TDO3 (Jacobson et al. 2010; Jiang et al. 2012; Herb et al. 2014) both in terms of ability to simulate conditions of low abundance, and in the response to increases of air temperature for a cool-water fish species, yellow perch. Results indicate that for yellow perch on Fish Lake, Wisconsin, years with the highest COSD values match years with the lowest yellow

perch abundance, as estimated with CPUE values, whereas TDO3 values do not match low perch abundance. The advantage of COSD method is its ability to account for magnitude of stress conditions and length of strength conditions. Using the COSD metric to quantify oxythermal stress, air temperatures were perturbed and results reveal that COSD values become more variable as the July – September air temperatures increase.

6.3 Recommendations for future work

While Chapters 2 and 3 give evidence that lake depth and surface area impact lake responses to changing climate, future modeling studies could investigate changes over a larger range of lake sizes. Such a modeling effort would more clearly delineate effects of depth and surface area through the creation of artificial modeling lakes. This would enable development of empirical equations describing response differences based on depth and surface area in addition to identifying possible lake sizes where significant shifts in response would be expected. Furthermore, this modeling study only described lakes that are all eutrophic, and results may not hold true for oligotrophic or mesotrophic lakes. A more expansive, purely modeling effort, could further investigate the role of lake trophic status on response to climate changes, providing more information on lake response to develop mitigation and adaptation efforts.

Results from Chapter 4 are promising in their indication that fish habitat could be maintained under changing climate through phosphorus loading reductions, but fish ecologists and managers would benefit greatly from increased knowledge on the number and types of lakes that could be impacted as well as the fish species that could be maintained. Cisco was chosen in this study in part because of the interest of those in the Wisconsin Department of Natural Resources to maintain and protect cisco populations in the state (John Lyons, personal communication). Other fish species may benefit from similar eutrophication management

strategies, while still others may face extirpation regardless of eutrophication efforts as warm-water fish expand their range northward and negatively interact with current populations (Sharma et al. 2011; Van Zuiden et al. 2016). More detailed analysis of range changes for cold-, cool-, and warm-water fish species in response to changes in air temperature and wind speed will help target management efforts to lakes where mitigation success is more likely.

A more detailed analysis of the COSD method and testing the predictive ability on other fish species in more lakes would further enhance the metric and support its use in investigating the impact of climate on oxythermal stress. Coupling the temperature and DO modeling approach with fish bioenergetics modeling might further refine COSD limits for varying fish species as well as investigate the effects of different timing, magnitude, and duration of stressful conditions. Recent research has identified winter temperatures as a threat to fish populations, specifically yellow perch, because short, warm winters impact spawning and reproductive success (Farmer et al. 2015; Feiner et al. 2016). A concept similar to that of COSD may enable modeling and future projections to investigate the effect of winter temperatures on reproduction.

Finally, for each of these modeling scenarios, perturbations of drivers were constant with time, but long-term and projected changes vary seasonally (Manabe et al. 2011) and diurnally (Vose et al. 2005; You et al. 2016), and these changes have caused asymmetric impacts on lake temperatures (Livingstone 2003; Wilhelm et al. 2006), dissolved oxygen (Snortheim 2015) and ecological responses (Winder and Schindler 2004; Straile et al. 2015; Coulter et al. 2016). Similar analysis as performed in this dissertation, but with focus on diurnally and seasonally asymmetric warming may further improve estimates and understanding of lake response to changing climate. Specifically, increases nighttime warming might further exacerbate lake warming and longer stratification as well as reduce ice cover because lakes tend to cool at night.

Seasonally heterogeneity in air temperature and wind speed changes may alter the response of stratification and in effect fish growth and reproduction cycles due to timing of temperature changes.

6.4 References

Adrian, R., C. M. O'Reilly, H. Zagarese, and others. 2009. Lakes as sentinels of climate change. Limnol. Oceanogr. **54**: 2283–2297.

Almeida, M. C., P. S. Coelho, A. C. Rodrigues, P. A. Diogo, R. Maurício, R. M. Cardoso, and P. M. Soares. 2015. Thermal stratification of Portuguese reservoirs: potential impact of extreme climate scenarios. J. Water Clim. Change **6**: 544. doi:10.2166/wcc.2015.071

Arvola, L., G. George, D. M. Livingstone, and others. 2009. The Impact of the Changing Climate on the Thermal Characteristics of Lakes, p. 85–101. *In* G. George [ed.], The Impact of Climate Change on European Lakes. Springer Netherlands.

Bueche, T., and M. Vetter. 2014. Future alterations of thermal characteristics in a medium-sized lake simulated by coupling a regional climate model with a lake model. Clim. Dyn. **44**: 371–384. doi:10.1007/s00382-014-2259-5

Butcher, J. B., D. Nover, T. E. Johnson, and C. M. Clark. 2015. Sensitivity of lake thermal and mixing dynamics to climate change. Clim. Change **129**: 295–305. doi:10.1007/s10584-015-1326-1

Comte, L., L. Buisson, M. Daufresne, and G. Grenouillet. 2013. Climate-induced changes in the distribution of freshwater fish: observed and predicted trends. Freshw. Biol. **58**: 625–639. doi:10.1111/fwb.12081

Coulter, D. P., M. S. Sepúlveda, C. D. Troy, and T. O. Höök. 2016. Species-specific effects of subdaily temperature fluctuations on consumption, growth and stress responses in two physiologically similar fish species. Ecol. Freshw. Fish **25**: 465–475. doi:10.1111/eff.12227

Desai, A. R., J. A. Austin, V. Bennington, and G. A. McKinley. 2009. Stronger winds over a large lake in response to weakening air-to-lake temperature gradient. Nat. Geosci. **2**: 855–858. doi:10.1038/ngeo693

Dokulil, M. 2014. Impact of climate warming on European inland waters. Inland Waters **4**: 27–40. doi:10.5268/IW-4.1.705

Farmer, T. M., E. A. Marschall, K. Dabrowski, and S. A. Ludsin. 2015. Short winters threaten temperate fish populations. Nat. Commun. **6**: 7724. doi:10.1038/ncomms8724

Feiner, Z. S., D. P. Coulter, S. C. Guffey, and T. O. Höök. 2016. Does overwinter temperature affect maternal body composition and egg traits in yellow perch Perca flavescens? J. Fish Biol. **88**: 1524–1543. doi:10.1111/jfb.12929

Heino, J., R. Virkkala, and H. Toivonen. 2009. Climate change and freshwater biodiversity: detected patterns, future trends and adaptations in northern regions. Biol. Rev. **84**: 39–54. doi:10.1111/j.1469-185X.2008.00060.x

Herb, W. R., L. B. Johnson, P. C. Jacobson, and H. G. Stefan. 2014. Projecting cold-water fish habitat in lakes of the glacial lakes region under changing land use and climate regimes. Can. J. Fish. Aquat. Sci. **71**: 1334–1348. doi:10.1139/cjfas-2013-0535

Honsey, A. E., S. B. Donabauer, and T. O. Höök. 2016. An Analysis of Lake Morphometric and Land-Use Characteristics that Promote Persistence of Cisco in Indiana. Trans. Am. Fish. Soc. **145**: 363–373. doi:10.1080/00028487.2015.1125949

Jacobson, P. C., H. G. Stefan, and D. L. Pereira. 2010. Coldwater fish oxythermal habitat in Minnesota lakes: influence of total phosphorus, July air temperature, and relative depth. Can. J. Fish. Aquat. Sci. **67**: 2002–2013. doi:10.1139/F10-115

Jeppesen, E., T. Mehner, I. J. Winfield, and others. 2012. Impacts of climate warming on the long-term dynamics of key fish species in 24 European lakes. Hydrobiologia **694**: 1–39. doi:10.1007/s10750-012-1182-1

Jiang, L., X. Fang, H. G. Stefan, P. C. Jacobson, and D. L. Pereira. 2012. Oxythermal habitat parameters and identifying cisco refuge lakes in Minnesota under future climate scenarios using variable benchmark periods. Ecol. Model. **232**: 14–27. doi:10.1016/j.ecolmodel.2012.02.014

Kerimoglu, O., and K. Rinke. 2013. Stratification dynamics in a shallow reservoir under different hydro-meteorological scenarios and operational strategies. Water Resour. Res. **49**: 7518–7527. doi:10.1002/2013WR013520

Kosten, S., V. L. M. Huszar, E. Bécares, and others. 2012. Warmer climates boost cyanobacterial dominance in shallow lakes. Glob. Change Biol. **18**: 118–126. doi:10.1111/j.1365-2486.2011.02488.x

Livingstone, D. M. 2003. Impact of Secular Climate Change on the Thermal Structure of a Large Temperate Central European Lake. Clim. Change **57**: 205–225. doi:10.1023/A:1022119503144

MacKay, M. D., P. J. Neale, C. D. Arp, and others. 2009. Modeling lakes and reservoirs in the climate system. Limnol. Oceanogr. **54**: 2315–2329. doi:10.4319/lo.2009.54.6_part_2.2315

Manabe, S., J. Ploshay, and N.-C. Lau. 2011. Seasonal Variation of Surface Temperature Change during the Last Several Decades. J. Clim. **24**: 3817–3821. doi:10.1175/JCLI-D-11-00129.1

O'Reilly, C. M., S. Sharma, D. K. Gray, and others. 2015. Rapid and highly variable warming of lake surface waters around the globe. Geophys. Res. Lett. **42**: 2015GL066235. doi:10.1002/2015GL066235

Sharma, S., M. J. Vander Zanden, J. J. Magnuson, and J. Lyons. 2011. Comparing Climate Change and Species Invasions as Drivers of Coldwater Fish Population Extirpations H. Browman [ed.]. PLoS ONE **6**: e22906. doi:10.1371/journal.pone.0022906

Snortheim, C. A. 2015. Meteorological drivers of oxygen depletion in Lake Mendota. University of Wisconsin-Madison.

Straile, D., O. Kerimoglu, and F. Peeters. 2015. Trophic mismatch requires seasonal heterogeneity of warming. Ecology **96**: 2794–2805. doi:10.1890/14-0839.1

Van Zuiden, T. M., M. M. Chen, S. Stefanoff, L. Lopez, and S. Sharma. 2016. Projected impacts of climate change on three freshwater fishes and potential novel competitive interactions. Divers. Distrib. **22**: 603–614. doi:10.1111/ddi.12422

Vose, R. S., D. R. Easterling, and B. Gleason. 2005. Maximum and minimum temperature trends for the globe: An update through 2004. Geophys. Res. Lett. **32**: L23822. doi:10.1029/2005GL024379

Wilhelm, S., T. Hintze, D. M. Livingstone, and R. Adrian. 2006. Long-term response of daily epilimnetic temperature extrema to climate forcing. Can. J. Fish. Aquat. Sci. **63**: 2467–2477. doi:10.1139/f06-140

Winder, M., and D. E. Schindler. 2004. Climate Change Uncouples Trophic Interactions in an Aquatic Ecosystem. Ecology **85**: 2100–2106.

You, Q., J. Min, Y. Jiao, M. Sillanpää, and S. Kang. 2016. Observed trend of diurnal temperature range in the Tibetan Plateau in recent decades. Int. J. Climatol. **36**: 2633–2643. doi:10.1002/joc.4517

Appendix A: Description of ice model component of DYRSEM – WQ – I

Portions of the model description are adapted from: Hamilton DP, MR Magee, CH Wu, and TK Kratz. Ice cover and thermal regime in a dimictic seepage lake under climate change. *In review* at Inland Waters

A.1 Ice modeling background

Previous models have coupled water temperature and ice cover with varying flavors of model development and implementation. For example, DYRESMI (Patterson and Hamblin 1988) fully coupled the DYnamic REservoir Simulation Model (DYRESM; Imberger and Patterson, 1981) with a two-component ice and snow model that incorporated two-dimensional effects of partial ice cover by using a minimum ice thickness criteria. Gosink (1987) similarly created DYRESMICE by coupling DYRESM with a snow-ice model and modified wind stress by applying a damping coefficient that decreased linearly from 1.0 to 0 as ice thickness increased from 0 to 10 cm. Mixed Lake with Ice (MLI; Rogers *et al.*, 1995) was an extension of DYRESMI (Patterson and Hamblin 1988) that included a three-component ice and snow model, snowmelt by rain, variable snow density, and snow and ice albedo. Recently, Oveisy and Boegman (2014) also coupled a three-component ice model to DYRESM in a method similar to that of Rogers *et al.* (1995). In addition to those coupled to DYRESM, others have developed ice and water temperature models, including ones added to the Minnesota Lake Model (MINLAKE) incorporating two-component ice and snow models (Gu and Stefan 1990) and sediment heat flux (Fang and Stefan 1996b) and the Dynamic Lake Model (DLM; (McCord et al. 2000).

A.2 Model description

A.2.1 Ice model

Here, a one-dimensional hydrodynamic lake-ice model (DYRESM-WQ-I) is developed and used to simulate vertical water temperature profiles and ice cover thickness in Fish Lake, Lake Wingra, and Lake Mendota. DYRESM simulates vertical water temperature, salinity, and density by using discrete horizontal Lagrangian layers of uniform properties that vary in thickness. More information on the hydrodynamic model simulation of water temperature and mixing can be found in Imberger and Patterson (1981) and Yeates and Imberger (2003). DYRESM-WQ-I, adds an ice sub-model to DYRESM (Hamilton and Schladow 1997) that is based upon the MLI model of Rogers *et al.* (1995) with alterations to two-way coupling of the water-column dynamics to the ice model and the addition of a time-dependent sediment heat flux for all horizontal layers. Coupling between the hydrodynamic and ice models is in both directions, with the hydrodynamic model determining heat flux at the ice-water interface and ice cover characteristics providing boundary conditions for the hydrodynamic model. Ice-snow model equations are embedded into DYRESM-WQ-I in the subroutine that performs thermal transfers at the surface, with ice, snow, and water temperature determined by fluxes at the surface and at the ice-water interface. Water temperature under ice is driven by heat fluxes between the ice-water interface and radiative fluxes through the ice layer into the water column. For brevity, equations for the model will not be given except for some fundamental or new equations.

Equations of the ice and snow model are based on a quasi-steady state assumption that the time scale for heat conduction through the ice is short relative to the time scale of meteorological forcing (Patterson and Hamblin 1988; Rogers et al. 1995). This assumption is

valid under a Stefan Number <0.1 (Hill and Kucera 1983). When the surface water temperature first drops below 0°C, the ice module is initiated with the initial ice thickness set to a minimum value of 5 cm to address effects of partial ice cover (Patterson and Hamblin 1988; Vavrus et al. 1996). The steady-state conduction equations are used with a three-component model that includes blue ice, white ice, and snow (see Eq. 1 and Fig. 5 of Rogers *et al.*, 1995). Shortwave radiation is allocated into two components, a visible (A_1=70%) and an infra-red (A_2=30%) spectral band. White ice, also called snow ice, is formed when the mass of snow exceeds the buoyancy of ice cover and water breaks through the ice layer. To determine whether flooding of the snow occurs, a force balance is used to determine the equilibrium depth of snow supported by the ice cover (Equation 13 in Rogers *et al.*, 1995). Snow conductivity is estimated from its density using an empirical equation (Ashton, 1986; Equation 12 in Rogers *et al.*, 1995), and snow compaction is based on the exponential decay formula (McKay, 1968; Equation 11 in Rogers *et al.*, 1995). Upward conductive heat flux between ice/snow cover and the atmosphere, q_0, is determined by numerically solving the quasi-steady state heat conduction equations (Rogers et al. 1995) and assigning appropriate boundary conditions to the water, ice/snow, and atmospheric interfaces. A heat flux balance at the ice or snow surface supplies the condition for surface melting (see Equation 6 and 7 in Rogers *et al*., 1995). Heat fluxes at the surface are derived from standard bulk aerodynamic formula in DYRESM (Hamilton and Schladow 1997) with modifications for vapor pressure over ice or snow (Gill 1982) and the addition of rainfall heat flux (Rogers et al. 1995).

Accretion or ablation of ice is calculated through the heat flux at the ice-water interface,

$$q_f = q_0 - A_1 I_0 \{1 - \exp(-\lambda_{s1} h_s - \lambda_{s1} h_e - \lambda_{s1} h_i)\} - A_2 I_0 \{1 - \exp(-\lambda_{s2} h_s - \lambda_{s2} h_e - \lambda_{s2} h_i)\} - Q_{si} h_s \quad \text{(A.1)}$$

where I_0 is the shortwave radiation penetrating the surface; λ and h are the light attenuation coefficient and thickness of the ice and snow components; *s*, *i*, and *e* subscripts represent snow, blue ice, and white ice respectively; and Q_{si} is a volumetric heat flux for formation of white ice, which is provided in Eq. 14 of Rogers *et al*. (1995). Ice and snow light attenuation coefficients are fixed to the same values as those given by Rogers *et al.* (1995). Reflection of shortwave radiation from the ice or snow surface is a function of surface temperature and ice and snow thickness (Vavrus et al. 1996). Albedo values are derived from these functions and vary from 0.08 to 0.6 for ice and from 0.08 to 0.7 for snow.

The rate of change of blue ice thickness at the ice-water interface is calculated based on the imbalance between q_f and the heat flux from the water to the blue ice, q_w:

$$\frac{dh_i}{dt} = \frac{q_f - q_w}{\rho_i L} \tag{A.2}$$

where ρ_i is the density of blue ice; q_w is given by the approximation of the conductive heat flux from water to ice; and L is the latent heat of fusion:

$$q_w = -K_w \frac{\Delta T}{\Delta z} \tag{A.3}$$

where K_w is molecular conductivity and ΔT is the temperature difference between the surface water and the ice, which occurs across an assigned depth Δz, which is adopted as 0.5 m based on Rogers *et al.* (1995). ΔT here is calculated from the hydrodynamic portion of the model, different from Rogers *et al.* (1995), who estimated change in water temperature from the net heat flux and

lake area and volume (see Equation 23, Rogers *et al*., 1995). A decision tree to update ice cover, snow cover, and water depth is provided in Figure A-1, and hydrodynamic and ice model parameters can be found in Table 1 of Magee et al. (2016)

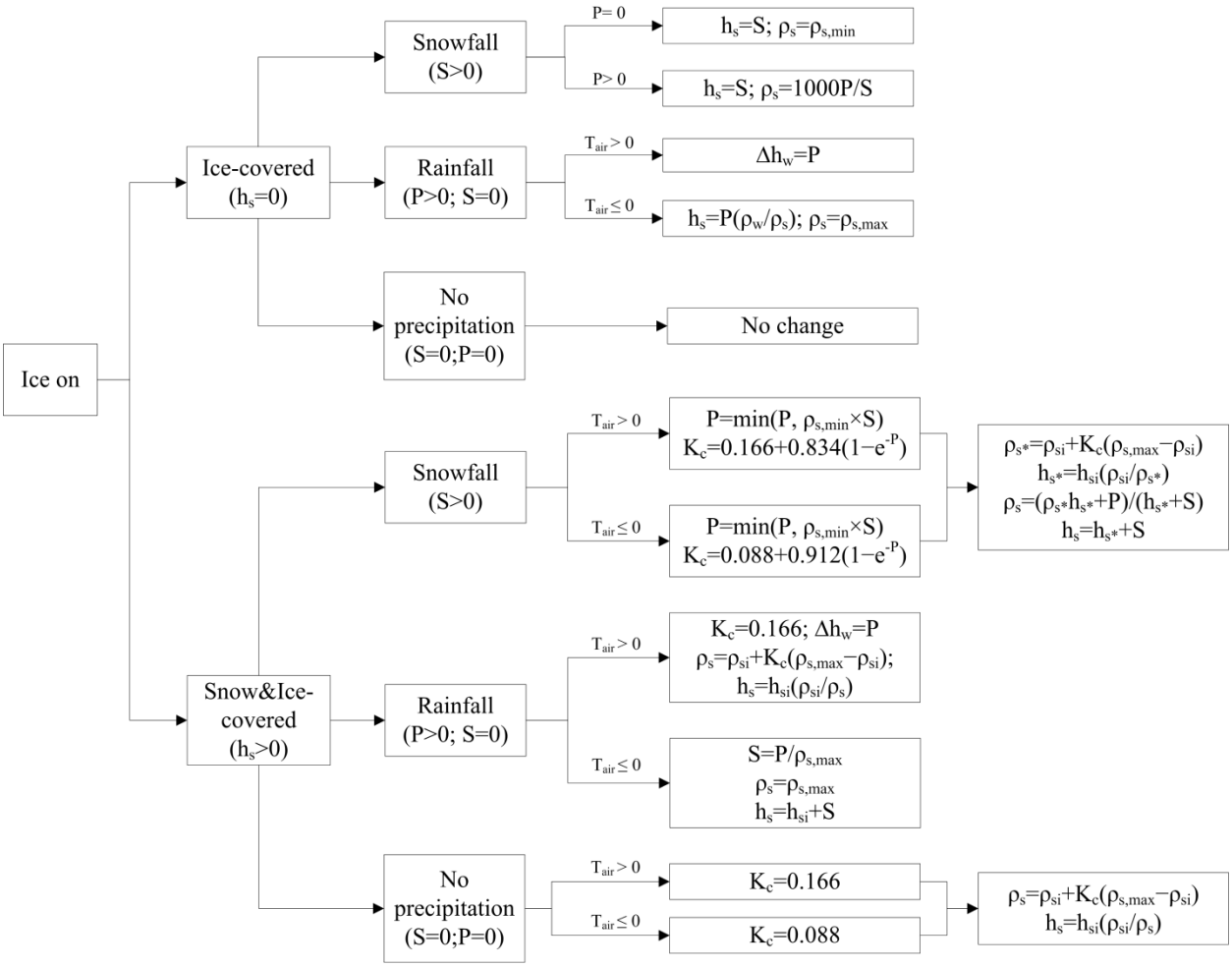

Figure A-1: Decision tree to update ice cover, snow cover, and water depth according to snow compaction, rainfall (P), and snowfall (S) on each day, and depth of snow cover (h_{si}) and snow density (ρ_{si}) for the previous day.

A.2.2 Sediment heat transfer

Since sediment heat transfer is important to water temperature beneath ice cover (Ellis et al. 1991; Tsay et al. 1992; Fang and Stefan 1996a, 1998), the model here incorporates sediment heat flux, a main external source of lake heating after freezing occurs, for all horizontal layers. This is the three-dimensional effect that a one-dimensional model cannot accurately portray;

however, in the model, the rate of heat transfer from the sediments to the water column in each layer is estimated by:

$$q_{sed} = K_{sed} \frac{dT}{dz} \quad \text{(A.4)}$$

where q_{sed} is the heat transfer, K_{sed} is the sediment conductivity (assumed constant), and $\frac{dT}{dz}$ is the temperature gradient across the sediment-water interface. $\frac{dT}{dz}$ is given by the equation:

$$\frac{dT}{dz} = \frac{T_s - T_w}{z_{sed}} \quad \text{(A.5)}$$

where T_s is the sediment temperature, T_w is the water temperature at the sediment surface (calculated from profiles simulated with DYRESM-ICE), and z_{sed} is the distance beneath the water at which the sediment temperature is constant. In Lake Mendota, sediment temperatures at 5 m varied little throughout the year (Birge et al. 1927). Since soils in the region are homogeneous, z_{sed} was set to 5 m for all three lakes. Data from Birge *et al.* (1927) is used to describe the variation of T_s with time:

$$T_s = 9.7 + 2.7 sin\left[\frac{2\pi(D-151)}{D_{year}}\right] \quad \text{(A.6)}$$

D is the number of days from the start of the year, and D_{year} is the total number of days for the year of interest (365 or 366). We use these equations in DYRESM-ICE to estimate the sediment heat fluxes for all three lakes.

A.2.3 Model input

Input for the model includes lake morphometry (lake volume and surface area as a function of elevation), initial vertical profiles for water temperature and salinity, Secchi depth, meteorological variables, and inflows/outflows, discussed in detail next. The model calculates the surface heat fluxes using meteorological variables: total daily shortwave radiation, daily cloud cover, air vapor pressure, daily average wind speed, air temperature, and precipitation. During the entire simulation period, all parameters/coefficients in the model are kept constant. The time step in the model for calculating water temperature, water budget, and ice thickness is 1 hr. Snow ice compaction, snowfall and rainfall components are updated at a daily time step, corresponding to the frequency of meteorological data input. Cloud cover, air pressure, wind speed, and temperature are assumed constant throughout the day, and precipitation is assumed uniformly distributed. Shortwave radiation distribution throughout the day is computed based on the lake latitude and the Julian day.

A.3 References

Birge, E. A., C. Juday, and H. W. March. 1927. The temperature of the bottom deposits of Lake Mendota; a chapter in the heat exchanges of the lake. Trans. Wis. Acad. Sci. Arts Lett. **XXIII**.

Ellis, C. R., H. G. Stefan, and R. Gu. 1991. Water Temperature Dynamics and Heat Transfer Beneath the Ice Cover of a Lake. Limnol. Oceanogr. **36**: 324–335.

Fang, X., and H. G. Stefan. 1996a. Dynamics of heat exchange between sediment and water in a lake. Water Resour. Res. **32**: 1719–1727. doi:10.1029/96WR00274

Fang, X., and H. G. Stefan. 1996b. Long-term lake water temperature and ice cover simulations/measurements. Cold Reg. Sci. Technol. **24**: 289–304. doi:10.1016/0165-232X(95)00019-8

Fang, X., and H. G. Stefan. 1998. Temperature variability in lake sediments. Water Resour. Res. **34**: 717–729. doi:10.1029/97WR03517

Gill, A. E. 1982. Atmosphere-Ocean Dynamics, Academic Press.

Gosink, J. 1987. Northern lake and reservoir modeling. Cold Reg. Sci. Technol. **13**: 281–300.

Gu, R., and H. G. Stefan. 1990. Year-round temperature simulation of cold climate lakes. Cold Reg. Sci. Technol. **18**: 147–160. doi:10.1016/0165-232X(90)90004-G

Hamilton, D. P., and S. G. Schladow. 1997. Prediction of water quality in lakes and reservoirs. Part I — Model description. Ecol. Model. **96**: 91–110. doi:10.1016/S0304-3800(96)00062-2

Hill, J. M., and A. Kucera. 1983. Freezing a saturated liquid inside a sphere. Int. J. Heat Mass Transf. **26**: 1631–1637. doi:10.1016/S0017-9310(83)80083-0

Imberger, J., and J. C. Patterson. 1981. Dynamic reservoir simulation model - DYRESM: 5, p. 310–361. *In* H.B. Fischer [ed.], Transport Models for Inland and Coastal Waters. Academic Press.

Magee, M. R., C. H. Wu, D. M. Robertson, R. C. Lathrop, and D. P. Hamilton. 2016. Trends and abrupt changes in 104 years of ice cover and water temperature in a dimictic lake in response to air temperature, wind speed, and water clarity drivers. Hydrol Earth Syst Sci **20**: 1681–1702. doi:10.5194/hess-20-1681-2016

McCord, S. A., S. G. Schladow, and T. G. Miller. 2000. Modeling artificial aeration kinetics in ice-covered lakes. J. Environ. Eng. **126**: 21–31.

McKay, G. 1968. Problems of measuring and evaluating snow cover. *Proceedings Workshop Seminar of Snow Hydrology*. Proceedings of the Secretariat Canadian National Committee for the IHD. 49–63.

Oveisy, A., and L. Boegman. 2014. One-dimensional simulation of lake and ice dynamics during winter. J. Limnol. **73**. doi:10.4081/jlimnol.2014.903

Patterson, J. C., and P. F. Hamblin. 1988. Thermal simulation of a lake with winter ice cover. Limnol. Oceanogr. **33**: 323–338. doi:10.4319/lo.1988.33.3.0323

Rogers, C. K., G. A. Lawrence, and P. F. Hamblin. 1995. Observations and numerical simulation of a shallow ice-covered midlatitude lake. Limnol. Oceanogr. **40**: 374–385. doi:10.4319/lo.1995.40.2.0374

Tsay, T., G. Ruggaber, S. Effler, and C. Driscoll. 1992. Thermal Stratification Modeling of Lakes with Sediment Heat Flux. J. Hydraul. Eng. **118**: 407–419. doi:10.1061/(ASCE)0733-9429(1992)118:3(407)

Vavrus, S. J., R. H. Wynne, and J. A. Foley. 1996. Measuring the sensitivity of southern Wisconsin lake ice to climate variations and lake depth using a numerical model. Limnol. Oceanogr. **41**: 822–831. doi:10.4319/lo.1996.41.5.0822

Yeates, P. S., and J. Imberger. 2003. Pseudo two-dimensional simulations of internal and boundary fluxes in stratified lakes and reservoirs. Int. J. River Basin Manag. **1**: 297–319. doi:10.1080/15715124.2003.9635214